

**POLITECNICO DI MILANO**  
FACOLTÀ DI INGEGNERIA INDUSTRIALE  
CORSO DI LAUREA SPECIALISTICA IN INGEGNERIA SPAZIALE



# **BOREAS**

An air-launched light satellite launcher design

Relatore: Prof. Michèle Lavagna

Co-relatore: Ing. Floriano Venditti

Tesi di laurea magistrale di

**Massimo Vetrivano, 711985**

Anno accademico 2009/2010

*As for the future, your task is not to foresee it, but to enable it.*

A. de Saint-Exupery

# Contents

<b>Acknowledgement</b>	<b>XVII</b>
<b>Sommario</b>	<b>XVIII</b>
<b>Abstract</b>	<b>XX</b>
<b>1 Introduction</b>	<b>1</b>
1.1 Small Satellite and Market . . . . .	1
1.2 Small-Medium Launcher . . . . .	4
1.3 Air launched vehicles . . . . .	11
1.3.1 Launch strategies . . . . .	11
1.3.2 Captive on top . . . . .	11
1.3.3 Captive on bottom . . . . .	16
1.3.4 Towed . . . . .	18
1.3.5 Aerial Refueled . . . . .	19
1.3.6 Internally carried . . . . .	21
1.4 Considerations . . . . .	23
1.4.1 Work organization . . . . .	25
<b>2 General configuration</b>	<b>27</b>
2.1 System presentation . . . . .	27
2.1.1 Safety concerns . . . . .	29
2.2 The vehicle propulsion design . . . . .	31

2.2.1	Z9 solid engine . . . . .	32
2.2.2	HM-7B cryogenic engine . . . . .	33
2.2.3	Bipropellant apogee engine,Astrium S400-12 . . . . .	34
2.2.4	Interstage and fairing . . . . .	36
2.2.5	Considerations . . . . .	37
2.3	Mass budget and sizing . . . . .	37
2.3.1	Cryogenic propellant system . . . . .	38
2.3.2	Second stage mass budget . . . . .	43
2.3.3	Third stage mass budget . . . . .	44
2.3.4	Interstage and fairing design . . . . .	48
2.4	Complete rocket configuration . . . . .	49
<b>3</b>	<b>Atmospheric configuration design</b>	<b>52</b>
3.1	Launcher and Aero-Module . . . . .	53
3.2	Carrier Aircraft . . . . .	59
3.2.1	Selection of aircraft types . . . . .	59
3.2.2	Modification to the carrier aircraft . . . . .	61
<b>4</b>	<b>Launcher dynamics: the release and ascent manoeuvres models</b>	<b>67</b>
4.1	Launcher dynamics models . . . . .	67
4.1.1	The release manoeuvre dynamics model . . . . .	68
4.1.2	The ascent phase dynamics model . . . . .	69
4.2	Atmospheric model . . . . .	71
4.3	Aero-Module actions definition . . . . .	73
4.4	Launcher actions . . . . .	74
4.4.1	Gravitational force model . . . . .	75
4.4.2	Aerodynamic drag model . . . . .	75
4.4.3	Thrust model . . . . .	75
4.5	Control law synthesis . . . . .	76



4.5.1	The first stage phase . . . . .	76
4.5.2	The second stage phase . . . . .	79
4.5.3	The third stage phase . . . . .	80
4.6	Release manoeuvre requirements . . . . .	82
4.7	Release Manoeuvres . . . . .	83
<b>5</b>	<b>Guidance and control simulation and results</b>	<b>86</b>
5.1	Release manoeuvre results . . . . .	86
5.1.1	Separation during horizontal flight . . . . .	86
5.1.2	Inclined separation manoeuvre . . . . .	91
5.2	Considerations . . . . .	95
5.3	Power ascent simulation . . . . .	97
5.4	Heat fluxes on fairing . . . . .	105
5.5	Flight trajectory optimization . . . . .	106
5.6	Performances . . . . .	108
<b>6</b>	<b>Design of Kerosene-LOx launcher</b>	<b>112</b>
6.1	Falcon I architecture . . . . .	112
6.2	Parametric design for liquid engine rocket . . . . .	114
6.3	Parametric design for the structures . . . . .	118
6.4	Optimization procedure . . . . .	119
6.4.1	Discussion . . . . .	120
6.4.2	Performance . . . . .	123
6.4.3	Direct insertion . . . . .	125
<b>7</b>	<b>Refined model for performances evaluation</b>	<b>127</b>
7.1	Rocket Attitude . . . . .	127
7.2	Rocket controller . . . . .	130
7.3	Results . . . . .	131
7.4	Consideration . . . . .	133

<b>8</b>	<b>Conclusions</b>	<b>134</b>
8.1	Innovative aspects . . . . .	134
8.2	Future developments . . . . .	135
	<b>References</b>	<b>139</b>
<b>A</b>	<b>Software Validation</b>	<b>140</b>
A.1	Comparison with Fortran . . . . .	140
A.2	Pegasus characteristics . . . . .	142
A.3	Test case . . . . .	144
A.4	Consideration . . . . .	146
<b>B</b>	<b>Genetic Algorithms</b>	<b>147</b>
B.1	Optimization based on genetic algorithms . . . . .	148
B.1.1	Components of the genetic algorithm . . . . .	149

# List of Figures

1.1	Distribution of world small satellite launched (1996-2006) and to be launched (1997-2016) by mass category . . . . .	2
1.2	Distribution of small satellite launched (1996-2006) and to be launched (1997-2016) by mass and altitude . . . . .	3
1.3	Distribution of small satellite launched (1996-2006) and to be launched (1997-2016) by mass and inclinations . . . . .	3
1.4	Scout rocket . . . . .	4
1.5	Volna launch from submarine . . . . .	5
1.6	Dnepr launcher . . . . .	7
1.7	Vega launcher . . . . .	8
1.8	Rockot launcher . . . . .	9
1.9	Leduc/Linguedoc and Space Shuttle <i>Approach and Landing Test</i> . . . . .	12
1.10	Spiral 50-50 credited ©Dan Roam . . . . .	12
1.11	Saenger II credited ©Mark Lindroos . . . . .	13
1.12	Interim HOTOL credited ©British Aerospace . . . . .	13
1.13	MAKS credited ©NPO Molniya . . . . .	14
1.14	Boeing AirLaunch credited ©Boeing . . . . .	15
1.15	Pegasus XL . . . . .	16
1.16	Yakovlev HAAL . . . . .	17
1.17	CNES concepts . . . . .	18
1.18	Astroliner . . . . .	19

## LIST OF FIGURES

---

1.19	Pathfinder credited ©Pioneer Rocketplane . . . . .	20
1.20	Drop of Minuteman missile C-5A in 1974 . . . . .	22
1.21	Darpa's Falcon rocket . . . . .	22
1.22	Velocity loss for a Sun-synchronous 200 km circular orbit . . . . .	25
2.1	General configuration . . . . .	28
2.2	Flight and launch phases . . . . .	28
2.3	Reference flight profile . . . . .	29
2.4	Possible launch sites . . . . .	30
2.5	Direct Insertion: first and second stage fall-out . . . . .	31
2.6	Z9 characteristics . . . . .	32
2.7	Z9 assumed thrust profile . . . . .	33
2.8	HM-7B engine characteristics . . . . .	34
2.9	S400-12 engine characteristics . . . . .	35
2.10	Third stage: general layout . . . . .	36
2.11	Payload envelope ( example for Pegasus launcher) . . . . .	37
2.12	Second stage tanks layout . . . . .	40
2.13	Pressure regulated vs blowdown system . . . . .	42
2.14	Third stage: installation on the launcher . . . . .	45
2.15	Propellant for de-orbiting . . . . .	47
2.16	Dimension for CoG estimation . . . . .	50
3.1	The Aero-Module . . . . .	52
3.2	Top view of the launcher with Aero-Module . . . . .	56
3.3	Centers of pressure position . . . . .	57
3.4	ESA/CNES A300 Zero-g and Airbus A330-200 . . . . .	60
3.5	Accommodation of the Launcher on an Airbus A330-200 . . . . .	62
3.6	Position of connections to the A/C and alternative position at rear side . . . . .	63
3.7	Beluga aircraft with the additional fins . . . . .	64

## LIST OF FIGURES

---

3.8	Telemetry reception system . . . . .	65
4.1	Initial condition . . . . .	70
4.2	Aerodynamic system . . . . .	74
4.3	Speed and position misalignment . . . . .	77
4.4	Third stage conceptual goals . . . . .	79
4.5	Third stage conceptual goals . . . . .	81
5.1	A/C and launcher position . . . . .	87
5.2	A/C and launcher relative module distance . . . . .	88
5.3	Horizontal separation and launcher speed components . . . . .	88
5.4	Normal loads on launcher . . . . .	89
5.5	Flight path angle . . . . .	90
5.6	Angle of attack . . . . .	90
5.7	Inclined release: A/C and launcher position . . . . .	92
5.8	Inclined release: A/C and launcher relative module distance . . . . .	92
5.9	Inclined release: horizontal separation and launcher speed components . . . . .	93
5.10	Inclined release: normal loads on launcher . . . . .	94
5.11	Inclined release: flight path angle . . . . .	94
5.12	Inclined release: angle of attack . . . . .	95
5.13	Attitude consideration . . . . .	96
5.14	Flight path angle relative to the orbital plane . . . . .	96
5.15	SSO at 600 km launch: altitude vs time . . . . .	98
5.16	SSO at 600 km launch: altitude vs time - detail . . . . .	99
5.17	SSO at 600 km launch: trajectory - 3D detail . . . . .	99
5.18	SO at 600 km launch: velocity vs time . . . . .	100
5.19	SSO at 600 km launch: acceleration vs time . . . . .	100
5.20	SSO at 600 km launch: thrust vs time . . . . .	101
5.21	SSO at 600 km launch: out-of-plane velocity vs time . . . . .	102

## LIST OF FIGURES

---

5.22	SSO at 600 km launch: angle of attack vs time . . . . .	102
5.23	SSO at 600 km launch: plane flight path angle vs time . . . . .	104
5.24	SO at 600 km launch: dynamic pressure vs time . . . . .	104
5.25	Heat fluxes on fairing . . . . .	106
5.26	Control laws . . . . .	107
5.27	Sensitivity on mass . . . . .	108
5.28	Sensitivity on initial in plane speed . . . . .	110
5.29	Sensitivity on fairing separation time . . . . .	110
6.1	Falcon 1 . . . . .	114
6.2	Nozzle definitions . . . . .	117
6.3	Mass breakdown . . . . .	122
6.4	Performance comparison in nominal condition . . . . .	123
6.5	LOx-Kerosene: sensitivity analysis . . . . .	124
6.6	Two burns insertion and direct insertion for kerosene-LOx launcher . . . . .	125
6.7	Two burns insertion and direct insertion for different Falcon launcher . . . . .	126
7.1	Rocket principal axis . . . . .	128
7.2	Attitude reference frames . . . . .	129
7.3	6 DoF Assembled launcher: Altitude and $\theta_r$ . . . . .	132
7.4	6 DoF Assembled launcher: parameters and thrust wrt plane . . . . .	132
7.5	Angle between $x_r$ projection on $z_p - y_p$ plane and orbital plane . . . . .	133
A.1	Fortran simulation results: Altitude . . . . .	141
A.2	Fortran simulation results: speed and acceleration . . . . .	141
A.3	Fortran simulation results: thrust and out of plane velocity . . . . .	142
A.4	Fortran simulation results: flight path angle and angle of attack . . . . .	142
A.5	Pegasus XL Performance Capability . . . . .	143
A.6	Pegasus's simulation results for 230 kg on 741 km circular orbit: altitude and $\theta_r$ . . . . .	145

*LIST OF FIGURES*

---

A.7	Pegasus's simulation results for 230 kg on 741 km circular orbit: acceleration and AoA . . .	146
B.1	Flow chart of a genetic algorithm . . . . .	150

# List of Tables

1.1	Scout-G launcher . . . . .	5
1.2	Dnepr launcher . . . . .	7
1.3	Vega data . . . . .	8
1.4	Rockot launcher . . . . .	9
1.5	Kosmos-3M launcher . . . . .	10
1.6	PSLV operational launcher . . . . .	10
1.7	Pegasus XL launcher data . . . . .	17
1.8	Air-launch method comparisons . . . . .	24
2.1	Second stage:parameters for sizing . . . . .	38
2.2	Second stage:propellant sizing . . . . .	39
2.3	Propellant used for tank sizing . . . . .	39
2.4	Second stage: tanks parameters . . . . .	39
2.5	Second stage:tanks parameters . . . . .	40
2.6	Material physical characteristics . . . . .	41
2.7	Constant $K_{type}$ for liquid propellant . . . . .	41
2.8	Mass tanks . . . . .	41
2.9	Second stage: pressurant gas sizing . . . . .	43
2.10	Second stage mass budget . . . . .	44
2.11	Third stage: maximum propellant required for 2000 km SSO . . . . .	46
2.12	Third stage: tanks sizing and mass estimation . . . . .	46



## LIST OF TABLES

---

2.13	Third stage: mass budget . . . . .	48
2.14	Interstage mass estimation . . . . .	49
2.15	Fairing mass estimation . . . . .	49
2.16	Elements mass and CoG with complete mass budget . . . . .	50
3.1	The Aero-Module: wing characteristics . . . . .	55
3.2	The Aero-Module: stabilizer characteristics . . . . .	56
3.3	The Aero-Module: trimming and centers of pressure . . . . .	56
3.4	Assumptions for trimming . . . . .	57
3.5	Aero-Module mass breakdown . . . . .	58
3.6	Characteristics and performances of candidate carrier aircrafts . . . . .	61
4.1	Temperature model coefficients . . . . .	72
4.2	Control coefficients for out of plane control . . . . .	79
4.3	Separation manoeuvre sequencing . . . . .	84
4.4	Aerodynamic characteristics for the Aero-Module . . . . .	85
4.5	Aerodynamic characteristics for Airbus A330 . . . . .	85
5.1	Third stage 570kg: initial condition . . . . .	97
5.2	Power ascent timeline . . . . .	98
5.3	Prandtl number and specific heat coefficient . . . . .	105
5.4	Control laws: performances comparison . . . . .	107
5.5	Sensitivity analysis on stage mass . . . . .	109
5.6	Sensitivity analysis on initial vertical sped and fairing separation . . . . .	111
6.1	Falcon 1: features . . . . .	113
6.2	Useful data for engine sizing . . . . .	115
6.3	Optimization kerosene/LOx launcher . . . . .	120
6.4	Optimization kerosene/LOx launcher . . . . .	120
6.5	Kerosene/LOx launcher: mass subdivision . . . . .	120

*LIST OF TABLES*

---

6.6	LOX-Kerosene launcher: engines characteristics . . . . .	121
6.7	LOX-Kerosene:Elements mass and CoG with complete mass budget . . . . .	121
6.8	Stage masses . . . . .	122
6.9	Comparison between assembled and kerosene launcher . . . . .	123
6.10	The Aero-Module for LOx-kerosene launcher: trimming and centers of pressure . . . . .	124
6.11	Sensitivity anlysis on kerosen launcher mass . . . . .	125
6.12	Comparison between direct and two burn insertion . . . . .	126
7.1	First stage <i>inertiae</i> . . . . .	129
A.1	Pegasus's main characteristics . . . . .	143
A.2	Pegasus's typical attitude and guidance modes sequence . . . . .	144
A.3	Pegasus's simulation parameters for 230 kg on 741 km circular orbit . . . . .	145

# Acronyms

**A/C** AirCraft

**ALV** Air Launched Vehicle

**AoA** Angle of attack

**CoG** Centre of Gravity

**CNES** Centre National d'Études Spatiales

**CPM** Conventional Payload Module

**DLR** Deutschen Zentrums für Luft-und Raumfahrt

**dof** degree of freedom

**ESA** European Space Agency

**FPA** Flight path angle

**NASA** National Aeronautics and Space Administration

**IMU** Inertial Measurement Unit

**ICBM** Inter Continental Ballistic Missile

**LEO** Low Earth Orbit

**LH2** Liquid Hydrogen

**LOx** Liquid Oxygen

**MRTT** Multi-Role Tanker Transport

MEOPMaximu Expected Operating Pressure

**OBDH** On Board Data Handling

---

<b>SL</b>	Sea Level
<b>SLV</b>	Small Launch Vehicle
<b>SMV</b>	Space Maneuver Vehicle
<b>SSO</b>	Sun-Synchronous Orbit
<b>TC</b>	TeleCommand
<b>TM</b>	TeleMetry
<b>TPS</b>	Thermal Protection System
<b>TVC</b>	Thrust Vector Control
<b>UDMH</b>	Unsymmetrical dimethyl-hydrazine
<b>VAC</b>	Vacuum
<b>wrt</b>	with respect to

# Acknowledgement

*To my father*

I would like to thank the Carlo Gavazzi Space S.p.A. where I had the opportunity to carry out this thesis.

A special mention goes to Mr. Floriano Venditti, who encouraged my work with his critical sense and who gave me many opportunities to exchange ideas. I would like to thank the guys of the Space Vehicle and Exploration Team, Emanuele, Igor and Filippo, that not only provided to me a clearer idea of what the industrial world is, but with who I also had many amazing and funny moments.

At the same time, a big thank goes, of course, also to all my friends and colleagues of the Space Engineering degree and of the Politecnico di Milano in general, with who I shared many hard and nice periods.

I would like to express my gratitude to the professors of Politecnico di Milano, that offered to me many opportunities to improve my education and that during these years have been with me throughout all the difficulties helping me to achieve this goal.

A heartfelt thank goes to my family and to all my true friends that always supported me. A final and special thank goes to my girlfriend Valentina, that pushed me to do always my best in any situation.

# Sommario

Il presente lavoro di tesi si inserisce nel contesto del Future Launcher Preparatory Programme (FLPP) dell'Agenzia Spaziale Europea (ESA); il programma nasce dal desiderio di ridurre i costi di lancio per sistemi spaziali di dimensioni contenute. Un aspetto chiave da analizzare in questo ambito riguarda la gestione razionale delle risorse e delle infrastrutture connesse alla totalità della fase di lancio: in particolare, la sostituzione del lancio del vettore dal suolo con il lancio da aereo permetterebbe di usufruire di un semplice aeroporto militare, di evitare i vincoli di carattere politico/nazionale, di semplificare le norme di sicurezza e di ridurre i requisiti sul sito stesso di lancio. Inoltre tale approccio consente una certa flessibilità per i satelliti di piccole dimensioni. Oggigiorno il progetto di tali satelliti deve tenere in considerazione che essi vengono lanciati come carico pagante secondario, il che implica la ricerca di un compromesso tra l'orbita disponibile e quella desiderata. Ciò causa spesso ritardi con un conseguente aumento dei costi. Il lancio aereo offre a questa classe di satelliti la possibilità di essere posizionati sull'orbita operativa desiderata senza ulteriori manovre ad alto costo quali i cambi di piano orbitale.

Il presente lavoro discute i risultati ottenuti dallo studio di fattibilità svolto per un lanciatore sganciato da aereo. Si è scelto di mantenere un approccio multidisciplinare nello studio che coinvolgesse gli aspetti di configurazione, propulsivi e di controllo. Si è effettuato uno studio dettagliato della dinamica del veicolo, dagli effetti legati alla strategia di sgancio fino all'immissione nell'orbita operativa. Si è prestata particolare attenzione all'impiego di componentistica già presente sul mercato o in attuale sviluppo per piccoli lanciatori, includendo tra i criteri di valutazione non solo le tipiche prestazioni di lanciatori (massa/quota) ma anche la modularità progettuale così da consentire l'impiego di differenti soluzioni propulsive. Lo studio svolto ha permesso di evidenziare e quantificare gli aspetti critici che maggiormente impattano sulla massa di carico pagante.

Il primo capitolo introduce le necessità di natura tecnica ed economica alla base di un

---

lanciatore leggero di tipo *air-launched* ed espone lo stato dell'arte nell'ambito di questa tipologia di lanciatori.

Il secondo e terzo capitolo espongono la configurazione iniziale e generale del lanciatore sviluppato a partire dall'obiettivo di costruire un *assembly* di componenti messi a disposizione dall'industria aerospaziale europea. Quanto riportato nel terzo capitolo é, inoltre, estendibile al lanciatore propulso da motori a kerosene e ossigeno, sviluppato nel sesto capitolo.

Il quarto capitolo analizza la manovra di rilascio del complesso, costituito dal missile e dal modulo alare, dall'aereo che ha il compito di portarlo nella zona di lancio e di garantire appropriate condizioni iniziali di volo.

Il quinto capitolo illustra la dinamica del vettore dopo il rilascio dall'aereo ed il distacco dalle ali, e riporta le prestazioni in termine di massa del carico pagante posta ad una certa quota su orbita circolare eliosincrona.

Il sesto capitolo discute la progettazione di un lanciatore con sistema propulsivo a base di kerosene e ossigeno liquido, in grado di garantire analoghe prestazioni. La motivazione di tale studio risiede nei possibili rischi legati alla presenza di sistemi propulsivi eterogenei, i quali caratterizzano il sistema assemblato.

Nel settimo capitolo si riporta un modello a sei gradi di libertà del lanciatore e discute le problematiche dovute alla perdite di prestazioni legate essenzialmente alla fase di distacco del modulo alare nella fase precedente all'ignizione del primo stadio.

## **Parole chiave**

ALV (Air Launched Vehicle); Controllo di vettore spaziale; Dinamica del razzo; Progettazione di traiettorie di lancio; Manovra di separazione in volo; Sistema propulsivo liquido; Progetto di missile.

# Abstract

The current thesis work can be considered as part of the Future Launcher Preparatory Programme (FLPP) of the European Space Agency (ESA); this programme arises from the wish to reduce the launch costs for small space systems. A key point to be analysed in such a field is relevant to a clever management of the resources and of the infrastructures linked to each launch phase: in particular, the substitution of a ground-based launch with an air-to-air launch that would allow to exploit a simple military airport, to avoid political and national issues, to simplify safety procedures and to reduce requirements on the launch base. Moreover, this approach increases also the flexibility of the small satellites. In fact, nowadays, the design of such satellites has to take into account the fact that they are launched as secondary payload, which implies the need to accept a compromise between the achievable orbit and the preferred one. This often causes delays and, then, an increase of the launch costs. An air-to-air launch from an airplane would offer to this class of satellites the possibility to be placed on the preferred operative orbit without any additional manoeuvre requiring a higher propulsive cost (e.g. plane changes).

The current work also discusses the results obtained during the feasibility study for a launcher released by a plane. A multidisciplinary approach has been selected, allowing to consider also the configuration, propulsion and control aspects. A detailed analysis of the launcher dynamics has been performed, taking into account all the phases of the mission, from the release strategies up to the insertion in the final orbit. Special attention has been focused on the use of off-the-shelf components and in the components that are currently under development for the small launchers, including among the evaluation criteria not only the performance of the launchers (e.g. mass, achieved orbit), but also the flexibility of their propulsive systems to face different missions. This study has also allowed to highlight and quantify the critical aspects that mainly impact the payload mass.

Chapter One introduces the technical and economical requirements that pushed towards the need of such a light launcher, type air-to-air, and provides the current status of the art



---

of this class of launchers.

Chapters Two and Three describe the initial general configuration of the developed launcher taking into account the objective to build an assembly of some components already available in the European aerospace industry market. What is reported in Chapter Three is also applicable to a launcher propelled with kerosene/oxygen engines (see also Chapter Six).

Chapter Four analyses the release manoeuvre of the whole system, that includes the missile, the wings module and the plane that has the goal to bring it up to the loading zone and to guarantee suitable initial flight conditions.

Chapter Five shows the launcher dynamics after the release from the plane and the separation of the vehicle from the plane wings surface. It provides also the performance of the launcher in terms of payload mass with respect the final height of the eliosynchronous circular orbit.

Chapter Six describes the design of a launcher with a propulsion system fueled with kerosene and liquid oxygen, and able to guarantee similar performances. The motivation of such a design is due to the possible risks that could be linked to the presence of different heterogeneous propulsion systems, which characterize the final assembly.

Finally, the last chapter, Chapter Seven, reports a six.degrees of freedom model of the launcher, and discusses about the problematics mainly due to the release mechanisms that could not provide the expected performances during the separation phase of the wings module.

## **Key words**

*ALV* (Air Launched Vehicle); Missile control; Rocket dynamic; Ascent trajectory optimization; Separation flight manoeuvre; Liquid propulsion system; Rocket design.

# Chapter 1

## Introduction

This thesis focuses on the multidisciplinary study to assess the feasibility for an air-launched launcher for small satellites. The thesis was conceived and developed within the Space Vehicles and Exploration Department at Carlo Gavazzi Space Spa, Milan, under the supervision of the Engineer Floriano Venditti, between April 2009 and March 2010.

The name of the studied system, Boreas, after the name of the Roman God of Northern winds, stands for Bipropellant Operational Responsive European Air-launched System and has been chosen because explanatory of the its main features.

In fact, the most important design driver has been to identify a flexible and responsive launcher subjected to a limited number of constraints, requiring short forewarnings before to be launched, and exploiting the european launch areas that are mainly localized over the Atlantic Ocean.

The current chapter highlights motivations for air-launched systems offering their current state of development too.

### 1.1 Small Satellite and Market

The interest of a dedicated launch system follows the recent proliferation of micro-satellite platforms and the increasing success of the associated applications. In particular, it is due to:

- numerous successful technology demonstration experiences based on micro-satellites, for Science or Defense applications with gradual increase in instrument performance,

- constant improvements of quality versus cost,
- rebirth of interest for constellations ( e.g. Rapid eyes, Orbcomm2, numerous project worldwide etc.) and formation flying,
- increasing number of operational applications becoming accessible to small satellites: communications, intelligence gathering, early warning, space surveillance, different types of observation, etc.,
- evidence of the vulnerability of the large space systems, i.e. their complexity, high launch and recurrent costs due to long period of development, the difficulty of tailored mission for small satellites,
- increasing interest for the *Responsive Space* approach in the U.S. and other countries (China, etc.); this approach prefers small size systems in order to reduce global costs and delays, thanks also to the reduced size of the required facilities and space-ports, to limit the safety launch concerns, and to facilitate the implementation of new technologies

The current market for small satellites (less than 500 kg) is more active in the micro-satellites range (40-150 kg, refer to [1]). Over the last few years there has been a strong increase in demand for launching of that class of satellites, for which more and more platforms are available<sup>1</sup>.

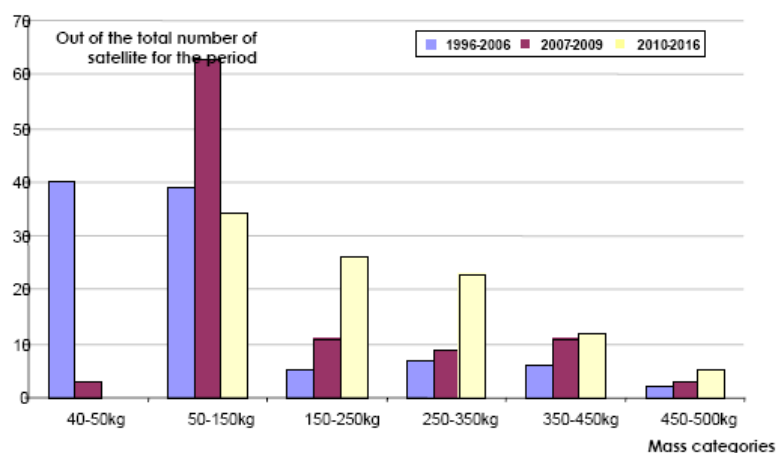


Figure 1.1: Distribution of world small satellite launched (1996-2006) and to be launched (1997-2016) by mass category

<sup>1</sup>figures reported in this paragraph have been elaborated in the *Euroconsult Market Study*(see [1]) for small LEO satellites

## 1.1. SMALL SATELLITE AND MARKET

This increase in number might also be accompanied by an increase in satellite masses (increase from 150 to 200 kg, or even more) in order to optimize mission yields.

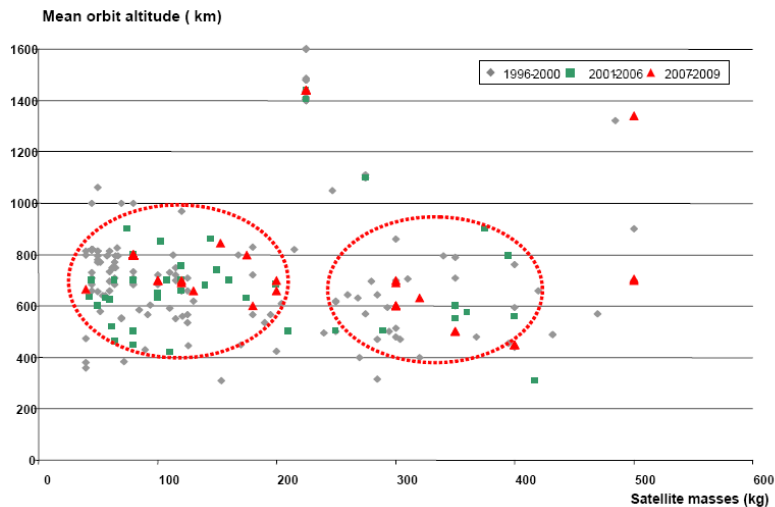


Figure 1.2: Distribution of small satellite launched (1996-2006) and to be launched (1997-2016) by mass and altitude

As it can be seen in figure 1.2, most of the satellites to be launched in LEO have a mass that is less than 500kg, that is the target payload mass for the launcher studied in this thesis.

Satellites, which will be launched in the next years, have as preferred injection orbit the Sun-synchronous orbit (SSO):

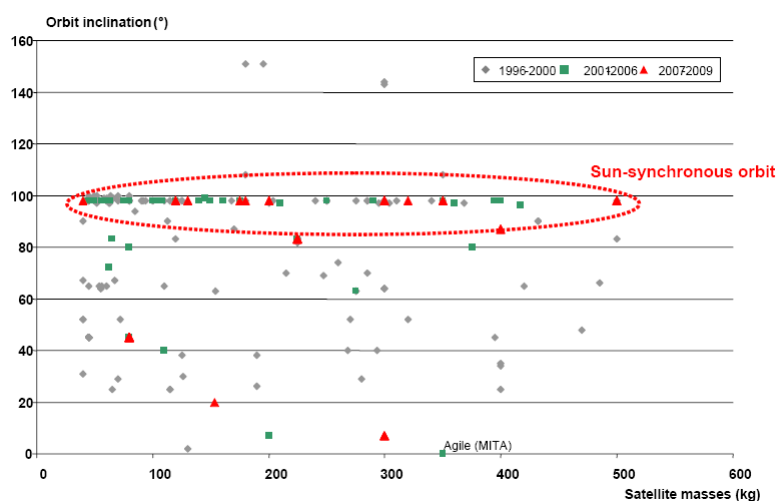


Figure 1.3: Distribution of small satellite launched (1996-2006) and to be launched (1997-2016) by mass and inclinations

For this reason the study of launch vehicles targeted to small satellites into Sun-synchronous orbit is definitely needed. The launch of small satellites can be accomplished via two different alternative launch systems, that are the traditional one performed from a ground facility by using a small-medium launcher, or the one exploiting the use of air launch vehicles. The state of the art according to the two aforementioned classes is briefly presented in the following, to better highlight their limitations and possible rooms for new solutions.

## 1.2 Small-Medium Launcher

In the past years Small launchers derived from military ballistic nuclear rockets. The U.S. Scout family rockets were launch vehicles designed to place small satellites into orbit around the Earth and were operative in the period 1961-1994.

- Scout

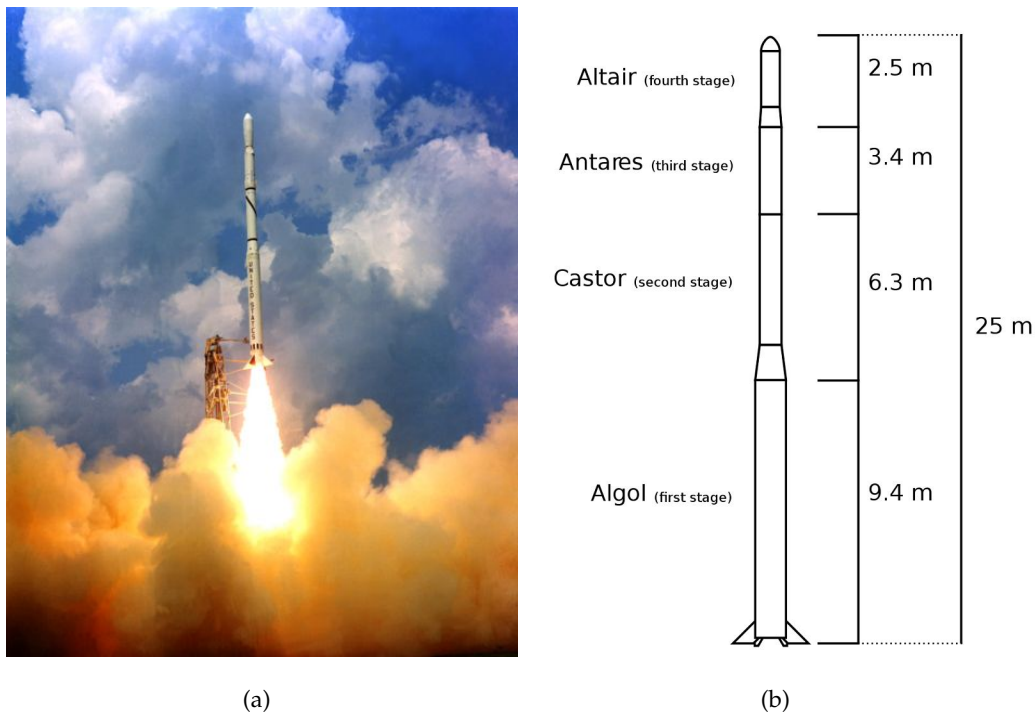


Figure 1.4: Scout rocket

The Scout four-stages rocket was the first (and for a long time, the only) orbital launch vehicle to be entirely composed of solid fuel stages. The first successful orbital launch of a Scout, on February 16, 1961, delivered the Explorer 9 in its final

orbit the Explorer 9, a 7kg satellite used for performing studies about the density of the atmosphere. The main dedicated launch complex was the Wallops Flight Facility. Scout capability grew dramatically over the years. Originally able to place a 59-kilogram payload in a nominal 552-kilometer circular orbit, Scout performance was improved, increasing its capability up to put a 208-kilogram payload into the same orbit. Thanks to this launcher, Italy became the third space country putting on orbit its first satellite, San Marco 1, in 1964. Italian was also the heaviest satellite it had ever placed in orbit which weighed more than 270 kilograms. Scout increased its load-carrying capability up of the 350 percent with respect its original capability with only a little increase in size of its stages. The mean cost per launch was about 10 million U.S. dollars.

	1 <sup>st</sup> Stage Algol	2 <sup>nd</sup> Stage Castor	3 <sup>rd</sup> Stage Antares	4 <sup>th</sup> Stage Altair
Gross mass [kg]	14320	4424	1637	301
Propulsion type	Solid	Solid	Solid	Solid
Thrust [kN]	622.8	266.9	80.0	26.7
Burning time [s]	82	41	4x	34

Table 1.1: Scout-G launcher

- Volna

Ballistic rockets play a predominant role as favourite light launcher vector . This is due essentially to the great availability of this kind of missile, mainly from former soviet countries.



Figure 1.5: Volna launch from submarine

The Ukrainian space launch vehicle Volna , is a converted submarine-launched ballistic missile used for launching artificial satellites into orbit.

The main advantage of this kind of launch method stands in the fact that it allows to reduce safety concerns linked to the ground launch.

The Volna is a 3 stage launch vehicle that uses hypergolic liquid propellant.

The warhead section is used for the payloads that can be either put into orbit with the help of an additional boost engine or travel along a sub-orbital trajectory to be recovered at the landing site. Volna can be launched from Delta III class submarine or from land based facilities. The Volna missile weighs 35 tons, and has a length of 14.2 metres and a range of 8000 kilometres.

Because of its mobile launch platform the Volna launch vehicle can reach a large number of different inclinations and could increase its performance to low Earth orbit by launching from equatorial sites.

All flights to date have taken place from the Barents Sea. From this site the Volna can lift 100kg into a 400km high orbit with an inclination of 79 degrees. The warhead section can accommodate a payload of up to 1.3 m<sup>3</sup>.

For sub-orbital missions the payload can be either a recoverable vehicle of up to 720kg or research equipment placed in a descent vehicle of up to 400kg (no other data are available about the Volna launcher).

- Dnepr The Ukrainian Dnepr is three-stage rocket using storable hypergolic liquid propellants (refer to [2]). The launch vehicles used for the launch of satellites are missile withdrawn from service with the Russian Strategic Rocket Forces and stored for commercial use. The Dnepr are traditionally launched from Baikonur in Kazakhstan and recently from the new Cosmodrome at the Dombarovsky launch base, near Yasny, in the Orenburg region of Russia.

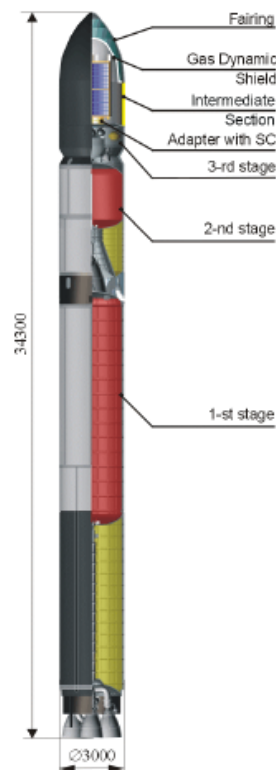


Figure 1.6: Dnepr launcher

The baseline version can lift 3600 kg into a 300 km low earth orbit at an inclination of 50.6 degrees , or 2,300 kg to a 300 km sun-synchronous orbit.

	1 <sup>st</sup> Stage	2 <sup>nd</sup> Stage	3 <sup>rd</sup> Stage
Gross mass [kg]	208900	47380	6266
Propulsion type	Hypergolic liquid	Hypergolic liquid	Hypergolic liquid
Thrust [kN]	4520	755	18.6
Burning time [s]	130	190	317

Table 1.2: Dnepr launcher

- Vega

Vega is a programme of the European Space Agency (ESA) geared to developing a launcher for small and medium satellites (see [3]). Its development began in 1998 and the first launch, which will take place from the Guiana Space Centre, is planned for 2011. It is designed to launch small payloads: 300 to 2,000 kg satellites for scientific and Earth observation missions to polar and low Earth orbits.

The reference Vega mission is a polar orbit bringing a spacecraft of 1,500 kilograms



## 1.2. SMALL-MEDIUM LAUNCHER

to an altitude of 700 kilometers.

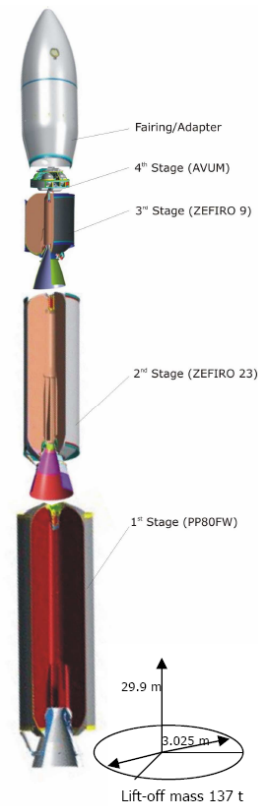


Figure 1.7: Vega launcher

Vega is a single-body launcher with three solid rocket stages, the P80 first stage, the Zefiro 23 second stage, the Zefiro 9 third stage, and a liquid rocket upper module called AVUM.

	1 <sup>st</sup> Stage P80	2 <sup>nd</sup> Stage Zefiro 23	3 <sup>rd</sup> Stage Zefiro 9	4 <sup>th</sup> Stage Avuum
Gross mass [kg]	95796	25751	10948	785
Propulsion type	Solid	Solid	Solid	Hypergolic liquid
Thrust [kN]	2261 SL	1196SL	225- Vac(TBC)	2.45-VAC
Burning time [s]	106.8	71.7	117	up to 667

Table 1.3: Vega data

- Rockot Rockot is a fully operational, three stage, liquid propellant Russian launch vehicle which is being offered commercially by EUROCKOT Launch Services for launches into low earth orbit (see [4]). EUROCKOT, a German-Russian joint venture company was formed specifically to offer this vehicle commercially.

## 1.2. SMALL-MEDIUM LAUNCHER

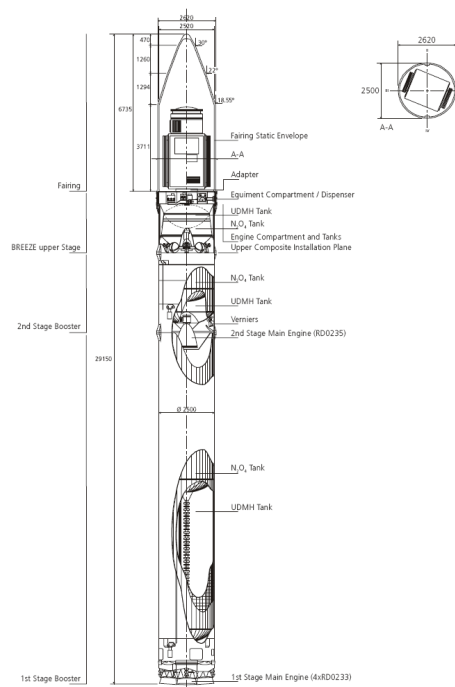


Figure 1.8: Rockot launcher

The gross mass of the launcher is 107000 kg and it is able to deliver a 1950kg payload to a 200km circular orbit with an inclination of 63 degrees.

	1 <sup>st</sup> Stage	2 <sup>nd</sup> Stage	3 <sup>rd</sup> Stage
Propulsion type	Hypergolic liquid	Hypergolic liquid	Hypergolic liquid
Thrust [kN]	2070-VAC	240-VAC	20-VAC
Burning time [s]	121	183	max 1000

Table 1.4: Rockot launcher

- The Kosmos-3M is a Russian expandable space launch vehicle (see [5]). It is a liquid-fuelled two-stage rocket, first launched in 1967 and with over 410 successful launches to its name. The Kosmos-3M uses nitrogen tetroxide as an oxidizer to lift roughly 1500 kg of payload to LEO and nearly 800 to SSO. The launch facility are located in Russia at Plesetsk and Kapustin Yar.

## 1.2. SMALL-MEDIUM LAUNCHER

---

	1 <sup>st</sup>	2 <sup>nd</sup> Stage
Gross mass [kg]	87200	20640
Propulsion type	Nitric acid-hydrazine	Hypergolic liquid
Thrust [kN]	1486	883
Burning time [s]	131	700

Table 1.5: Kosmos-3M launcher

- Polar Satellite Launch Vehicle

The Polar Satellite Launch Vehicle (PSO) launch vehicles were developed by Indian Space and Research Organization (ISRO) to launch its own remote sensing satellites (IRS series) into sun-synchronous orbits (see [6]). PSLV is a four stage core vehicle with additional strap-on solid boosters. The core vehicle possesses an unusual design consisting of two solid-propellant stages (1st and 3rd stages) and two liquid stages (2nd and 4th stages).

The standard version of the PSLV has four stages using solid and liquid propulsion systems alternately and six strap-on boosters. Currently it has capability to launch 1678 kg to 622 km into sun synchronous orbit. The total mass of the operational launcher is 294000 kg.

The PSLV-CA, CA meaning *Core Alone*, model does not include the six strap-on boosters used by the PSLV standard variant. The fourth stage of the CA variant has 400 kg less propellant when compared to its standard version. It has the capability to launch 1100 kg to 622 km sun synchronous orbit.

	0 Stage boosters	1 <sup>st</sup> Stage	2 <sup>nd</sup> Stage	3 <sup>rd</sup> Stage	4 <sup>th</sup> Stage
Propulsion type	Solid	Solid	N2O4/UDMH	Solid	Hypergolic liquid
Thrust [kN]	502.6	4860	725	328	14
Burning time [s]	44	105	158	83	425

Table 1.6: PSLV operational launcher

As it can be seen there is a broad variety of small-medium launcher developed with the aim of targeting LEO orbits with small satellites. Many countries, on the other hand, have focused their effort on big launchers (China and Japan). This choice implies that such satellites have to be delivered as secondary payload with delays and increasing costs waiting for a suitable mission.

## 1.3 Air launched vehicles

Air launched vehicles differ in the methodologies they are connected to the transporting vehicle and in the releasing solutions.

The most relevant solutions are reported hereinafter.

### 1.3.1 Launch strategies

The main launch strategies can be categorized into five launch method categories:

1. captive on top - the launcher is placed on the top of the carrier
2. captive on bottom - the launcher is positioned on the bottom or on a wing of the carrier
3. towed - the launcher is dragged and dropped thanks to the use of a tow
4. aerial refueled - the launcher flies at high altitude where it is refueled in order to access to low orbit; it combines air-brahe propulsion and rocket propulsion
5. internally carried - the launcher is accommodated in the air-carrier bay

Several examples are reported in the following discussion for each launch method.

### 1.3.2 Captive on top

The benefits of the captive on top launch method are:

1. the capability to carry a large launch vehicle on top of the carrier aircraft,
2. the possibility to use a carrier aircraft with little clearance between fuselage and ground at take-off,
3. the proven separation strategy during US Space Shuttle *Approach and Landing Test* campaign in , and in Leduc/Languedoc in 1946 (see figure 1.9)

Drawbacks include

1. penetrations on the windward side of the launch vehicle's thermal protection system (TPS) for attachment hardpoints

2. possible extensive modifications (high cost) to the carrier aircraft.

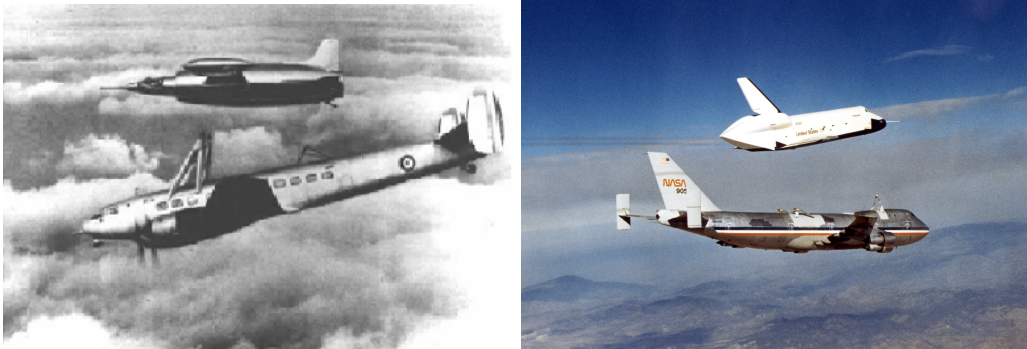


Figure 1.9: Leduc/Linguedoc and Space Shuttle *Approach and Landing Test*

Also the launch vehicle must be provided with active controls at release from the carrier aircraft and the launch vehicle wings must to be large enough to support it at separation from the carrier aircraft. Examples include:

- Spiral



Figure 1.10: Spiral 50-50 credited ©Dan Roam

The Spiral 50-50 represents a very advanced concept that is still not possible with today's technology since it requires advanced materials, thermal protection system (TPS), and engines. It was financed from 1965 to 1978 by the Soviet government and consisted of an air-breathing Mach 7 booster aircraft powered by 4 hydrogen-burning air-breathing turbo ramjets, an expendable two-stage rocket, and a one-person orbital spaceplane. Take-off gross weight was projected at 127000 kg . A proof-of-concept prototype of the orbital spaceplane was flown at least 3 times from 1976 to 1978 after being airdropped from a Tu-95 aircraft. The program was canceled due to development cost.

- Saenger II



Figure 1.11: Saenger II credited ©Mark Lindroos

Saenger II represents a very advanced concept that is still not possible with today's technology. It was funded from 1985 to 1994 by the Messerschmidt-Boelkow-Bloehm company and the German Ministry for Research and Development. It consisted of a large air-breathing Mach 6.6 booster aircraft powered by 6 coaxial turboramjets and a small rocket-powered upper stage (HORUS). The HORUS would be able to deliver a crew of two persons and 3000 kg of payload to LEO. Take-off gross weight was designed at over 340000 kg. As part of the program a liquid hydrogen ramjet was run for 25 seconds in a simulated Mach 4 environment by MBB in 1991. The program was canceled due to development cost.

- Interim HOTOL



Figure 1.12: Interim HOTOL credited ©British Aerospace

The British Aerospace Interim HOTOL was studied from 1989 to 1991 and was an air-launched version of the original HOTOL that eliminated the ambitious combined cycle air-breathing propulsion system for four modified Russian LH2-LOX rocket engines. The carrier aircraft was to be a Ukrainian An-225 Mriya aircraft, currently the world's largest aircraft.

Modifications to the aircraft include adding two Lotarev D-18 engines to increase number of engines to 8. The Interim HOTOL would separate from the carrier aircraft at Mach 0.8 at 9200 m. Its wings would assist its pull up for the ascent to orbit and it would return via a gliding re-entry and conventional runway landing.

Interim HOTOL represents an advanced concept that is still not possible with today's technology. It required fueling with densified super cooled LH2 and LOX to prevent propellant boil-off during the climb and cruise to the launch point.

External carriage of the Interim HOTOL meant that its propellants underwent both radiation heating from the sun and convective heating from the atmosphere. The designers of Interim HOTOL were unable to achieve a satisfactory solution to its stability and control problems.

Reusable launch vehicles must control their center of gravity (CoG) position both during ascent and reentry. During the wing borne portion of flight, the CoG must be reasonably close to the wing's lift or center of pressure (CP). With engines mounted in the rear, then empty CoG is dominated by the engine location, and the wings must be in the rear for reentry.

- MAKS

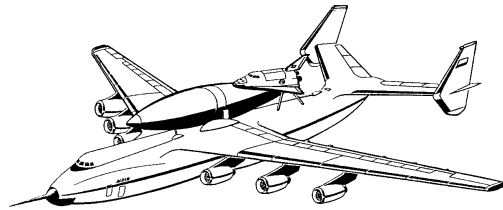


Figure 1.13: MAKS credited ©NPO Molniya

NPO Molniya developed MAKS5 in a draft project that was completed in 1989. The MAKS would have to consist of a manned version (MAKS-OS), and unmanned cargo carrier (MAKSC), a sub orbital demonstrator (MAKS-D), and an advanced fully reusable unpiloted version (MAKSM), similar to the Interim HOTOL.

The MAKS-OS is shown in figure 1.13 it weighed 590000 kg on takeoff. It consisted of a An-225 carrier aircraft that would be piggy-back the 272000 kg MAKS to an altitude of about 9200 m and 250 m/s, an external tank, and a 18150 kg and 19.2 m long spaceplane designed for 100 reuses. It would be able to carry a crew of two and a payload of 8160 kg to a 185 km 51deg inclination orbit and was powered by two tripropellant engines designed for 15 re-uses. These engines initially used RP-LOX and then switched to higher specific impulse LH2-LOX at reduced thrust later in the trajectory. This reduced the size of the external tank and was expected to reduce the mass of the engines to half as compared to pure LH2-LOX engines. MAKS pioneered the idea of an orbiter pushing an external tank. This significantly reduced the tank's weight as compared to a fully reusable integral tank.

Pushing the external tank also allowed easier aborts strategy since during the atmospheric portion of the ascent trajectory the external tank was always denser than the orbiter. This means the orbiter and external tank would naturally separate if released. The orbiter and external tank concept also reduced the amount of orbital maneuvering propellant required.

Finally, the external tank concept solved the stability and control problem that plagued Interim HOTOL. The MAKS concept required the development of new TPS materials for the orbiters leading edges since it had a smaller radius (and hence higher heating rate and temperatures) than the Buran's leading edges. It also required the use of supercooled propellants to prevent propellant boiloff.

The orbiter's payload capability appears a bit optimistic, resulting as the 50% of the orbiter's empty weight. The larger Space Shuttle is capable to carry less than of less than 30% of its empty weight. Finally, the fully reusable MAKS-M would require advanced materials for the tanks as well as a solution to ascent and reentry stability and control problems.

- Boeing AirLaunch



Figure 1.14: Boeing AirLaunch credited ©Boeing

Conceived in 1999, AirLaunch is a feasible system design based on today's technology. Its design goals were to keep development and recurring costs to a minimum. It can support two configurations, one able to place a Space Maneuver Vehicle (SMV) into LEO, the other to put on orbit civil, commercial and military payloads with a Conventional Payload Module (CPM). Solid motor wall thickness is several times thicker (and heavier) than a liquid fueled propellant tank wall thickness. Also the solid propellant itself provides some structural strengthening, particularly in compression. Note that the SMV is a small, unpiloted reusable spacecraft designed to support a variety of military space missions ranging from



satellite deployment to terrestrial and orbital support.

### 1.3.3 Captive on bottom

The benefits of the captive on bottom launch method include:

1. proven and easy separation from carrier aircraft,
2. leeward side penetrations,
3. hard points on the launch vehicle that reduces some TPS concerns,
4. and the option of sizing the wings smaller than required for flight at the release altitude and airspeed ( thanks to an initial loss of height and consequent increase of speed up to the engine ignition) .

Drawbacks include :

1. limits on the launch vehicle size due to clearance limitations on the carrier aircraft (wrt ground)
2. high cost of carrier modifications.

A carrier aircraft designed for this kind of launch vehicle can eliminate clearance limitations.

- Pegasus



Figure 1.15: Pegasus XL

American Pegasus and current version Pegasus XL are the world's only operational air launch system. The Pegasus launcher consists of expendable 3 stage solid rocket

### 1.3. AIR LAUNCHED VEHICLES

---

boosters with wings attached to the first stage. It is launched from Orbital Science's L-1011 Stargazer carrier aircraft at 11500 km of altitude at a local Mach number of 0.82. It can deliver a 450 kg payload into a 185.2 km equatorial orbit.

Mass at launch[kg]	Length [m]	Diameter [m]	Wingspan [m]
23500	17.6	1,27	6.7

Table 1.7: Pegasus XL launcher data

- Yakovlev HAAL



Figure 1.16: Yakovlev HAAL

Initially conceived in 1994 at Ukrainian Yakovlev as Burlak (barge-hauler) and now called High Altitude Aerial Launcher (HAAL), this concept is possible with today's technology. The system would consist of a two stage expendable rocket launched from the Tu-160 *Blackjack* swing-wing supersonic bomber at an altitude of 13800m and Mach 1.7 . The 31750 kg launch vehicle is based on a Russian InterContinental Ballistic Missile (ICBM). It is fueled with non-cryogenic propellants (N<sub>2</sub>O<sub>4</sub>/UDMH) and is carried under the Tu-160. Launch price is estimated at \$5 million for delivering a 1150 kg payload to a 185 km orbit. Development cost is estimated at \$100 million.

- Airborne Micro Launcher (MLA)

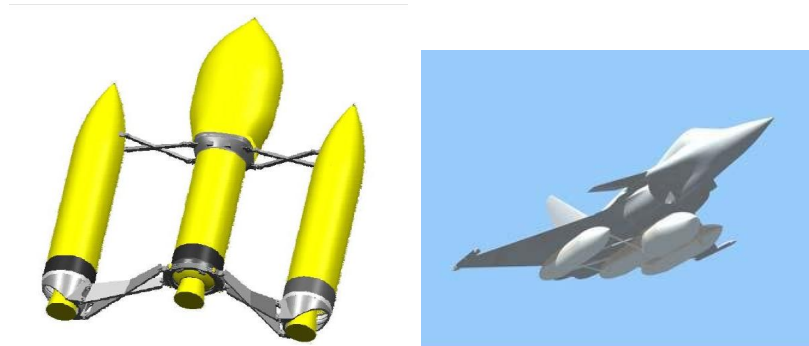


Figure 1.17: CNES concepts

The French National Centre of Space Studies (CNES) in collaboration with the German Aerospace Center (DLR) is currently developing project studies for a launcher dedicated to micro-satellites. A candidate configuration is the Airborne Micro Launcher (MLA).

The 9 tons MLA vehicle is capable of putting a 150 payload kg payload to a SSO. It is carried by a Rafale fighter up to 16000 m and then dropped.

The MLA concept supported is by a fighter aircraft which has the ability to maximize the benefit due to an airborne launch thanks to the dynamic capabilities of the aircraft (optimization of the kinematics at separation such as altitude, velocity and flight path angle). Such capabilities also offer the possibility to imagine a simplified sequence of jettisoning and a launcher without important aerodynamic support (big wings like Pegasus, parachute like QuickReach, etc.). Drawbacks are the limited mass and volume due to the aircraft capability, and some constraints such as the train trap deployment, aerobrakes, ground clearance, etc.

#### 1.3.4 Towed

The primary benefits of a towed concept are:

1. easy separation from the towing aircraft and
2. low cost modifications on the towing aircraft.

The main drawbacks are:

1. safety concerns including the abort strategy in case of broken towlines during flight and at take-off,

### 1.3. AIR LAUNCHED VEHICLES

---

2. propellant boil-off unless supercooled propellants are used since there it is not possible to replenish the propellant consumed by the towed launched through the towing lines aircraft.
3. the sizing of the launch vehicle wings and landing gear for take-off with a full propellant load and the design of a sophisticated flight control system during aerotowed phase.

- Kelly Space's Astroliner



Figure 1.18: Astroliner

This vehicle was conceived in 1993 and received over \$6 million in NASA funding, the Kelly Space and Technology Astroliner concept is a combined jet and rocket powered aircraft that was to be built using existing technology and off the shelf components. The fully fueled 326600 kg Astroliner would be towed off on a runway using the thrust of its own jet engines and the excess thrust provided by a stripped down Boeing 747 acting as a tow aircraft.

At 6000 m, the tow line would be dropped and once clear of the 747, the Astroliner would light its rocket engines. It is expected to accelerate up to Mach 5 and then to coast to 120km altitude. Clear of the atmosphere its nose would open and release a 25400 kg upper stage capable of placing a 4550 kg payload into LEO. Except for towing, new technologies were not expected to be needed for the Astroliner.

Although the Astroliner's basic towing concept seems to be possible, it is still unfeasible with today's technology.

#### 1.3.5 Aerial Refueled

The principal benefits of aerial refueling are:

### 1.3. AIR LAUNCHED VEHICLES

---

1. reduction of the size of the carrier aircraft'wing and landing gear,
2. no limitations to the size of the launcher

Drawbacks are:

1. no reduction of the size of jet engines because they must be sized to maintain flight level for a fully fueled carrier aircraft,
  2. hazardous release of the payload from the payload bay of the launcher
- Pioneer Rocketplane



Figure 1.19: Pathfinder credited ©Pioneer Rocketplane

This concept was conceived in the late 1990's and received \$2 million in NASA funding. The Pioneer Pathfinder Rocketplane<sup>10</sup> concept is a combined jet and rocket powered aircraft that had to be built using existing technology and off the shelf components. It would use its two turbofan engines for take-off, rendezvous, and refueling with a 747 aerial tanker where it would take on 59000 kg of LOX, doubling its gross weight up to 123500 kg .

This refueling concept would reduce the size of the Pathfinder's wings and landing gear to about one half of an aircraft that had to carry all its oxidizer at take-off. Once separated from the 747, it would light on its single RD-120 engine and it was expected to climb to 130 km altitude and Mach 15. Once outside the atmosphere, it would open its payload bay doors and release a 15500 upper stage capable of placing a 2000 kg satellite into LEO.

Except for LOX aerial transfer, new technologies were not expected to be needed for

Pathfinder. Although the Pathfinder's basic aerial refueling concept seems possible, it is still unfeasible with today's technology. Even with the savings in landing gear and wing weight, the Pathfinder is expected to carry 4.6 times its empty weight in propellant, crew, and upper stage.

Using realistic weights and today's technology Pathfinder staging could not occur at published Mach 15. It would still be subject to significant aerodynamic pressure during staging making release from Pioneer Rocketplane payload bay extremely hazardous.

#### 1.3.6 Internally carried

The main benefits of internally carried concepts include:

1. little or no modifications to the carrier aircraft (lowers both development and operations cost);
2. major propellant boil-off elimination concerns since the launch vehicle is not subject to either radiation heating from the sun or convective heating from the airstream;
3. access by the maintenance crew to the launch vehicle until the launch, which reduces the safety concerns about carrying a launch vehicle with a manned carrier aircraft.

The launch vehicle is in a safe environment inside the carrier aircraft and maintenance and safety problems can be detected and solved.

Moreover, internal carriage eliminates weather induced launch failures (such as the Shuttle Challenger) by launching into a known and benign environment, the stratosphere. Furthermore, the carrier aircraft offers a protection, until the carrier has reached the release altitude. Internally carried launch concepts are also able to carry heavier launch vehicles and release them at higher altitudes compared to the externally carried ones.

In fact, the latter shows a higher carrier aircraft drag because of launcher presence. Taking into account that the carrier aircraft's jet engines thrust is designed in order to balance the drag of the only aircraft, this drives to the need to reduce the reachable altitude or the overall gross weight.

Main drawbacks of internal air launch are:

1. the launch vehicle must be sized to fit inside the carrier aircraft,

### 1.3. AIR LAUNCHED VEHICLES

---

2. LH<sub>2</sub>-LOX powered launch vehicles can not be carried because air and gaseous hydrogen explode over a wide range of mixture ratios - 4% to 76% by hydrogen volume ratio - This is not a safe situation for the interior of a cargo airplane,
3. hazardous separation phase due to the interference between launch vehicle and carrier aircraft.



Figure 1.20: Drop of Minuteman missile C-5A in 1974

The first internal-carried air launched test was done on 24 October 1974 when a C-5A Galaxy dropped a 35400 kg LGM-30A Minuteman I missile using drogue chutes to extract the missile and its 3600 kg launch sled, as shown in figure 1.20.

- Falcon Small Launch Vehicle (SLV) program

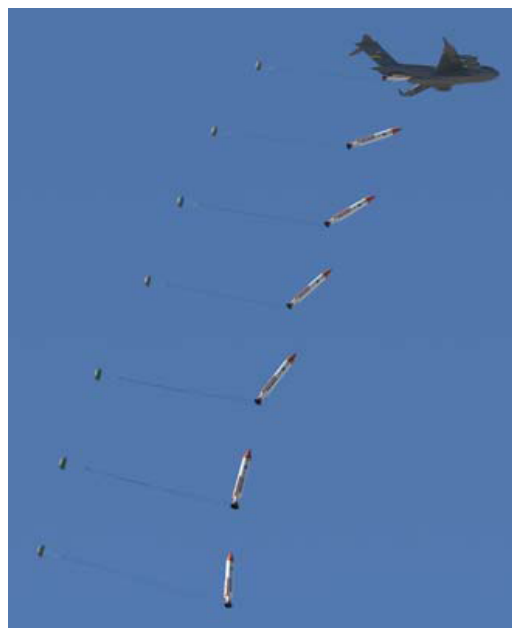


Figure 1.21: Darpa's Falcon rocket

The American Falcon SLV program started in 2003 with the main goal of developing a vehicle able to deliver a 500 kg satellite to a 200km circular orbit for less than \$5 million, within 24 hours of notice. Currently it costs about \$20 million to launch a satellite of this size into space and the lead time can be also years. The 33 tons rocket, contained in the fuselage of a C-17, is extracted by an air drop and launched. Tests on a mock-up have confirmed the safety of the launch procedure.

Other similar internally carried launchers are the French HORUS (High Operational Responsive and Versatile System) and Vozdushny Start (Air Start) planned by the Russian Energia in collaboration with Polyot and Antonov companies.

## 1.4 Considerations

The classical launchers dedicated to the small satellites market lack of competition, for two main disadvantages:

1. scale effect, which implies the launch of smaller satellites due to bigger mass ratio
2. fixed cost, which are due to expensive ground facilities and complex operation before and after launch which has to be compliant with safety launch policy

The study of airborne launchers could represent a solution to many problems thanks to :

1. use of a re-usable, existing and very reliable first stage to carry the launcher above the denser layer of atmosphere, that is an aircraft;
2. gain on the total mass of the vehicle due to lower velocity losses with consequent propellant mass savings,
3. reduction of the ground facilities size, with the removal of the launch pad, and constraints (safety in close range), and possibility to launch from the European continent with the advantage of proximity to the customer.

Among the different air-launch methods some figures of merit can be highlighted, driving towards the choice of the studied launcher. Table 1.8 shows a summary:



#### 1.4. CONSIDERATIONS

Air-launched strategy	System complexity	Technological readiness	Reliability	Flexibility	Development costs
Captive on top	Simple system	Proven method	Secure manoeuvre	Dependent on air-carrier	Medium for expandable vehicle
Captive on bottom	Simple system	Proven method	Proven reliability	Dependent on air-carrier	Medium for expandable vehicle
Towed	Simple release manoeuvre but accurate active gear control needed	Not tested. Some examples for airplanes available	Safety concerns about the towlines resistance	Dependent on air-carrier	Medium-high
Aerial refueled	Complex system with different propulsion type	Aerial refueling proven but need of taylorred system design	Hazardous payload release	Not dependent on air-carrier	High - reusable launch vehicle
Internally carried	Simple system	Method under test for solid propellant	Air-drop influences performances	Dependent on air-carrier	Low

Table 1.8: Air-launch method comparisons

The towed and aerial refueled strategies have been discarded because they are the most complex and need technological improvements with high costs of development. At same time, the internally carried strategy has not been considered due to the hazards relevant to the cryogenic propulsion that has been chosen as the second stage of the launcher studied. The captive on bottom solution results the best option taking into account the reduced clearance under the wings and fuselage of European Airbuses, which could represent a huge problem during take-off.

Taking into account the main sources of velocity losses (thrust loss due to atmosphere, drag loss, out-plane control loss, gravity loss) and one of the launcher developed in this work (the one based on kerosene and liquid oxygen propellants), it is possible to evaluate

the benefits that such a launcher would provide if launched directly from air (air-launch) or from ground (ground-launch). These benefits are shown in figure 1.22.

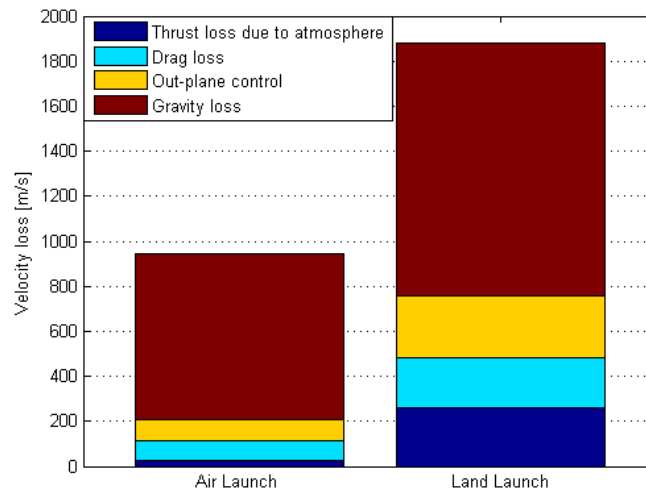


Figure 1.22: Velocity loss for a Sun-synchronous 200 km circular orbit

In particular, it has to be noted that there is a benefit with respect each of the main sources mentioned above.

### 1.4.1 Work organization

The report firstly focuses on the overall vehicle preliminary design: the engines, are borrowed by already flown launchers, such as Ariane IV and Ariane V, and by Vega which is next to the first launch(first months of 2011):

- Z23 solid propulsion engine from Vega's second stage
- HM-7B cryogenic engine used on third stage of Ariane IV and on Ariane V upper stage

In this way beyond the reliability and the well known performances which have been proved in previous launches and tests, those choices help in containing development costs, reducing the development phase to only components integration and lift off and early phase of flying studies. These latter includes also the release from the plane, that represents the most hazardous manoeuvre of the entire launch.

Moreover, the choice of the carrier, e.g. one among Airbus' planes, wants to create an economical return and heritage for European industry.

The chapters from two to five deal with the design of the launcher using off-the shelf components, the aerodynamic configuration, the study of the release manoeuvre from the plane, and the definition of the launcher performances.

Chapter six analyzes the possibility to develop a tailored launch vehicle based on kerosene-LOx motors, with the freedom of design the motors and the mass distribution of rocket. This choice is due essentially to some difficulties relevant to the use of cryogenic propellants and the risk for humans.

Chapter seven wraps up the work done by giving some critical review and considerations according to aspects emerged during the air launched feasibility study and addresses further developments for the future.

## Chapter 2

# General configuration

In this chapter the general configuration of the captive on top air-launched vehicle will be exposed. Then the chapter will describe the launcher module, whose propulsion elements are the main drivers for the estimation of final mass and of the size of the system, and that have great impacts on the launcher performances in terms of maximum payload mass to deliver to LEO.

### 2.1 System presentation

The overall launch system, as shown in figure 2.1, is composed by the following elements:

- the carrier aircraft A330-200 that has been chosen among the Airbus family (see chapter 3); it has the task to carry the Aero-Module and the launcher to the release place at an altitude of about 11000 m;
- the wing module, named Aero-Module (described in chapter 3 and 4), which has the function of lifting the complex formed by the launcher and the Aero-Module itself from the carrier aircraft;
- the launcher which has to deliver the payload to the final orbit; the design orbit, as exposed in section 1.1, is Sun-synchronous, which is easily accessible through air-launch from Europe (see chapter 5).

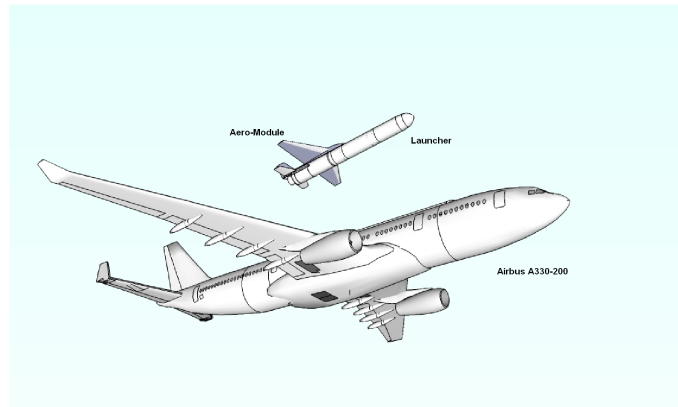


Figure 2.1: General configuration

For what concerns the launcher, the number of stages has been set to three as input of the work coming from CGS and basing on existing small launchers as Volna and Pegasus (see section 1.2), while the propulsion engines have been chosen among the available European ones as described in section 1.4.1.

In order to distinguish the flight and launch phases and to allow to understand how each stage is connected to the other one, a schematic view is proposed in figure 2.2:

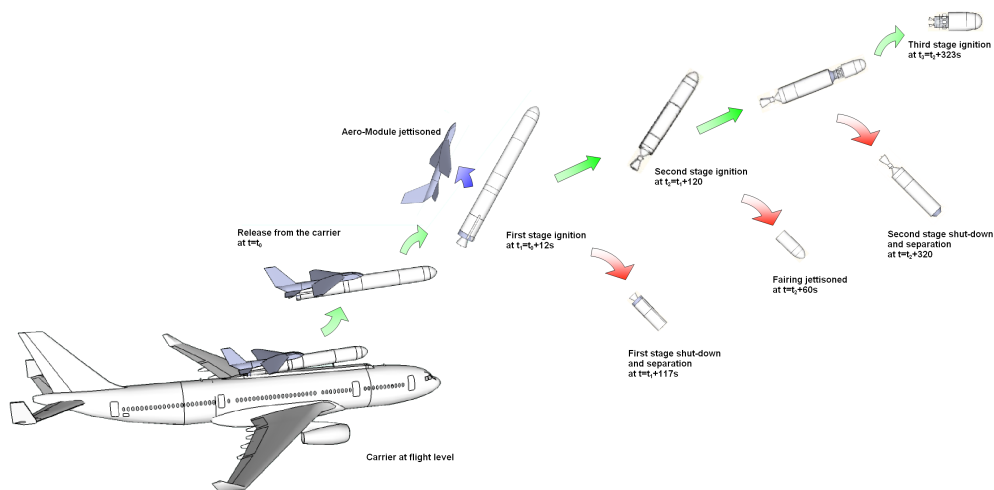


Figure 2.2: Flight and launch phases

The launch can be conceptually divided in two phases:

1. the release manoeuvre, which is a non propelled phase, during which the Aero-Module with the launcher leaves the carrier plane

2. the ascent phase, that starts with the ignition of the first stage, when the Aero-Module is jettisoned from the launcher, and finishes with the third stage burn-out, when the payload reaches the target orbit.

It is important to note that during the ascent phase of the launcher a control system acts in order to direct the thrust properly and achieve the target orbit.

Taking into account that the major driver and principal purpose of the design reported hereafter is to deliver a payload of approximately 300 kilograms on a 600 kilometers Sun-synchronous circular orbit, the assumptions applied to the design are the following:

1. a fixed first stage
2. a variable propellant mass of the second stage
3. a variable propellant mass and total mass of third stage, payload included

This strategy leads to the flight profile reported in the figure 2.3:

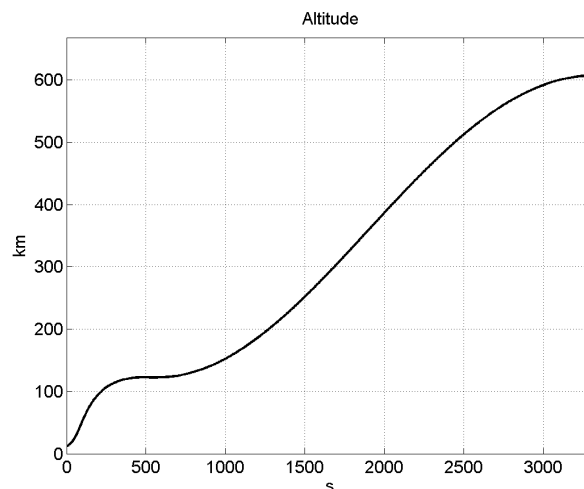


Figure 2.3: Reference flight profile

### 2.1.1 Safety concerns

The general idea is launching from Europe, offering the chance of inserting satellites on inclined orbit of particular interest for commercial and scientific purposes. The main difficult, nowadays, is that small-medium satellites are launched as secondary payloads and need a series of maneuvers that reduce the effective payload mass and field of application of the satellite.

## 2.1. SYSTEM PRESENTATION

---

Even with launches from airplane, airports and release areas must be defined, to be compliant with safety rules; to this end the ocean represents the best area for safe release. Several launch areas can be identified with respect to the final orbit requests.

The most suitable launch area can be chosen according to the customer:

1. high inclined orbits are such as Sun-synchronous take advantage of high latitude site of launch
2. low and medium inclined orbits are favored by low latitude

Having all that in mind, the following launch areas are here proposed:

1. Norwegian Sea, north-east of Scotland, between 60 deg latitude and Arctic circle (67 deg latitude) and between -10 and 0 degrees of longitude
2. Atlantic Ocean, south-west of Iceland, between 60 deg latitude and Arctic circle (67 deg latitude) and between -26 and -22 degrees of longitude
3. Atlantic Ocean, near Canary Islands, between 25 and 32 degrees of latitude and -25 and -15 degrees of longitude

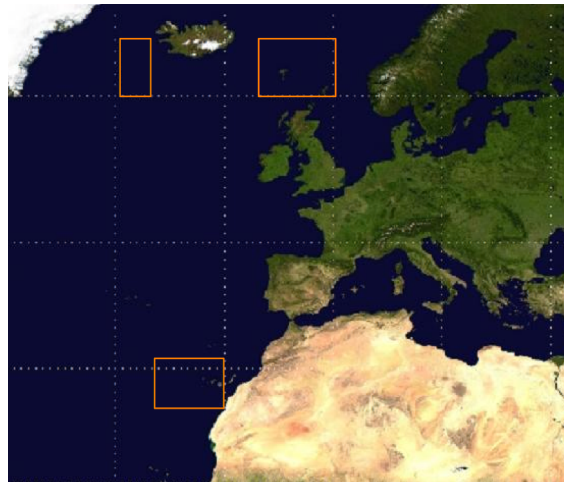


Figure 2.4: Possible launch sites

The choice of the last implies that only retrograde orbits can be obtained for safety reasons that require to avoid flying above very populated regions, that it will occur for other launches.

By launching from the first and second sites, the vehicle flies above Arctic and western

part of Alaska and a possible impact area for the expended 2nd stage are located in the Pacific Ocean

The presence of those locations is due to safety concerns about the stages' range:

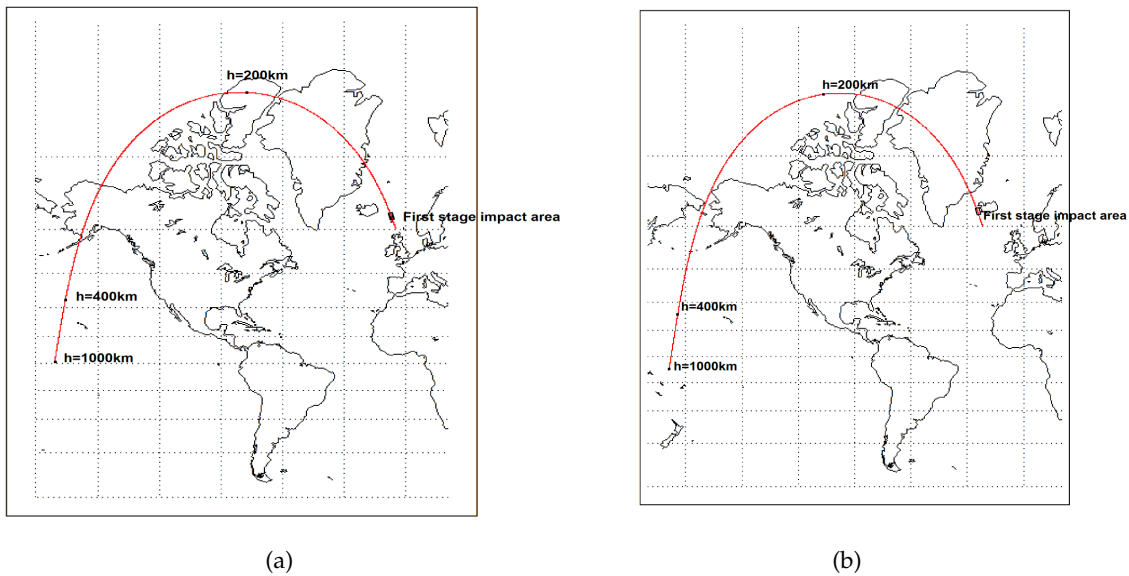


Figure 2.5: Direct Insertion: first and second stage fall-out

As it can be seen in fig 2.5 for these payloads launched at high latitude, it is possible that especially second stages may impacts relatively populated areas in the continental north America.

The first site is reachable from the Middle-Europe, although it is preferable to reduce the flight time of the carrier, while in the second case it is preferable to start carrier operations from the British Isles or Iceland.

Polar and nearly polar orbits, included Sun-synchronous orbit, represents an interesting field from commercial and military point of view.

The most important element of the general configuration is represented by the launcher propulsion system, which has great impact on the performances. For this reason the vehicle propulsion design will be analyzed priorly to the other. launch vehicle aspects

## 2.2 The vehicle propulsion design

As anticipated in the first chapter, main components of launcher come from the existing ones. Europe sees its principal rocket suppliers in companies involved in the Ariane and Vega development, which has, as its principal products, the Ariane and Vega launchers.



## 2.2. THE VEHICLE PROPULSION DESIGN

---

As the current study focuses on small launchers for Europe, those projects are assumed as reference for any already available component. The Ariane has proven a great reliability, while the Vega is still under at the time this document has been written (May 2010).

The following engines have been considered for the current study:

1. first stage Z9 solid engine under development and test in Vega rocket (see section 2.2.1)
2. second stage HM-7B cryogenic engine used in the the 3rd stage of Ariane IV and V (see section 2.2.2)
3. third stage and apogee maneuver bipropellant motor Astrium S400-12 (see section 2.2.3)

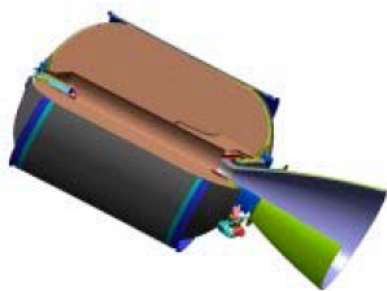
At the same time, it is necessary to consider other vital elements, which have a considerable impact on the final mass and on the size of the launcher, as:

- the inter-stage adapters
- the fairing

Other components, such as the telemetry and telecommunications unit, the control system, the separation system etc., have been considered for the system final mass estimation but will be not treated in detail in the next paragraphs.

### 2.2.1 Z9 solid engine

First stage has the task of driving the rocket up to the orbital plane or not far from it, leaving dense layers of atmosphere and giving a certain speed to the second stage. Z9 engine is produced by Avio and has not flown so far. Figure 2.6 shows Z9 main characteristics:



Dimensions	Mass
Body diameter 1.9m	Propellant mass 10115 kg
Overall length 3.85 m	Mass at ignition 10950 kg

Figure 2.6: Z9 characteristics

The mass budget includes TVC actuators and units. Z9 diameter represents the maximum transversal dimension for the entire rocket. The use of Z9 grants a significant thrust with a specific impulse of  $295s$ . Because this engine is still under test and its development results are confidential, only few data about its thrust profile are available. The performance, shown in figure 2.7, has been estimated, assuming that the maximum thrust is given in the first 40s of firing and then decreases linearly. This trend has been considered also during the performance analysis reported in chapter 5.

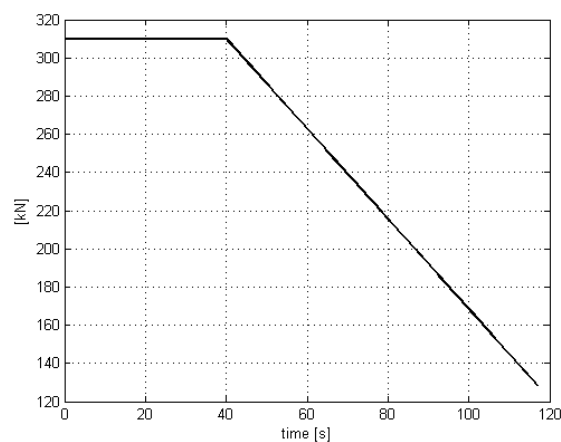


Figure 2.7: Z9 assumed thrust profile

An issue is represented by its nozzle that has been sized to maximize vacuum thrust, and therefore its performance are decreased during the first phase of the launch because of the static losses due the different pressure. The real effects on performance embraces also shocks in the nozzle that would further decrease the effective thrust. For this reason it would be necessary to adapt its dimensions to a lower altitude (as from 12 to 70km), which would reduce the mass of the nozzle. In next chapter only static losses has been considered.

### 2.2.2 HM-7B cryogenic engine

The main task of the second stage is to drive the launcher with a very small error up to the payload final orbital plane, and to provide the right flight path angle in order to achieve enough speed and altitude for the third stage. HM-7B engine, produced by SNECMA, has been already used on the third stage of Ariane IV and is still present also in one version of the Ariane V standard upper stage (ECA). It is a non-throtteable and non-restartable gas generator cycle engine, whose main characteristics are reported in figure 2.8:



Overall length	2.01m
Nozzle Diameter	0.99m
Mass	165kg
Thrust in vacuum	64800N
Mass flow rate	14.82kg/s
Chamber pressure	36.1
Mixture ratio	6:1
Gimbal capability	+/-3

Figure 2.8: HM-7B engine characteristics

### 2.2.3 Bipropellant apogee engine, Astrium S400-12

This kind of motor has been selected for the third stage of the launcher. This engine can provide the following functions:

- to insert the launcher into the transfer orbit,
- to insert the launcher from the transfer orbit into the payload final orbit,
- to perform orbital manoeuvres for collision avoidance and for multi-payload release,
- to perform de-orbiting manoeuvre for the third stage, when this is required by the debris mitigation policy.

Propulsion functions are implemented by the well-proven Astrium S400-12 bipropellant engine, which has been selected for its performances, reported in figure 2.9, and reliability.

The third stage accommodates also the payload, an attitude control system and most of the avionic system.



Throat diameter	16.4mm
Nozzle end diameter	244mm
Nozzle expansion ratio	244mm
Mass engine with valve	3.60kg
Thrust,nominal, in vacuum	420N
Specific impulse,nominal	318
Thrust range	340-440N
Mass flow rate,nominal	135g/s
Mass flow rate,range	110-142g/s
Mixture ratio,nominal	1.65
Mixture ratio,range	1.50-1.80
Chamber pressure	10bar
Qualified single burn life	1.1hrs
Qualified accumulated burn life	8.3hrs
Qualified cycle life	100hrs

Figure 2.9: S400-12 engine characteristics

Thrust level provided by one single engine would be sufficient to perform the manoeuvre but long firing due to the low resulting acceleration impacts on the manoeuvre precision. For example a total amount of 1000 m/s will be needed to insert the vehicle properly on a 600 km orbit, and the burning time will be about 1200s.

Moreover, a lower firing time would allow to increase the precision of the manoeuvre. A possible solution would be to increase the number of the engines, but this would increase also the propulsion system mass. Therefore, taking into account these aspects, the third stage have been provided with only two of these engines.

The internal volume of the third stage encloses the propulsion system together with the two tanks for MMH and  $N_2O_4$  with the pressurant tank of helium. Instead, the avionics unit have been accommodated on the external surface of the third stage structure. A thermal protection shield could be required for protecting the electronic units from plume radiation.

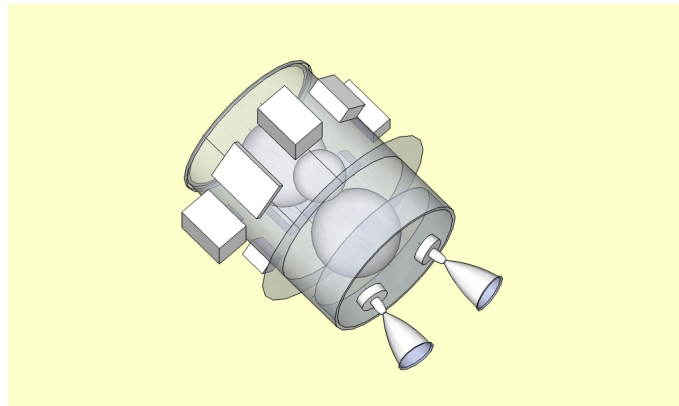


Figure 2.10: Third stage: general layout

Motors should be mounted with thrust directions converging approximately toward the system symmetry axis; in this way if one engine failed, the mission would not be compromised, assuming that attitude control system is able to compensate the induced momentum around the center of mass of the launcher.

### 2.2.4 Interstage and fairing

The link between first and second stage is ensured by an adapter, whose dimensions are essentially due to HM-7B nozzle. It has to be built in order to guarantee the necessary stiffness for withstanding static and in-flight loads. Static loads are given by the hard points necessary to connect the launcher to the airplane and to the wings during the first phase of flight. Another connection to the carrier is expected to occur on the top of the second stage. These hard points are described in chapter 3 but their design will not be part of this work.

Fairing encapsulates the third stage, which is composed by a primary structure of about 1000mm diameter, on which the standard payload interface ring of 937mm is mounted on the top. For what concerns the choice of the fairing envelope this has been assumed similar to the Pegasus one:

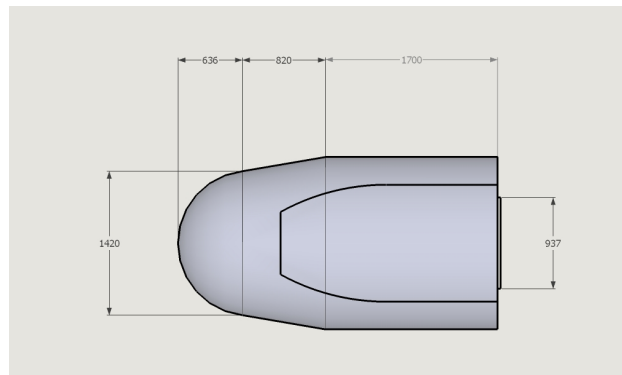


Figure 2.11: Payload envelope ( example for Pegasus launcher)

As shown in figure 2.11, the total volume for the payload accommodation is more than  $5m^3$  and it is composed by a cylinder of 1.7m of diameter and 1.7m of height. This configuration could allow to avoid the need to use deployable systems (as solar arrays and antennas) on the payload.

### 2.2.5 Considerations

The diameter of the launcher is set by the first stage case to 1.9m, which implies that second stage takes the same dimension, as well as the fairing. This latter are connected to the second stage, providing a safe distance from the payload in order to reduce shocks. An interstage between the second and the third stage is not required as the third stage case is directly connected to the second stage structure.

Different configurations of the third stage could be envisaged thanks to its lighter structure and to the fact that the fairing loads are not transferred to the third stage itself. This solution allow to accommodate larger payloads without to increase the third stage mass, that instead affects the maximum payload mass that can be delivered on orbit.

Finally, given a certain mission profile, an increase of the fairing mass has only small effects on the system performances, while these are greatly influenced by when the fairing separation occurs (see chapter 5).

## 2.3 Mass budget and sizing

First stage is assumed fixed in terms of dimensions and masses but in the sensitivity analysis on mass of chapter 5 it will be considered. Other elements, such as structures and

tanks, have been sized in order to fit some constraints, for propellant system essentially due to physical considerations, while structural elements like interstage adapter have been conservatively defined.

#### 2.3.1 Cryogenic propellant system

The following criteria has been applied to identify a proper range for second stage burning time:

- long burning times produce an increase of the mass with a consequent reduction of acceleration in the initial phase of firing; low accelerations result in noticeable gravity losses, with final orbit altitude decrease or mission abort
- low burning times produce light second stages; in this way acceleration is limited by max load value, when the mass is given by the almost empty second stage and the third stage.

A value of 380s has been selected in order to limit maximum acceleration to less than 5g for a third stage of 570kg, which permits significant performances of the launcher, even if payload mass increases. In this way, if third stage weight would be less or more of about 130 kg, loads would not change significantly. For best performances it would be needed to establish a variable burning time, which implies building a specific rocket for each mission. This is not possible and, once sized second stage, there are other parameters to work on to in order to obtain best results in terms of mass on circular orbit; these will be defined in chapter 5.

Required propellant mass has been calculated on the base of HM-7B characteristics, some of which reported in table 2.1:

firing time	380s
mass flow	14.82kg/s
mixture ratio	6:1
additional LH2 for nozzle cooling	6%
margin on residual propellant	1%

Table 2.1: Second stage:parameters for sizing

Therefore, cryogenic propellant masses contained in the second stage tanks are therefore:

	Mass kg
LOX	4875
LH2	861
total mass	5736

Table 2.2: Second stage:propellant sizing

The sizing of the tanks in terms of volume has to consider a larger value of propellant mass, in particular of LH2 for two main reasons:

- presence of gaseous hydrogen and oxygen during operations and flight, which tends to increase dramatically tank pressure
- cooling of propellant lines and maintaining hydrogen and oxygen in liquid state

Actually the latter can be provided by the carrier aircraft, during ground taxi and captive flight, with important modifications to the carrier, or , more simply, to the Aero-Module, allowing some mass reduction in terms of propellant, tanks and coatings.

Limiting to a conservative configuration additional 40kg of LH2 have been envisaged, estimating 1 hour for the operations on ground and 2 hours of flight at cruise altitude, with a thermal insulation on tanks, which leads to the the results reported in the table 2.3:

	Mass kg
LOX	4875
LH2	901

Table 2.3: Propellant used for tank sizing

The tank volumes are estimated on the base of these values and of the parameters reported in table 2.4:

LOX density	861 $kg/m^3$
LH2 density	5736 $kg/m^3$
margin on volume	5%

Table 2.4: Second stage: tanks parameters

the tank layout foresees the use of hemispherical tank caps as shown in figure 2.12:



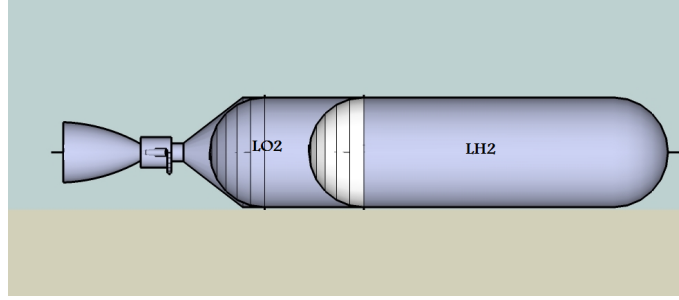


Figure 2.12: Second stage tanks layout

Remembering that launcher diameter is driven by Z9 engine of 1.9 m, and assuming a 25 mm thermal insulation thickness, the useful diameter decreases to 1.85m and the encumbrance of tanks results in table 2.5:

	Volume [ $m^3$ ]	Length [m]
LO2 tank	4.5	1.68
LH2 tank	13.36	5.64
Overall	17.86	7.32

Table 2.5: Second stage:tanks parameters

Eventually tanks mass for cylindrical vessel with hemispherical ends can be evaluated using the following formulas (see [7]):

$$P_b = k_{safety} M E O P \quad (2.1)$$

$$t = \frac{P_b R}{F_{tu}} \quad (2.2)$$

$$M = A \cdot t \cdot \rho \quad (2.3)$$

where

- $P_b(Pa)$  is the burst pressure of tank multiple of the maximum operating pressure ,
- $k_{safety}(-)$  is the margin of safety,
- $F_{tu}(Pa)$  is the tensile ultimate stress,
- $t(m)$  is the tank thickness,
- $R(m)$  is the radius,
- $M(kg)$  is the tank mass

### 2.3. MASS BUDGET AND SIZING

---

- $\rho(kg/m^3)$  is the material density, and
- $A(m^2)$  is the total area.

For spherical shape tanks the mass is given by:

$$M = \frac{3}{2}PV \frac{\rho}{F_{tu}} \quad (2.4)$$

where  $V(m^3)$  is the tank volume.

Metallic tank has been considered<sup>1</sup> with characteristics shown in table 2.6.

Material	$\rho[kg/m^3]$	$F_{tu}[GPa]$
Aluminum 2091	2780	0.441
Titanium	4429	1.103

Table 2.6: Material physical characteristics

Furthermore parametric formulas are applicable to tanks for space applications, based on volume, *MEOP* and tank typology in the form of (refer to [8]):

$$M = V \cdot MEOP / K_{type} \quad (2.5)$$

These formulas come from the application of a statistical approach to the problem, and the constant  $K_{type}(-)$  is given in terms of standard deviation in table 2.7:

Type of tank	Range ( $\pm 1s$ )( $m^2/s^2$ ) · 10 <sup>4</sup>	Range ( $\pm 2s$ )( $m^2/s^2$ ) · 10 <sup>4</sup>
Diaphragm	1.53 - 2.97	0.81 - 3.69
Surface Tension	2.28 - 4.36	1.24 - 5.40
No Propellant Management Device	3.41 - 4.71	2.76 - 5.36

Table 2.7: Constant  $K_{type}$  for liquid propellant

It can be seen that the results fall in a large range of values, depending on the type of tank and trust level. Eventually mass is obtained as shown in table 2.8:

	LO2 tank	LH2 tank
Analytical approach	63kg	152kg
Statistical approach	57kg	134kg

Table 2.8: Mass tanks

---

<sup>1</sup>this choice together with margin is very conservative with respect to composite material.

where for the second approach diaphragm tanks have been considered with a conservative value of  $K_{type} = 2.4$ . The first results have been held because it represents the worst case.

Liquid propulsion system needs a pressure fed system. There are two types of fed system:

1. pressure-regulated system supplying constant or nearly constant tank pressure, hence constant pressure to the engine throughout the engine firing time;
2. blowdown system - this is simpler, has few parts in design and usually weighs less than the regulated system, but tank pressure and thrust continuously drop during the firing timeline.

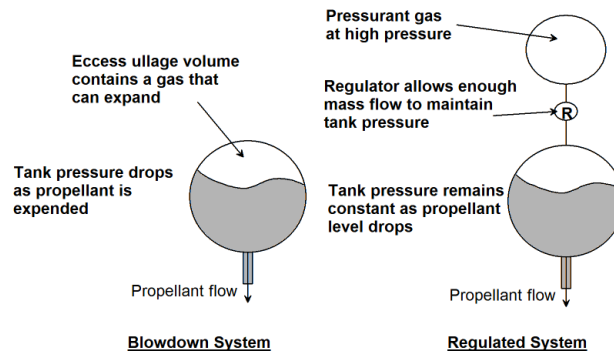


Figure 2.13: Pressure regulated vs blowdown system

In order to get maximum performances the first kind has been chosen<sup>2</sup>. The most popular pressurant gas is helium because it is inert and lightweight. An alternative is nitrogen, or hydrogen for only LH2, or oxygen for LO2. The use of nitrogen implies more mass, meanwhile hydrogen and oxygen require two different store tanks with the same result. For this reason helium pressurant mass and tank have been sized by applying the following formula which assumes isentropic temperature change:

$$T_f = T_i \left( \frac{P_f}{P_i} \right)^{\frac{\gamma-1}{\gamma}} \quad (2.6)$$

where

- $T(K)$  is the temperature

---

<sup>2</sup>it is a compelled choice because of the HM-7B with constant thrust

- $P(Pa)$  is the pressure
- $\gamma$  is the isentropic parameter of the gas.

considering that subscript  $i$  and  $f$  refer to the initial condition in pressurant tank and the final condition in pressurized tanks. The pressurant mass is then given by (see [9]):

$$m_g = \frac{P_t V_t}{R_g T_g} \left( \frac{\gamma}{1 - \frac{P_t}{P_g}} \right) \quad (2.7)$$

where

- $m_g(kg)$  is the gas pressurant mass,
- $R_g(J/kg \cdot K)$  is the gas constant,
- $T_{g-t}(K)$  is the temperature respectively in the pressurant tank and in the propellant tank,
- $P_{g-t}(Pa)$  is the pressure respectively in the pressurant tank and in the propellant tank,

Usually the typical initial pressure is about 200 bar, lower helium mass is obtained for higher temperature, which is assumed to be 290K. Pressurant tank could be a monolithic titanium tank but it would be weightier, and so a composite overwrapped pressure vessel has been selected and its main characteristics are reported in table 2.9:

Mass	Volume [ $m^3$ ]	Radius [ $m$ ]
14	0.42	0.465

Table 2.9: Second stage: pressurant gas sizing

### 2.3.2 Second stage mass budget

The empty mass of the second stage is very important for the performance of the launcher. Therefore a detailed sizing has been carried out. Table 2.10 reports the obtained results:

### 2.3. MASS BUDGET AND SIZING

Item	Mass [kg]	Remarks
LH2 tank	152	Sizing with nominal pressure 300000 Pa Safety factor 2, additional margin 50% Aluminum alloy 2019
LO2 tank	63	Sizing with nominal pressure 220000Pa Safety factor 2, additional margin 50% Aluminum alloy 2019
Helium tank	18	Sizing with 200bar, titanium alloy
Helium	14	
Thermal insulation	50	density $50kg/m^3$ , 25mm thick
Structural item	128	Thrust cone, lower ring, upper ring, fairing I/F, 3rd stage I/F
HM-7B engine	165	actual datum
TVC system	20	
Separation system	35	Mass pertaining to 2nd stage of separation system with fairing, 1st stage, 3rd stage. It includes batteries and electronic units
Roll control system	20	
Range safety unit	10	
Total	678	
Margins	101	20% on total mass, excluding HM-7B engine mass
<b>Empty mass</b>	<b>775</b>	Rounding in excess

Table 2.10: Second stage mass budget

The empty weight represents about the 12 per cent of the second stage gross mass that is slightly higher than similar launcher where this value is 10 per cent. In this way it is confirmed the correctness of the conservative assumptions.

#### 2.3.3 Third stage mass budget

Third stage is accommodated above the second stage through a conical adapter, which is part of the second stage:

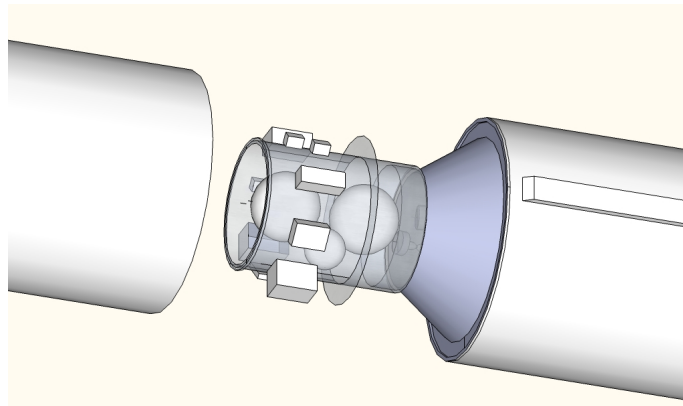


Figure 2.14: Third stage: installation on the launcher

On the left of the figure 2.14 the fairing is shown in order to highlight the interface with only the second stage on the top of its outer ring. The configuration results in a very compact third stage. In this way it has not to carry loads deriving from vibrations of fairing. Furthermore it is not required an interstage, and shocks loads on the payload caused by fairing separation are damped out by the long structural path.

The mass estimation is the result of an iteration process between stage sizing, where the stage definition depends on the propellant mass to be embarked, and performance analysis.

The sizing of the two propellant tanks and helium pressurant tank starts from the identification of the maximum difference of speed to be impressed by the third stage. From this point of view the most demanding mission concerns the launch into higher SSO orbits: a 2000km limit has been assumed. Limiting to a 2000km circular orbit and to an overall mass of 570 kg for third stage, some considerations can be done concerning the speed required and the propellant masses. Tsiolkovsky's formula has been used to calculate the propellant mass required to perform speed variation, given initial mass and specific impulse of the engine (see [10]):

$$m_{required} = M_{initial} \cdot \left( 1 - \exp \left( -\frac{\Delta v}{I_{sp}g} \right) \right) \quad (2.8)$$

where

- $m_{required}(kg)$  is the required mass for manoeuvre,
- $M_{initial}(kg)$  is the initial mass of the system,
- $\Delta v(m/s)$  is the speed variation in the manoeuvre,
- $I_{sp}(s)$  is the specific impulse,

### 2.3. MASS BUDGET AND SIZING

---

- $g(m/s^2) = 9.81m/s^2$  is the reference gravity acceleration.

Table 2.11 reports the propellant that has been calculated for a 570kg third stage:

Manoeuvre	$\Delta v$	Propellant mass	Elements involved
First ignition	525 m/s	89 kg	Assembly 3rd stage+ P/L
Orbital insertion	445 m/s	65 kg	Assembly 3rd stage+ P/L
CAM	40 m/s	5 kg	Part with P/L, part only 3rd stage
De-orbit to 400km perigee	375 m/s	22 kg	Only 3rd stage
<b>Total</b>		<b>181 kg</b>	

Table 2.11: Third stage: maximum propellant required for 2000 km SSO

On this base tank sizing and mass budget has been determined, assuming:

- 10% margin on mass,
- two equal tanks for  $N_2O_4$  and MMH at 17 bar nominal pressure,
- a helium pressurant tank at 170bar,
- spherical tanks in titanium,

Under these assumptions, a simple linear law has been derived on the base of available data from past experience and used to estimate the overall mass of three tanks (see [8]):

$$M_{tank} = 0.11 \times M_{propellant}$$

and  $M_{propellant}(kg)$  is the propellant mass. Thus:

$$M_{tank} = 0.11 \times 181kg = 20kg$$

which includes helium needed. Table 2.12 shows the computed tanks sizes:

	MMH	$N_2O_4$	Helium
Diameter	560mm	560mm	320mm or $2 \times 250mm$
Mass	20kg		

Table 2.12: Third stage: tanks sizing and mass estimation

When defining the mass of third stage for the purpose of performance analysis, the propellant to be used for manoeuvring and for de-orbit is not available for first and

second ignition purpose, but have to be carried anyway. This does not forbid to use in particular cases part of that allocated for de-orbit once third stage reaches an altitude lower than 2000 km.

Propellant stored for de-orbiting depends on the specific mission. A simplified, conservative linear model has been used for this purpose:

$$M_{deorbit} = 0.011 \times H_{circularorbit}$$

where  $H(km)$  represents the altitude from ground of the initial circular orbit.

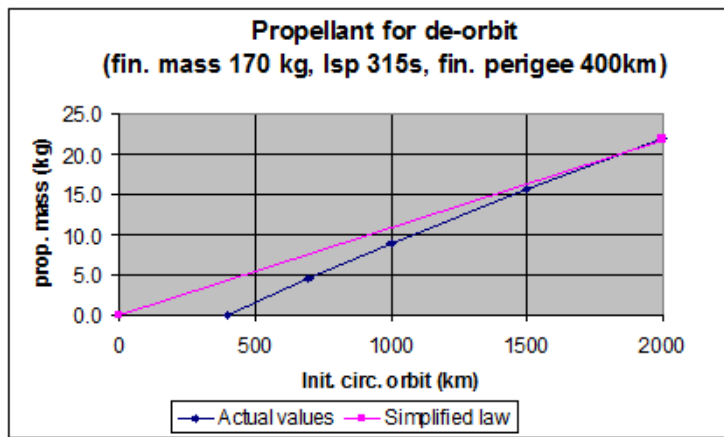


Figure 2.15: Propellant for de-orbiting

Other equipment and items have been estimated as a fraction of the mass of the propulsion system. They are the following::

- battery and power distribution unit
- inertial measurement unit
- on board computer
- data acquisition/ drive electronics
- separation control unit
- telemetry unit
- harness

Finally mass estimation can be resumed in the next table:



Item	Mass [kg]	Item	Mass [kg]
Propellant tanks	20.0	Structure	22
Engines (2)	7.2	P/L interface ring	18
Piping, valves etc.	6	Attitude control system	15
<b>Total prop system</b>	33.2	Avionics	60
		<b>Total non prop. systems</b>	115
<b>Total dry mass</b>		<b>20kg</b>	
Manoeuver/de-orbit propellant		$5 + 0.011H_{circularorbit}$ kg	
Total		$153 + 0.011H_{circularorbit}$ kg	
<b>Total with 25% margin</b>		<b><math>191 + 0.011H_{circularorbit}</math> kg</b>	

Table 2.13: Third stage: mass budget

Table 2.13 highlights the use of noticeable margin during sizing and mass estimation which takes in account all the uncertainties about the system.

### 2.3.4 Interstage and fairing design

The interstage between first and second stage is a careful element which has to undertake axial, lateral and random loads without deformations that could cause the structure collapse.

Stresses acting on fairing cross section are given by:

$$\sigma = \frac{F}{A} + \frac{M}{I}r \quad (2.9)$$

where

- $I(kg \cdot m^2)$  is the inertial momentum about the section,
- $A(m^2)$  is the cross section area,
- $M(Nm)$  is the momentum applied, and
- $r(m)$  represents the distance from the neutral axis (coincident with the centre of the annular ring that is the cross section).

The thickness and so the interstage mass is computed when the stress is equal to the yield stress of aluminum. Table 2.14 reports the structure sizing, using a margin of safety of 2 on forces with a margin of 25% on the result:

Thickness [mm]	Length [m]	Mass [kg]
2.5	3.2	170

Table 2.14: Interstage mass estimation

The fairing mass has been derived on the base of other launchers data. As reference the mass and scale factor of the Vega launcher have been used, and it has been chosen as fairing surface the one of a cylinder with the same diameter and length:

$$M_f = M_{ref} \cdot \frac{A_f}{A_{ref}} \quad (2.10)$$

where

- $M(kg)$  is the fairing mass,
- $M_{ref}(kg)$  is the reference fairing mass,
- $A_f(m^2)$  is the fairing area,
- $A_{ref}(m^2)$  is the reference fairing area.

Applying a 20% of margin, fairing mass is obtained:

	Diameter [m]	Length [m]	Mass [kg]
Vega	2.66	7.88	490
ALL-V	1.9	5.115	196

Table 2.15: Fairing mass estimation

## 2.4 Complete rocket configuration

The launcher CoG position along the longitudinal axis has been calculated on the base of the mass budget and of the given system geometries:

## 2.4. COMPLETE ROCKET CONFIGURATION

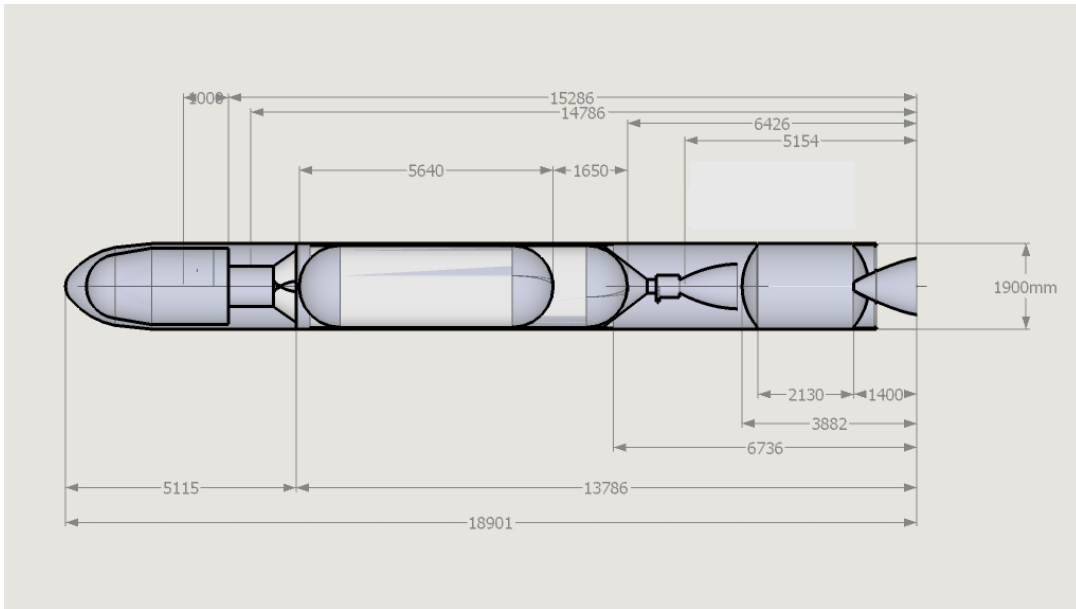


Figure 2.16: Dimension for CoG estimation

Item	Mass [kg]	CoG [mm]
2nd structure	213.6	10071
Z9 prop	10115	2465
Z9 empty	835	2250
I/S 1-2	170	5154
LOX	4875	7251
LH2	901	10896
2nd stage engine	165	5114
LH2 Tank	183.6	10896
LO2 tanks	74.4	7251
He+devices	82	13600
3rd stage	270	14786
Fairing	200	17708
Payload	300	16286
<b>Rocket</b>	<b>18385</b>	<b>5000.06</b>

Table 2.16: Elements mass and CoG with complete mass budget

Considering to some extent uncertainties and minor adaptations of some dimensions, the CoG position range is with respect to the launcher base:

$$5000 - 5025\text{mm}$$

#### 2.4. COMPLETE ROCKET CONFIGURATION

---

Furthermore third stage mass and assembly have great influence on the CoG with severe consequences on the separation manoeuvre. Considering variable payload from 150 to 400 kg, CoG varies considerably in the following range:

$$4900 - 5100mm$$

The CoG longitudinal position is important for the investigations on the separation manoeuvre, as the aerodynamic stability characteristics of the system have to be defined on the base of such position. Thus it is important to arrange payload in order to reduce CoG displacements.

## Chapter 3

# Atmospheric configuration design

The definition of aerodynamic characteristics of the rocket and the aerodynamic module, which has the task of giving the rocket favorable initial conditions leaving safe the carrier aircraft, it is essential to assess system performances.

Before the launcher first stage engine ignites, the launcher has to separate from the carrier. For a captive on top air-launch, this operation would not be possible without the Aero-Module. As it can be seen in fig.3.1 the Aero-Module is basically a plane. Its wing provides lift for a pull-up maneuver after release from the carrier; a horizontal stabilizer gives pitch stabilization and a vertical fin is used for directional stability.

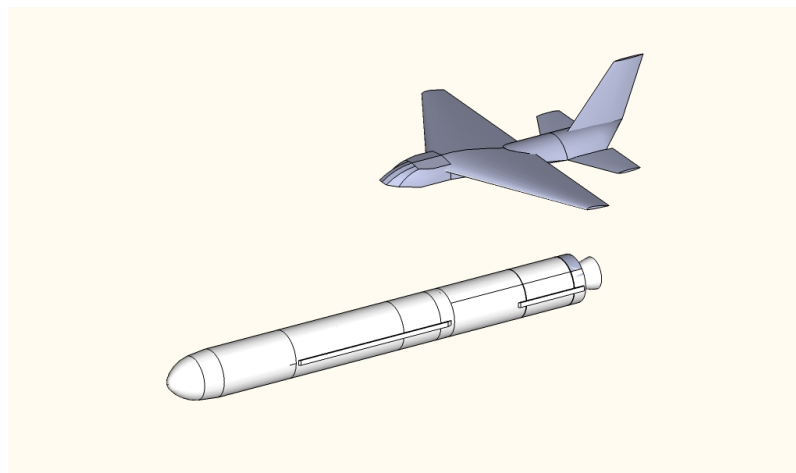


Figure 3.1: The Aero-Module

Flight in close proximity of a plane represents a critical point because the aerodynamic turbulence can produce an interference that, in the worst case, can produce the collision and the loss of the mission.

For what concerns the Aero-Module, it has been assumed to be a passive element able to pull-up the launcher without control surfaces, notwithstanding the awareness of the need for a possible control system, because the aim was to proof the conceptual feasibility of the separation manoeuvre. Some requirements have driven the definition of the Aero-Module, which has not been dimensioned.

Moreover, this chapter deals with the choice of a suitable carrier plane able to perform the separation manoeuvre at high altitude and accommodate the Aero-Module and launcher.

## 3.1 Launcher and Aero-Module

A preliminary aerodynamic definition of the launcher has been performed in order to evaluate and investigate the separation manoeuvre in a simple but meaningful way.

In order to implement the separation approach outlined in the chapter 4, the following configuration has been identified and, following a first definition iteration, the conceptual feasibility of the separation maneuver has been demonstrated. An Aero-Module is foreseen, mounted on the rear part of the launcher. This Aero-Module is used only during the phase that starts with the release from the aircraft to first stage ignition; just before the first stage ignition when the Aero-Module is separated from the launcher. The Aero-module is conceived basically as a structural item, passive, with no moving control surface. In order not to modify existing items (e.g., the Z9 stage), it is mechanically fixed to the interstage element and to a ring mounted at the base of first stage case. The launcher in itself is essentially a cylindrical body with a nose. The nose shape has some influence of the position of the center of pressure (CP), a conical nose providing a CP slightly more rearward than a rounded nose. After separation of the Aero-module, the attitude control (pitch, yaw) is performed by the TVC.

A wing is required to provide the lift for performing the pull-up maneuver following separation from the aircraft.

The aerodynamic configuration has been trimmed in such a way to perform the separation maneuver without the need for movable control surfaces.

The aerodynamic definition has many goals:

1. to grant a meaningful initial speed to the launcher at least a 100m/s vertical component at 12000m altitude;
2. to limit the maximum load during pull-up less than 3-g; the system has to naturally

tend toward angles of attack (AoA) able to provide the desired lift;

3. to provide a condition corresponding to slightly more 1-g normal load for the wing at the speed,  $v_{release}$ , and altitude,  $h_{release}$  of interest, at the beginning of the pull-up manoeuvre; this makes the manoeuvre fast, reducing the possibility for the Aero-Module to collide with the carrier.

The maximum value of loads has been set in order to limit the transversal load applied to the payload and to the Aero-Module wing (usually for wing the maximum value is 2.5 g; an upper limit higher implies to strengthen the wing).

Furthermore, the aerodynamic configuration must be stable in pitch, because oscillations could reduce the altitude reached by the Aero-Module and launcher and could be dangerous for the carrier aircraft. Pitch time response shall be such to be compatible with the overall separation maneuver duration from release to ignition. Two aspects should be considered in this case:

1. the pitch response must also be such that the pull-up maneuver, with the increase of AoA and g-level during the maneuver itself, is performed in a suitable time frame to get the desired initial conditions for ignition; a fast response time would increase g-levels and pitch oscillations would occur before the desired conditions are obtained; a slow pitch response time implies larger velocity losses, making less effective the manoeuvre.
2. at release and just after it, it would be beneficial not to have a large normal load factor (a value between 1 and 1.5 g could be adequate), in order to reduce aerodynamic effects on the A/C fin; this would also help in the accommodation of the launch vehicle on the A/C, as the relative angle of the launcher with respect to the A/C at separation could be smaller, simplifying accommodation and reducing cruise drag.

Some elements has assumed in order to estimate the aerodynamic configuration, because there are more variables than available equations:

1. the  $C_{l_\alpha}$  for both wing and tail
2. linear variation of the lift coefficient
3. drag coefficient as a fraction of  $C_{l0}$

4. zero-lift corresponding to 0 deg. of AoA
5. the aspect ratio for both wing and tail

Summarizing the method used for identify a proper launch configuration, which will be well explained in chapter 4:

1. from the desired lift at equilibrium, a required AoA for the wing is obtained (desired lift corresponding to 1-g) by vertical equilibrium

$$M_{launcher+Aero-Module} = 0.5\rho v_{release}^2 S_{wing} \cdot C_{l_\alpha} AoA;$$

2. from the desired pitch oscillation frequency, the proper position of the tail and of the wing are obtained (the investigations led to a satisfactory pitch oscillation frequency of 0.05 Hz, 20s period) by

$$I_{launcher+Aero-Module}/f_{configuration}, C_l, C_d = \omega^2;$$

3. then, from the equilibrium to pitch rotation at 100m/s, the setting of the tail pitch (the fixed angle of the horizontal surface 0-lift line with respect to the wing 0-lift line) is identified by momentum equilibrium  $f(configuration, C_l, C_d, AoA, tailpitch) = 0$ .

A first configuration of the wing has been defined as it results in table 3.1:

Span	Surface	Aspect ratio	$C_{l_\alpha}$
12 m	31 $m^2$	4.5	0.12deg <sup>-1</sup>

Table 3.1: The Aero-Module: wing characteristics

From the stability point of view, the center of pressure of the launcher body is located well in front of the launcher center of gravity (CoG), which, because of the relatively heavy first stage, is placed rearward at about 5000 mm from the nozzle base. Therefore some tail surfaces have to be introduced to provide a stable system in pitch and yaw. The top view of the launcher with the Aero-Module is shown in figure 3.2.



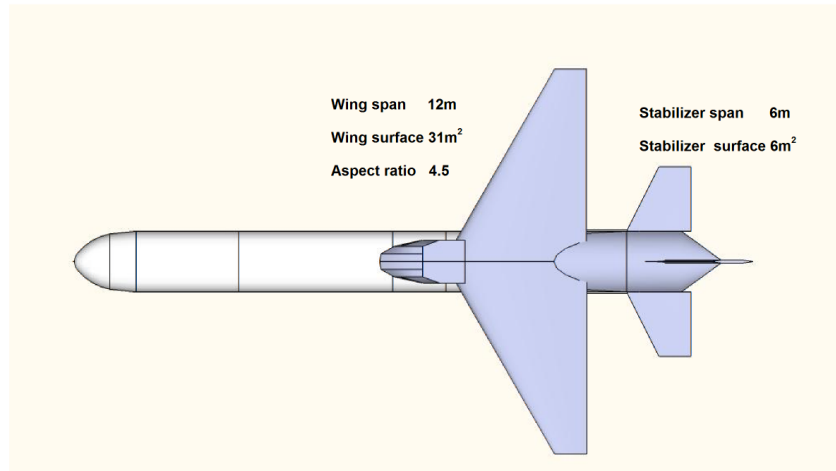


Figure 3.2: Top view of the launcher with Aero-Module

The investigations has led to horizontal surfaces with the general layout shown in figure 3.2:

Surface	$C_{l_\alpha}$
$6 m^2$	$0.12deg^{-1}$

Table 3.2: The Aero-Module: stabilizer characteristics

The above aspects are inter-related, but following very few iterations a solution is found, as reported in table 3.3:

AoA to provide 1-g lift	6.5deg
Arm of the horizontal surface lift wrt CoG	4.3 m (geometrically defined)
Arm of the body-wing lift wrt CoG	0.73 m in front of CoG
Horizontal surface pitch setting	1.8deg

Table 3.3: The Aero-Module: trimming and centers of pressure

Figure 3.3 shows the position of those significant points:

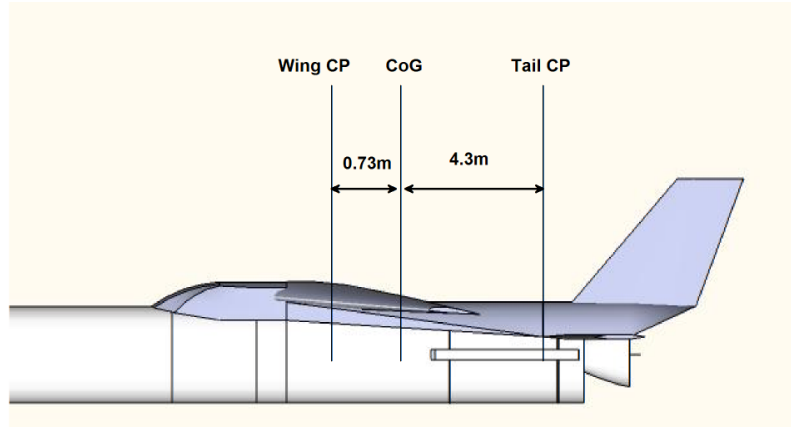


Figure 3.3: Centers of pressure position

Altitude an initial velocity has been assumed, while pitch moment has been calculated after the mass budget. Those results are reported in table 3.4:

Altitude:	≈ 11000 m
Velocity:	240 m/s
Pitch Moment of inertia about CoG:	500000kgm <sup>2</sup>

Table 3.4: Assumptions for trimming

Although the Aero-Module sizing is not the main objective of this work, mass has been estimated by using statistical approach for transportation system (refer to chapter 4 of [11]), doing some assumptions, because this value is necessary for the release manoeuvre:

- the wing mass

$$M_{wing} = 0.0667 * M_{dry} (b / \cos \Lambda_{1/2})^{0.75} (1 + (1.905 \cos \Lambda_{1/2} / b)^{0.5}) (n_{ult})^{0.55} \left( \frac{b / \cos \Lambda_{1/2} / t_r}{M_{dry} / S_{wing}} \right) \quad (3.1)$$

- $M_{wing}$  is the wing mass
- $M_{dry}$  (kg) is the dry mass of the system, estimated as 300kg
- $\Lambda_{1/2}$  (deg) is the sweep angle at 50% of the chord, assumed 45degrees,
- $b$  (m) wing span,
- $S_{wing}$  (m<sup>2</sup>) is the wing surface,
- $t_r$  (m) is the root thickness, assumed 0.3m (similar to Pegasus value)
- $n_{ult}$  is a contingency factor, here assumed very conservatively as equal to 4;

- the tail horizontal surface mass

$$M_h = S_h \left( 0.05836 \left( \frac{S_h^{0.2} v_d}{\cos \Lambda_h} \right) - 1.41 \right) \quad (3.2)$$

- $M_h$  is the tail horizontal surface mass
- $S_h(m^2)$  is the tail horizontal surface,
- $v_d(m)$  would be the dive speed, here assumed as the maximum speed at separation (i.e. 240m/s)
- $\Lambda_h(deg)$  is the sweep angle at 50% of the chord, assumed 45degrees,

- the tail vertical surface mass

$$M_v = S_v \left( 0.05836 \left( \frac{S_v^{0.2} v_d}{\cos \Lambda_v} \right) - 1.41 \right) \quad (3.3)$$

- $M_v$  is tail vertical surface mass
- $S_v(m^2)$  is the vertical surface, assumed as  $5m^2$
- $v_d(m)$  would be the dive speed, here assumed as the maximum speed at separation (i.e. 240m/s)
- $\Lambda_v(deg)$  is the sweep angle at 50% of the chord, assumed 45degrees,

- fuselage mass

$$M_F = 0.23 \left( v_d \frac{l_T}{b_F + h_F} \right)^{0.5} S_G \quad (3.4)$$

- $M_F(kg)$  is the fuselage mass
- $l_T(m)$  is the length of the fuselage between the 25% of the wing and the 25% of the tail, about 5m
- $b_F(m)$  is the fuselage maximum width, about 2m
- $h_F(m)$  is the fuselage maximum height, assumed 1.2m
- $S_G(m^2)$  is the fuselage total surface, calculated by  $\pi b_F l_T$

Table 3.5 reports the mass breakdown and total mass of the Aero-Module:

Element	Mass [kg]
Wing	360
Tail horizontal surface	236
Tail vertical surface	92
Fuselage	120
Aero-Module+20%margin	995

Table 3.5: Aero-Module mass breakdown

Margin has been used for considering the attachment point on the launcher and separation system.

## 3.2 Carrier Aircraft

The choice of a plane which allows to perform certain manoeuvres during the release of the assembly represented by the launcher plus the Aero-Module is difficult because many aspects have to be considered, first of all the cost of the plane and its possibly required modifications to support the launcher.

As it has been mentioned in section 1.4, captive on top air-launch has been chosen to assure a safe release and mainly to reduce modifications for a captive on bottom air-launch. In fact the latter requires either a safety clearance between fuselage and ground at take-off or a robust and large wing to maintain the rocket attached. Both solutions are likely to require either a big airplane or a great deal of structural and aerodynamic corrections, which entail major costs.

### 3.2.1 Selection of aircraft types

An aircraft suitable for acting as a carrier has been identified in the class of the Airbus A330. Also the Airbus A300 could be useful for air-launch (see [12] and [13]). Larger aircraft such as the A340 and A380 could also accommodate the launcher, but would be expensive to acquire, modify and operate.

Other aircraft could be considered, for example Boeing airliners of the same category of A300 and A330, or other large transport aircraft. The Airbus solution has been preferred in order to deal only with European industry.

The A330-200 version is the basic configuration used for A330 military configuration in service as air-refueling tanker, MRTT, Multi-Role Tanker Transport, in UK and other non-European countries.

MRTT is likely to enter into service in other European air forces in next years.

The possibility to adapt one or more of these aircrafts as launcher carrier while retaining the air-refueling capabilities is considered as a viable concept: the aircraft would be normally used for its military missions; whenever a launch mission is in view, it would be reconfigured to the carrier configuration in few days and after having performed the launch it would be returned to its military service.

### 3.2. CARRIER AIRCRAFT

---

This solution would allow to dramatically reduce recurring costs related to carrier operations from the launch cost point of view. This is even more important when a low launch rate is envisaged, especially in the first year of operations. Furthermore non-recurring costs related to the acquisition of the plane would take advantage of this approach.

The viability of this approach is outside the scope of the study and would depends on political and strategic aspects.

However it highlights the general idea of using the airplane also for other missions, sharing acquisition and operating costs with other users.

Another possibility in line with this concept is to use the ESA/CNES A300 Zero-g (fig. 3.4):



(a)

(b)

Figure 3.4: ESA/CNES A300 Zero-g and Airbus A330-200

it is about 5m shorter than the A300-200 but it can work as well as A300-200.

By properly adapting the plane to carry and release the launcher, it could be used for both functions: parabolic flight and launch missions.

Table 3.6 shows the main characteristics and performances of the identified aircrafts types. For A330-200 data are relevant to freighter version, A330-200F, which should be very closer to the tanker configuration. For A300-B2(101), the smaller aircraft able to transport to a meaningful distance the launcher can be taken into account.

	<b>A330-200F</b>	<b>A300-B2(101)</b>
Operating empty weight	109000 kg	86000kg
Max take-off weight	233000	137000
Max payload (structural limit)	63500	30500
Range with max payload	About 7000km	About 1600km
Range in a carrier configuration	More than 5000km	More than 1000km
Max altitude [m]	11253	13000
Max cruise speed	$M=0.86$	$M=0.82$
Max speed with launcher	$M > 0.80$	$M < 0.80$

Table 3.6: Characteristics and performances of candidate carrier aircrafts

The range in the carrier configuration has to be considered as the max distance from airport for launch, with the capability to return to base with fuel reserves.

#### 3.2.2 Modification to the carrier aircraft

The carrier aircraft has to be modified in order to carry and release the launcher. The sizing of this modifications has not been performed in this work because the work deals with the feasibility of the launch strategy and of the launcher vehicle. Nevertheless the type of interventions on the carrier has been studied because it is vital to the carrier requirements definition.

The piggyback installation allows to reduce such modifications with respect to an underbelly mounting. In fact, for the identified aircraft, the clearance between the fuselage and the ground is about 2.3 m for the A330-200.

Considering the 1.9 m diameter of the launcher and the additional encumbrance of the launcher wing, appendages and mounting structures, an underbelly position would require a recessed installation to have enough clearance during landing (with the launcher attached) and during rotation at take-off.

Such installation affects the pressurized structure of the fuselage and of the wing box resulting in a major modification of the plane, which would require a redesign of the fuselage/wing box, structural testing and expensive implementation of the modification and certification.

For the A330-200, it seems that the modification would not affect the landing gear wells; on the contrary on the A300-B2, the main landing gear would have to be repositioned.

The launcher fin dimensions would provide an additional problem for installation in an

underbelly.

Therefore the piggyback solution has been preferred, because it can be easier implemented on the aircraft.

Figure 3.5 shows the chosen accommodation layout on the Airbus A330-200:

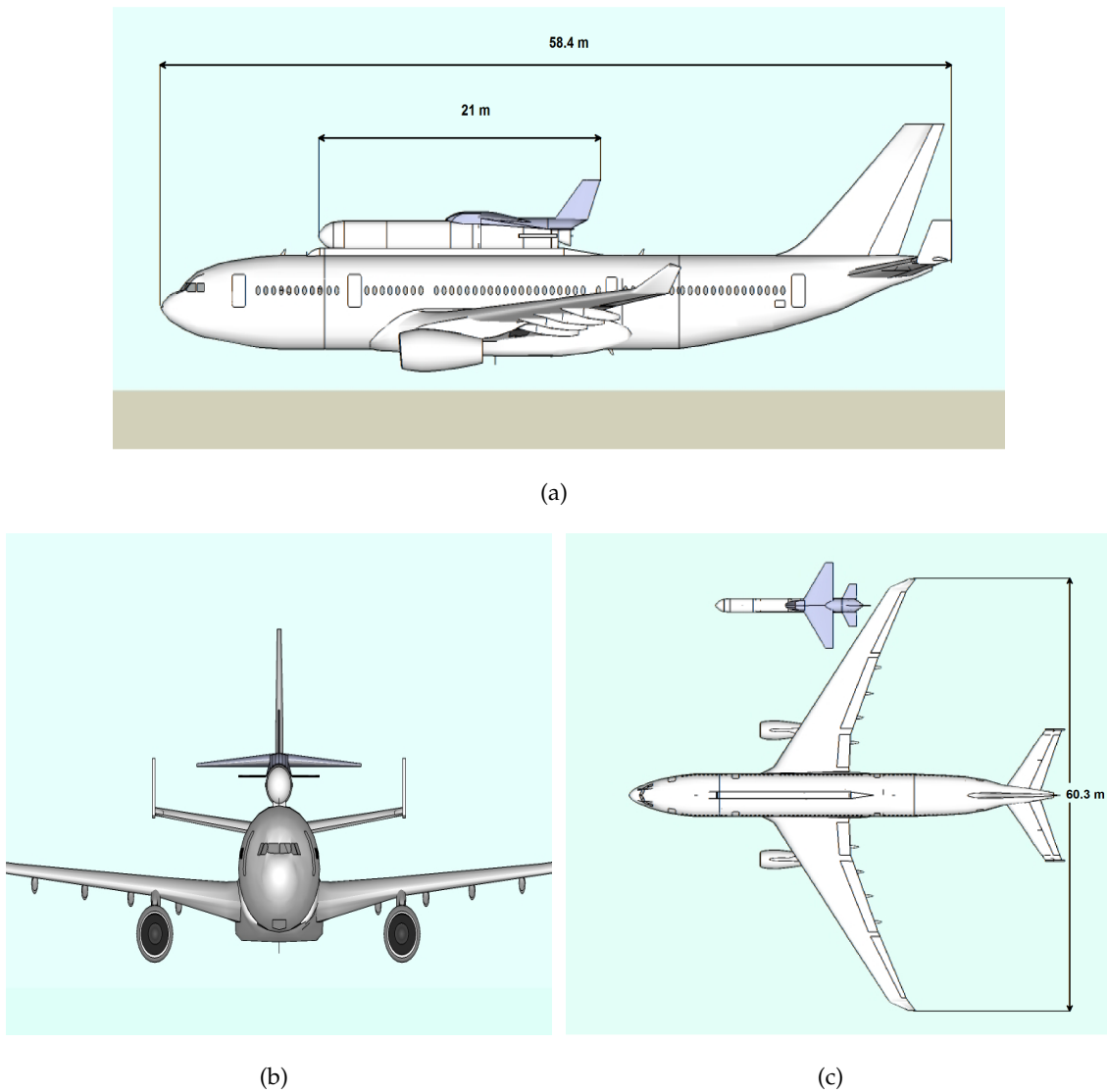


Figure 3.5: Accommodation of the Launcher on an Airbus A330-200

The conceptual allocation and general dimensions comparison for the launcher and the carrier displays that the launcher with the Aero-Module represents a third of the the airplane length.

Hereafter the main modifications to be introduced on the aircraft for transporting and releasing the launcher are preliminarily identified; these modifications are important but they can be considered of an order of magnitude less complicated than the ones described

for an underbelly mounting:

- Attachment points: the Launcher shall be attached at two points (see figure 3.6); the front point in correspondence of the upper part of second stage; the rear point at the rear of the first stage or at the interstage; a launcher erecting mechanism could be required at the front point.

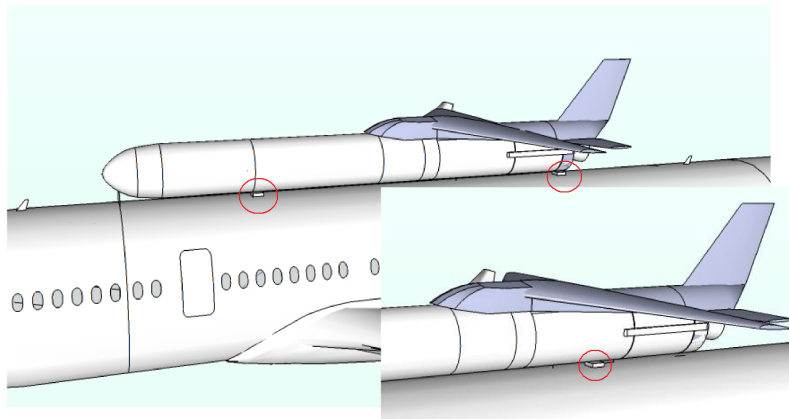


Figure 3.6: Position of connections to the A/C and alternative position at rear side

- Structure to carry the Launcher loads from the two attachment points to the wing box structure of the aircraft; a significant strengthening of the fuselage structure between the attachment points and the wing box will be required; this modification will be the most impacting in terms of weight on the aircraft. The structural modification could be implemented with high safety factors in order to reduce testing/certification requirements.
- Fairing structure between the Launcher and the A/C fuselage could have to be strengthened to reduce structure deformations which could damage the payload.
- Additional fins could be required to improve directional stability (if required); in fact the launcher body puts part of the A/C vertical stabilizer in its shadow; furthermore the launcher body in itself for its position on the aircraft could reduce to some extent directional stability. The solution for the additional fins could be the one used on the Beluga aircraft, the extensively-modified Airbus used for large volume transport:





Figure 3.7: Beluga aircraft with the additional fins

two fins have been installed at the tip of the horizontal stabilizer (see the two trapezoidal surface marked with a big 4 in fig. 3.7).

- A/C flight control software could be impacted in case the separation maneuver is performed in an automatic mode; also management of emergency/abort modes would also be impacted. Otherwise modification to A/C on-board software could be very limited.

All operations will be monitored by the launcher control station, which would provide the following functions:

- keep the launcher under control and check it until separation from the aircraft;
- interface with the aircraft
- provide a telemetry link with the ground

Telemetry generally operates only in the microwave frequencies (S-band and above). It is needed to provide in-flight data flow to the launcher control station, and to monitor all the powered ascent phases. As reported in figure 3.8, during the first phases of flight till 150 km telemetry could be provided to the airplane, while in the following phases the data will be received by the ground station.

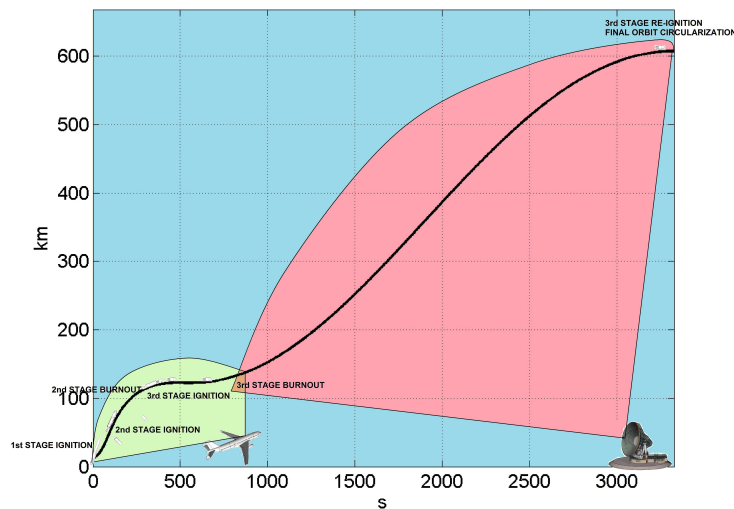


Figure 3.8: Telemetry reception system

The launcher when attached to the aircraft could require some services as:

- electrical power provided during the carrier flight especially for long range,
- payload bay conditioning,
- cryogenic fluid temperature control, needed for second stage
- launcher erection.

Those services shall be controlled by the launcher control station which will receive electrical power from the aircraft. Other equipment required for above services shall be part of the on-board launcher control station or shall be mounted outside the aircraft (e.g. conditioning equipment could be placed inside the A/C-launcher interface fairing, as well as erection driving system).

It has to be underlined that:

- no structural modification should be required to the wing, front fuselage, rear fuselage; horizontal stabilizers with vertical fins could be directly derived from the ones of the Beluga A/C;
- there would be not impact on landing gears (configuration, strength, operations);
- propulsion system, and other on-board systems, except electrical system and possible re-routing of lines in the mid fuselage, remain unchanged;

- avionics and on-board software undergo to minimal changes to take into account the presence of the launcher and its position with respect to the plane during the release.

With the exception of:

- the mid fuselage structural strengthening,
- the re-routing of lines (electrical, hydraulic, pneumatic,...) in the mid fuselage,
- all required interface provisions,

all other modifications could be introduced as a kit which is installed in preparation for the launch mission; this approach, as also said above, would provide a great flexibility of operations mainly when the launch rate is not so high to require a dedicated carrier A/C (10-12 launches per year). The kit would include mainly:

- the Launcher Control Station,
- the external fairing system, including various equipment,
- the two additional fins.

In this way the aircraft, whenever not used for the launch missions, would be reconfigured to a normal configuration, with the possibility to be used for its usual task, with the only impact of few thousands of kg of additional mass, but for the rest (aerodynamics, performance, operations etc.) unrestricted.

## Chapter 4

# Launcher dynamics: the release and ascent manoeuvres models

This chapter deals with the modeling of the launcher dynamics. The launch can be conceptually divided in two phases:

1. the release manoeuvre, which is a non propelled phase, during which the Aero-Module with the launcher leaves the carrier plane,
2. the ascent phase, that starts with the ignition of the first stage, when the Aero-Module is jettisoned from the launcher, and finishes with the third stage burn-out, when the payload reaches the target orbit.

After introducing the dynamics equation of both phases, the chapter will explain in detail the actions applied on the system during the launch.

Although the release manoeuvre is carried out first, the ascent phase, especially the initial condition on the first stage, imposes some requirements on how the first part of the launch has to be performed, in terms of initial state variable. For this reason, the launcher dynamics model of section 4.1 deals with those models, as they occur during the launch, but the launcher control law synthesis will be introduced first in order to set the requirements and expose the release strategies.

### 4.1 Launcher dynamics models

In both the release manoeuvre and the ascent phase, a 3 degrees of freedom model (dof) has been used. Actually this degrees of freedom are distributed in different modes:

1. in the release manoeuvre the body, represented by the Aero-Module and launcher, has two translational degrees of freedom in the local horizon vertical plane and it can moves only in this plane; moreover, the body can rotate around the axis normal to this plane, thus completing the number of dof;
2. during the ascent phase the body has been assumed as dimensionless, and so the body can moves in the 3D space.

Furthermore, for what concerns the release manoeuvre is important to estimate the relative position of the launcher with respect to the A/C. This one has been modeled as a 2dof, notwithstanding it can also perform articulated manoeuvres, which entail higher spatial gap between the launcher and the A/C.

#### 4.1.1 The release manoeuvre dynamics model

As introduced in section 4.1, a 3D model has been adopted, just representing the dynamics in the vertical plane, and only the translational dynamics has been represented for the A/C. It has been here assumed that the guidance for the rotational dynamics can be followed by the real A/C.

The launcher has two translational degrees and one rotational degree. Pitch rotations is a fundamental parameter that enters in the dynamics of the launcher to check for the manoeuvre feasibility.

The model for the separation studies uses the following general equations ( see [14]):

$$\frac{dv_x}{dt} = \frac{(F_{x_{wing}} + F_{x_{tail}})}{M_l} \quad (4.1)$$

$$\frac{dv_z}{dt} = \frac{(F_{z_{wing}} + F_{z_{tail}})}{M_l} \quad (4.2)$$

$$\frac{d^2\beta}{dt^2} = \frac{(\mathbf{F}_{wing} \times \mathbf{d}_{wing} + \mathbf{F}_{tail} \times \mathbf{d}_{tail})}{I_l} \quad (4.3)$$

where the momentum equation is given in baricentricral frame and

- $v_x(m/s)$  and  $v_z(m/s)$  are the speed components defined in a local horizontal reference system (figure 4.2)
- $M_l(kg)$  is the mass of the launcher and Aero-Module
- $\mathbf{F}_{wing}(N)$  and  $\mathbf{F}_{tail}(N)$  represent the overall forces acting respectively on the wing and the tail, sums of lift,  $L(N)$  and drag,  $D(N)$ , forces acting on wing and tail, including the gravitational action  $-M_l g$ ;

- $I(kg \cdot m^2)$  is the pitch moment of inertia of the launcher and Aero-Module;
- $\mathbf{d}_{wing}$  and  $\mathbf{d}_{tail}$  are the centers of pressure vector distances from CoG;
- $cd_0^{wing}$  is the shape drag coefficient which includes the contribution of that of the launcher scaled on the wing area;

Eqs.4.1 and 4.2 have been also exploited to describe the A/C dynamics.

Section 4.3 will explain in particular the aerodynamic forces, which represents the main components acting on the body, together with the gravity action (explained in section 4.4.1).

#### 4.1.2 The ascent phase dynamics model

Launcher motion can be described by the use of a simple three degrees of freedom approach. The launcher is assumed as a material point, with no dimension, subjected to drag, thrust and gravitation forces:

$$\frac{d\mathbf{v}}{dt} = \frac{1}{m} (\mathbf{T}-\mathbf{D}) - \mathbf{g} \quad (4.4)$$

which is a vectorial equation, where:

- $\mathbf{T}(N)$  is the engine thrust
- $\mathbf{D}(N)$  is the aerodynamic drag
- $\mathbf{g}(m/s^2)$  is the gravitational acceleration
- $m(kg)$  is the mass of the launcher

Two reference frame has been used:

1.  $[x, y, z]$  is the inertial frame where x-axis is represented by the nodal axis, i.e.the intersection between equatorial and orbital plane, z-axis points north and y-axis completes the right-handed frame
2.  $[x_p, y_p, z_p]$  is a local orbital plane frame, where  $x_p$  is the versor corresponding to on plane projection of vector distance from Earth centre,  $z_p$  is parallel to the normal to the plane  $\mathbf{n}$ , and  $y_p$  completes the right-handed frame

In order to set the initial state conditions in the inertial frame, some considerations have to be done:

1. the initial state vector for the propelled phase coincides with the final state condition of the release phase. The latter is formally given in the local reference frame to be coincident with the orbital reference frame;
2. for each orbital plane inclination,  $i(deg)$ , and launch latitude,  $Lat(deg)$ , there is a corresponding longitude,  $Long(deg)$  which descends from spherical geometric consideration; because launch latitude and longitude are fixed, this means only that there is a launch window that has no impact on analysis;
3. the launcher speed in the inertial frame is the sum of the initial condition expressed in the local frame and the contribution due to the Earth rotation.

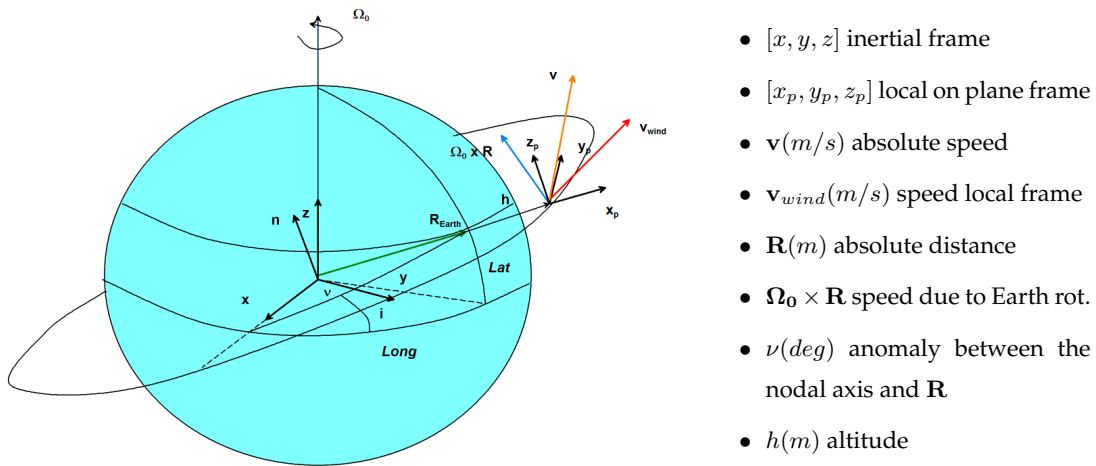


Figure 4.1: Initial condition

In this way:

$$\sin Long = \frac{\tan Lat}{\tan i} \quad (4.5)$$

$$\sin \nu = \frac{\sin Lat}{\sin i} \quad (4.6)$$

Given position and speed in local frame, the equivalent vectors  $v_{wind}(m/s)$  in the inertial frame result:

$$\mathbf{R} = A_{rot} \mathbf{R}_{local} \quad (4.7)$$

$$\mathbf{v}_{wind} = A_{rot} \mathbf{v}_{local} \quad (4.8)$$

where

- $A_{rot}$  is the rotational matrix necessary to pass from the local frame to the inertial

frame

$$A_{rot} = \begin{bmatrix} \cos \nu & \sin \nu \cos i & \sin \nu \sin i \\ -\sin \nu & \cos \nu \sin i & -\sin \nu \cos i \\ 0 & -\sin i & \cos i \end{bmatrix} \quad (4.9)$$

- $v_{local}(m/s)$  is the speed in the local horizon

Initial speed is then:

$$\mathbf{v} = \mathbf{v}_{wind}^0 + \boldsymbol{\Omega}_0 \times \mathbf{R} \quad (4.10)$$

where

- $\mathbf{v}(m/s)$  is the vector velocity in the inertial frame,
- $\mathbf{v}_{wind}^0$  is the initial speed in the local frame, coincident with the wind speed,
- $\boldsymbol{\Omega}_0(rad/s)$  is the Earth rotational speed and
- $\mathbf{R}$  is the absolute position.

Once the initial condition has been given in the inertial reference frame, all the other variable can be managed in this system, thus avoiding to calculate the rotation from the local to the inertial frame.

## 4.2 Atmospheric model

During the ascent the launcher passes through all the atmospheric layers. It is necessary to model all the significant atmospheric aspects that influence the launcher, since the external pressure affects the thrusters performances, as shown in section 4.4.3, and the density contributes to the aerodynamic drag, as described in section 4.4.2.

To take into account the variation of air thermodynamic characteristics, model 1976 Standard Atmosphere has been used because it is easy to introduce in the simulator tool developed (refer to [15]).

Temperature varies linearly with geopotential altitude:

$$h_{geo} = h \frac{R_{Earth}}{h + R_{Earth}} \quad (4.11)$$

$$T_e = T_k(h_{ref}) + L_h \cdot (h - h_{ref}) \quad (4.12)$$

where:



- $T_e(K)$  is the environmental temperature at the altitude  $h(km)$ ,
- $T_k(h_{ref})(K)$  is the reference temperature in Kelvin at  $h_{ref}$ ,
- $h(km)$  is the actual altitude,
- $h_{ref}(km)$  the reference altitude,
- $L_h(K/km)$  is the thermal lapse.

Defining  $v$  and  $\delta$  as the fraction of the reference pressure and temperature respectively,  $P_0(Pa)$  and  $T_0(K)$ , at sea level, pressure and density can be evaluated. If thermal lapse is equal to zero (for example between 11 and 20 km, see table 4.1):

$$v = P_{fraction} \exp\left(-GMR \frac{h - h_{ref}}{T_0}\right) \quad (4.13)$$

otherwise:

$$v = P_{fraction} (\delta)^{GMR/L_h} \quad (4.14)$$

where

- $GMR = 34.163195km/K$  is a constant
- $\delta(-)$  is the ratio  $T_e/T_0$
- $P_{fraction}(Pa)$  is pressure fraction in the altitude range between  $h_k$  and  $h_{k+1}$

Table 4.1 reports those significant constants:

$h_{ref}[km]$	$T_k(h_{ref}) [K]$	$L_h [K/km]$	$P_{fraction}$
0	288.150	-6.5	1
11	216.650	0.0	2.233611e-1
20	216.650	1	5.403295e-2
32	228.650	2.8	8.5666784e-3
47	270.650	0	1.0945601e-3
51	270.650	-2.8	6.6063531e-4
71	214.650	-2.0	3.9046834e-5
84	186.946	-2.0	3.68501e-6

Table 4.1: Temperature model coefficients

Then pressure and density result:

$$P_a = P_0 v \quad (4.15)$$

$$\rho = \rho_0 \frac{v}{\delta} \quad (4.16)$$

where:

- $P_a(Pa)$  is the environmental pressure used in eq. 4.26
- $\rho(kg/m^3)$  is the air density used in eq. 4.23 and in the aerodynamic forces definition of next section.

### 4.3 Aero-Module actions definition

A linear law for the lift coefficient and a parabolic law for the drag one has been adopted:

$$\mathbf{L}_{wing} = q \cdot S_{wing} \left( cl_0^{wing} + cl_{\alpha}^{wing} \cdot \alpha \right) \cdot [v_z \ v_x]/v \quad (4.17)$$

$$\mathbf{L}_{tail} = q \cdot S_{tail} \left( cl_0^{tail} + cl_{\alpha}^{tail}(\alpha + \alpha_t) \right) \cdot [v_z \ v_x]/v \quad (4.18)$$

$$\mathbf{D}_w = -q \cdot S_{wing} \left( cd_0^{wing} + \frac{k(cl_{wing})^2}{\pi \lambda} \right) \cdot [v_x \ v_z]/v \quad (4.19)$$

$$\mathbf{D}_t = -q \cdot S_{tail} \left( cd_0^{tail} + \frac{k(cl_{tail})^2}{\pi \lambda} \right) \cdot [v_x \ v_z]/v. \quad (4.20)$$

where

- $\mathbf{L}_{wing}(N)$  and  $\mathbf{L}_{tail}(N)$  are the wing and tail lift forces respectively;
- $\mathbf{D}_{wing}(N)$  and  $\mathbf{D}_{tail}(N)$  are the wing and tail drag forces respectively;
- $q(Pa) = \frac{1}{2}\rho v^2$  is the dynamic pressure;
- $v(m/s)$  is the speed norm;
- $\beta(rad)$  is the angle formed by launcher axis and the local horizon;
- $cl_0^{wing}(-), cl_0^{tail}(-)$  is the wing and tail lift coefficient at 0deg AoA;
- $cd_0^{tail}(-)$  is the tail shape drag coefficient;
- $cd_0^{wing}$  is the shape drag coefficient which includes the contribution of that of the launcher scaled on the wing area;
- $\alpha(deg)$  is the AoA.

The angle of attack  $\alpha$ , needed to have the aerodynamics actions completely known, can be derived :

$$\alpha = \beta - \arccos \frac{v_x}{v} \quad (4.21)$$

where the term  $\arccos \frac{v_x}{v}$  represents the flight path angle.

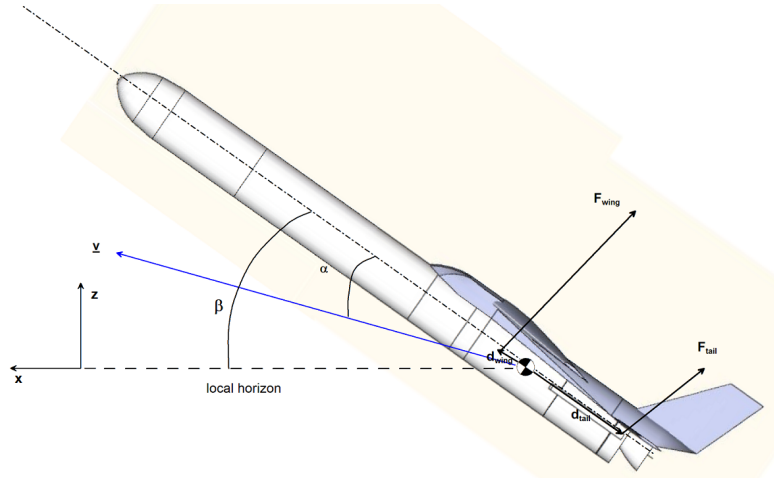


Figure 4.2: Aerodynamic system

Note that the aerodynamic interference between A/C and the Aero-Module has not been taken into account for this study.

#### 4.4 Launcher actions

The actions the launcher undergoes throughout the whole launch phases are:

1. gravitational force
2. aerodynamic force, i.e. the drag force (the lift components on the launcher has been neglected)
3. thrust, intended as magnitude since the vectorial definition in the different ascent phases are discussed in section 4.5

Each of them needs to be modeled to settle the dynamics equations and eventually define the control strategy. In the followings selected models are introduced.

#### 4.4.1 Gravitational force model

Gravitational force, expressed as acceleration, varies with altitude:

$$\mathbf{g} = -\frac{\mu}{R^3}\mathbf{R} \quad (4.22)$$

where  $\mathbf{R}(m)$  is the vector distance from Earth center. This simple model has been assumed since the ascent phase for first and second stages lasts less than 9 minutes, and gravitational perturbations effects would not be appreciable.

#### 4.4.2 Aerodynamic drag model

Aerodynamic drag is obtained by classical relationship:

$$\mathbf{D} = \frac{1}{2}\rho C_d S v_{wind} \mathbf{v}_{wind} \quad (4.23)$$

where

- $C_d(-)$  is the drag coefficient,
- $S(m^2)$  is the cross section area,
- $\mathbf{v}_{wind}(m/s)$  is the vector speed with respect to Earth and is defined by manipulating eq.4.10:

$$\mathbf{v}_{wind} = \mathbf{v} - \boldsymbol{\Omega}_0 \times \mathbf{R} \quad (4.24)$$

- $v_{wind}(m/s)$  is the speed norm of  $\mathbf{v}_{wind}$ .

In fact wind has been assumed to move rigidly with ground.

#### 4.4.3 Thrust model

Available thrust, in terms of magnitude, is less than the nominal one described in paragraph 2.2, mainly for first stage. Thrust profile is given in terms of operation in vacuum. Actual conditions must take into account the pressure conditions at the exit section of the thruster which depends on nozzle dimension and chamber pressure and temperature. The general expression of thrust is reported below (refer to [10]):

$$T = \frac{dm_f}{dt} u_{exit} + (P_e - P_a) \cdot A_e \quad (4.25)$$

where:

- $T(N)$  is the thrust norm,
- $\frac{dm_f}{dt} (kg/s)$  is the mass flow rate of the exhausted gases,
- $P_a(Pa)$  is atmospheric pressure at the current altitude,
- $A_e(m^2)$  is the nozzle exit section.

This expression can be manipulated, to highlight known elements:

$$T = \frac{dm_f}{dt} u_{exit} + P_e A_e - P_a A_e = T_{vacuum} - P_a(h) \cdot A_e \quad (4.26)$$

This represents a simple way of proceeding, because nozzle works in conditions different from those of project, and other effects can spring, such as shock waves which worsen the overall nozzle performances<sup>1</sup>.

## 4.5 Control law synthesis

The launcher ascent has been split into three sequential phases, according to each stage ignition; the adopted philosophy within each phase is hereinafter reported:

1. first stage lifts up with a gravity turn manoeuvre, i.e. no control over path angle is actuated, except for that performed in order to put the launcher on the orbital plane; this is the usual procedure also for ground launcher if no orbital manoeuvre are done (refer to [16] and [17]);
2. second stage achieves completely the orbital plane and a controller tunes the path angle to eventually be almost zero;
3. third stage performs apogee manoeuvres and leaves the payload on target orbit.

The rocket is assumed to be dimensionless so that controller acts directly without any dynamics. The design of the mentioned phases are now discussed in more detail.

### 4.5.1 The first stage phase

Although the launcher starts its ascent on the orbital plane, the initial condition, in term of speed, causes a slight misalignment of the launcher for both position and speed as shown in figure 4.3:

---

<sup>1</sup>the nozzle could be re-design in order to give better performances between 12 and 100 km.

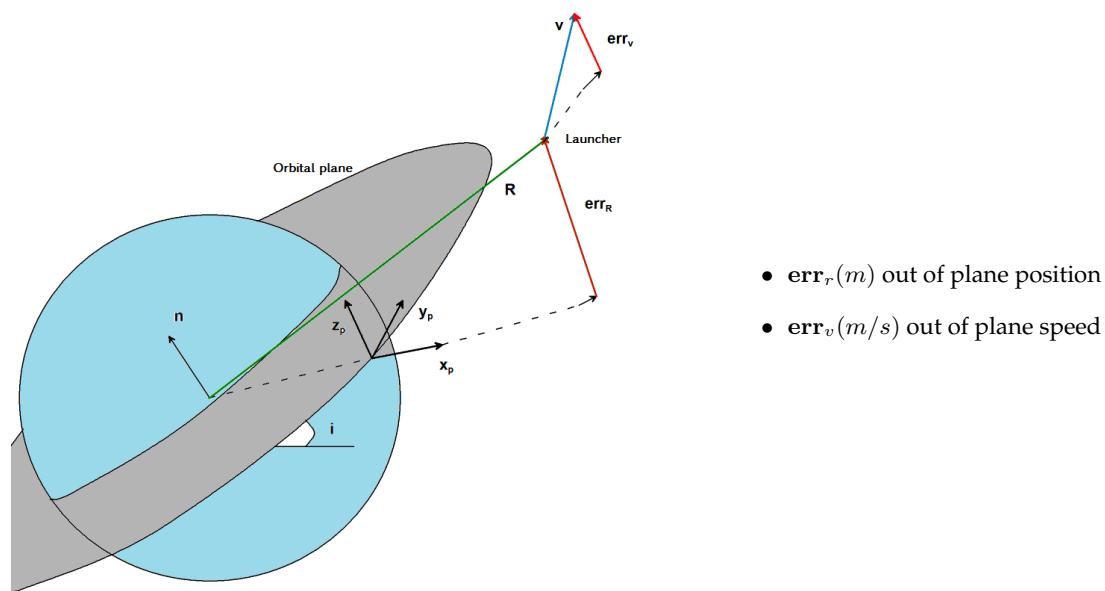


Figure 4.3: Speed and position misalignment

In general the initial absolute velocity vector of the launcher, at first stage ignition, is not contained in the nominal orbital plane, but it has an out-of-plane component which, in the case of the air-launched system, depends on Earth rotational velocity and on the launcher initial velocity with respect to the air. The Earth rotation contributes an initial velocity component which is directed eastward and reduces as launch latitude increases. For an equatorial launch this component, about 460 m/s, can be completely exploited to improve launch performance; but for highly-inclined orbits, an out-of-plane component appears which tends to bring the vehicle away from the desired orbital plane.

The launcher at ignition has an important horizontal velocity component; by choosing a proper flight heading, most of this component can be positioned in such a way to counteract the out-of-plane velocity effect of Earth rotation. At a launch latitude of 60 degrees for a 98deg. inclined nominal orbital plane, the out-of-plane Earth rotation contribution is about 225 m/s. A proper launch heading (westward) reduces overall out-of-plane velocity to 90 m/s, which can be much easier controlled. With this strategy, the effects of out-of-plane control on overall system performance are marginal.

During first stage the thrust has been split in two component:

1. an in plane thrust component directed along the in plane absolute speed components for the gravity turn manoeuvre;
2. an out-of-plane thrust component during first firing along the normal to the orbital plane  $\mathbf{n}$ .

It has to be pointed out that not all the out of plane speed and position could be zero at the end of the first stage. The on plane thrust is given by the following equation:

$$\mathbf{T}_p = T_p \frac{\mathbf{v}_p}{v_p} \quad (4.27)$$

where

- $\mathbf{v}_p(m/s)$  is the on plane absolute speed of norm  $v_p(m/s)$ ,
- $T_p(N)$  is the plane thrust norm, e.g. the total thrust available as given by eq. 4.26 minus the normal thrust  $T_p = \sqrt{T^2 - T_n^2}$

The normal thrust  $T_n$  acts to eliminate the remaining out-of-plane velocity component according to a proportional-derivative control law (commanded out-of-plane velocity value is zero). Working only along the normal to plane direction those components can be reduced thanks to a controller whose behavior can be described as a spring-damper system, with a force proportional to error on position  $err_R$  and speed  $err_v$  outside the plane, along normal direction:

$$T_n = -m(t) \cdot (K \cdot err_R + C \cdot err_v) \quad (4.28)$$

where

- $m(t)$  represents the launcher mass, varying with time, because force needed to change rocket motion decreases with mass according to Newton's laws;
- $K(1/s^2)$  is the spring constant and
- $C(1/s)$  is the damper constant.

The selection of those constants has been made considering the analogy with mechanical systems. As it can be infer by figure 4.4(a) and 4.4(b):

- high values of  $K/C$  ratio entail high frequency oscillations;
- low values of  $K/C$  make the zeroing of the out of plane errors very slow and inaccurate.

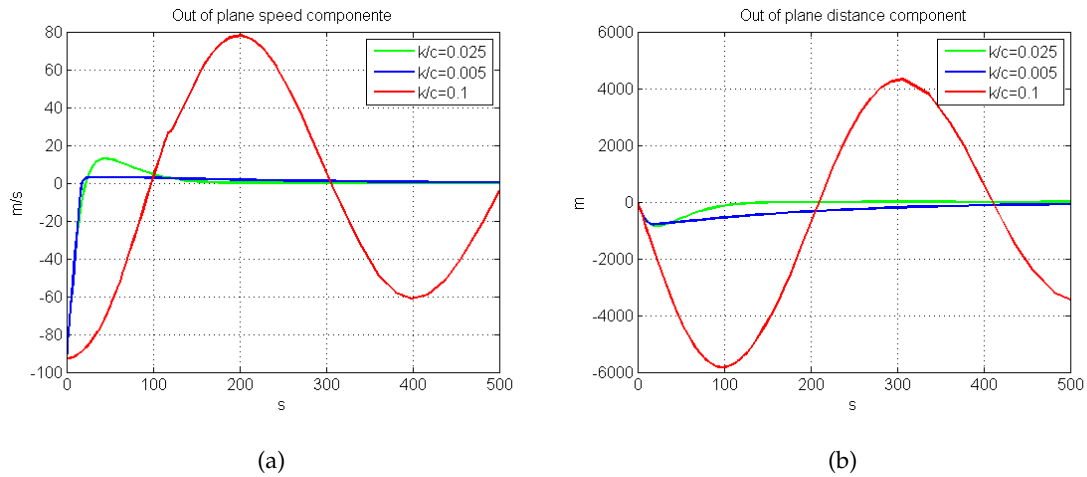


Figure 4.4: Third stage conceptual goals

In the case  $k/c = 0.1$  the propellant consumption results higher than those necessary to zeroing the out plane speed, about  $90m/s$ . In the second, where  $k/c = 0.005$  the propellant consumption bit lower than this quantity, because the out of plane thrust is unable to meet its task in a time compatible with the first stage burning time. The best value, able to perform the control manoeuvre required in a time of about 120s, has been calculated as  $k/c = 0.025$  given by the value reported in table 4.2:

$K = 0.0025/s^2$	$C = 0.1/s$
------------------	-------------

Table 4.2: Control coefficients for out of plane control

Moreover the maximum allowable out of plane component is limited by a maximum value. This value tends to decrease and, at the same time, also the requested out-of plane component reduces while the launcher reaches the plane. The higher out of plane control thrust is needed at the first stage ignition, and the maximum value depends on the launcher attitude. This has been set to the 50% of the total thrust corresponding to a  $\beta$  angle 60deg.

#### 4.5.2 The second stage phase

During second stage the trajectory control has been divided out-of-orbital-plane and into control in-the-orbital-plane. The first is the same dealt in the previous paragraph, meanwhile the second acts so that the flight path angle follows a control law defined in order to maximize performances.



A bi-dimensional control on orbital plane has been set, expressed in terms of in-plane path angle  $\theta_c$  and angle of attack  $\alpha_c$ . The controlled path angle is a decreasing function of initial path angle, that deriving from gravity turn, and time plus a dimensional parameter  $p(1/s)$ :

$$\theta_c = f(\theta_0, t, p) \quad (4.29)$$

It is expressed in the local orbital plane, which moves with the rocket; just recalling that  $z_p$  represents the normal to orbital plane and referring to figure 4.3 the  $y_p, z_p$  axis result:

$$\mathbf{x}_p = \frac{\mathbf{R} - err_R \mathbf{z}_p}{\|\mathbf{R} - err_R \mathbf{z}_p\|} \quad (4.30)$$

$$\mathbf{y}_p = \mathbf{z}_p \times \mathbf{x}_p \quad (4.31)$$

In-orbit plane control thrust designed is:

$$\mathbf{T}_{\mathbf{x}_p \mathbf{y}_p} = T_p \cdot (\mathbf{x}_p \sin(\alpha_c + \theta_c) + \mathbf{y}_p \cos(\alpha_c + \theta_c)); \quad (4.32)$$

where

- $T_p(N)$  is the in plane available thrust, i.e. the total thrust minus the out-of plane thrust:

$$T_p = \sqrt{T^2 - T_n^2} \quad (4.33)$$

- $\mathbf{T}_{\mathbf{x}_p \mathbf{y}_p}(N)$  is the thrust vector on components  $\mathbf{T}_{\mathbf{x}_p}(N)$  and  $\mathbf{T}_{\mathbf{y}_p}(N)$  on the orbital plane

and  $\alpha_c$  is obtained from (refer to [16]):

$$\alpha_c = \arcsin \left( \left( v \cdot \frac{d\theta_c}{dt} + \left( \frac{\mu}{R^2} - \frac{v^2}{R} \right) \cos \theta_c \right) m(t) / T_p \right) \quad (4.34)$$

where  $\mu(m^3/s^2)$  is gravitational constant for Earth. The control flight path angle  $\theta_c$  will be defined in section 5.5.

### 4.5.3 The third stage phase

The third stage phase goal can be one of the followings::

1. the engine starts working for a time corresponding to give the speed increase in order to reach the transfer orbit apogee, where the circularization occurs and final circular orbit is reached, as shown in figure 4.5-a;

2. a first burn to increase the velocity to get to the final circular orbit distance; a ballistic transfer; a final burn to circularize at apogee on the final operative orbit, as shown in figure 4.5-b.

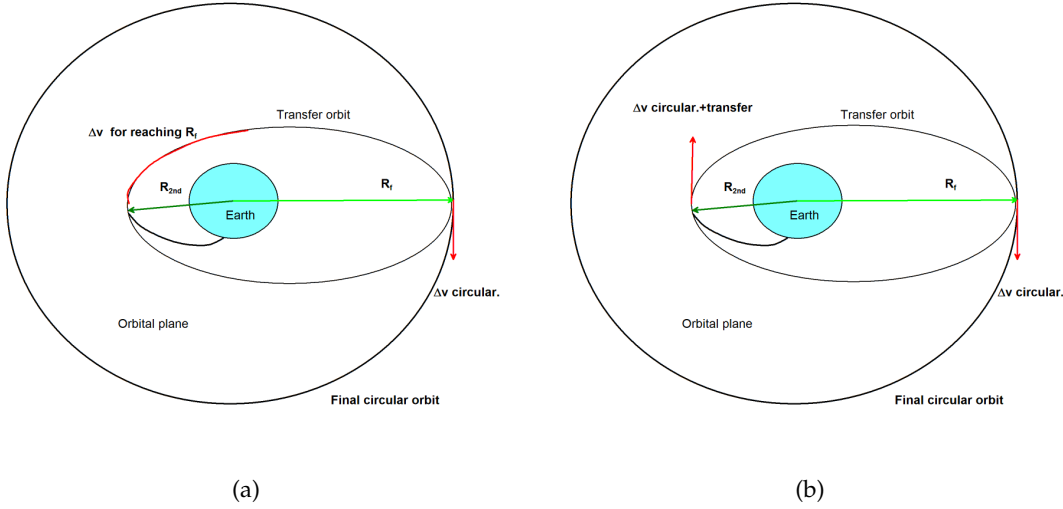


Figure 4.5: Third stage conceptual goals

Those approaches are similar and results are equivalent in the model. The only difference stay in that the third stage works as a complete stage in the first case meanwhile it acts only as an apogee motor in the second case. Actually, in the reality the first approach implies a propellant consumption to perform the control manoeuvre during the firing.

The first approach entails that thrust is aligned to the speed vector:

$$\mathbf{T} = T \cdot \frac{\mathbf{v}}{v} \quad (4.35)$$

where  $T(N)$  is the thrust given by the apogee motors. The second strategy considers impulsive maneuvers accomplished by the stage, therefore the impulsive mechanics is applied to define the required thrust.

$$a = \frac{R_{2nd} + R_f}{2} \quad (4.36)$$

$$\Delta v = \left\| \sqrt{\frac{2\mu}{R_{2nd-f}} - \frac{\mu}{a}} - \sqrt{\frac{\mu}{R_{2nd-f}}} \right\| + \left\| \sqrt{\frac{2\mu}{R_f} - \frac{\mu}{a}} - \sqrt{\frac{\mu}{R_f}} \right\| \quad (4.37)$$

where

- $a(m)$  is the transfer orbit semi-major axis
- $R_{2nd-f}(m)$  is the second stage burnout distance from the Earth centre

- $R_f(m)$  is the circular target orbit radius.

In this work the second approach has been in general used, but the section 5.3 shows the time integration with the first strategy up to the final orbit insertion.

## 4.6 Release manoeuvre requirements

The separation maneuver purpose is to:

- release the launcher from the aircraft,
- provide the suitable initial conditions for the ascent dynamics.

A driving requirement for the definition of the separation manoeuvre is that the manoeuvre itself must be safe for the launcher and for the A/C, that can be assessed evaluating the spatial gap between the launcher and the A/C. In general the requirements, needed in order to size the Aero-Module and to describe its dynamics, are a combination of 2 sources:

1. the launcher initial conditions at first stage ignition, and
2. the Aero-Module stability and structural requirements

It has to point out that those aspects are strictly interlaced, and no convergency of results would have been obtained, without the imposition of some assumptions. For what concerns the launcher requirements it has been assumed a vertical speed in the order of 100m/s. The remaining horizontal component descends from the integration and has also exploited to reduce the effects of Earth rotation when launching on high inclinations, by choosing a proper heading for the release manoeuvre.

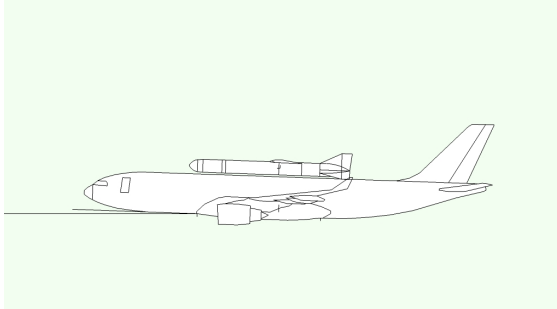
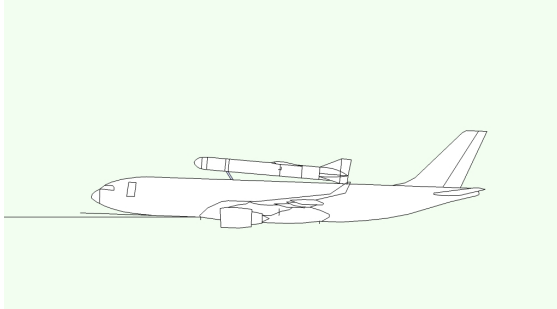
The main aerodynamic working assumptions for stability and structural requirements has been described in detail in section 3.1 and are hereafter briefly recalled:

- initial speed is that of the A/C,
- at incidence angle of 0 degrees there is not lift,
- at low incidence angle (less than 10degrees) the only wing is able of guarantee that lift is equal to weight at the release speed,

- shape drag coefficient equal to a fraction of lift coefficient,
- maximum load equal to 3,
- pitch oscillation frequency of 20s at the speed corresponding to a vertical component of 100m/s
- wing lift equal to launcher plus Aero-Module weight at the beginning of release manoeuvre.

## 4.7 Release Manoeuvres

Table 4.3 describes the in detail the separation manoeuvre as it has been conceived.

	
<p>1 Reached the Separation Area, the Carrier A/C, with the launcher as piggyback, accelerates to the maximum velocity, <math>M=0.81 / 240 \text{ m/s}</math> in horizontal flight, throttle 100%; altitude between 11000 and 12000 m, compatible with the carrier capabilities.</p>	<p>2 - The launcher is erected to provide a relative attitude with respect to the A/C; this is required to get the lift required for separation (see point 3 and 4) as studied in sec.5.1.1. The A/C could also perform a pull-up manoeuvre for release to occur at a moderate flight path angle as reported in sec.5.1.2.</p>

4.7. RELEASE MANOEUVRES

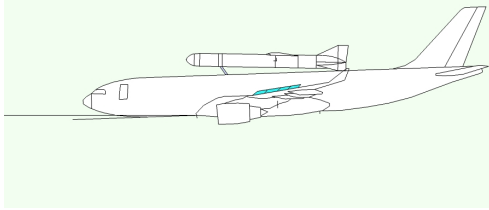
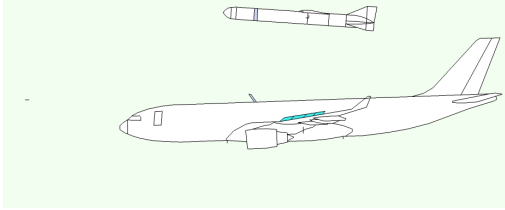
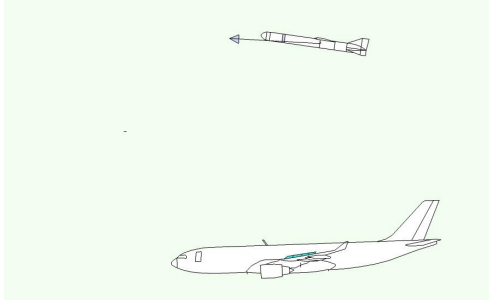
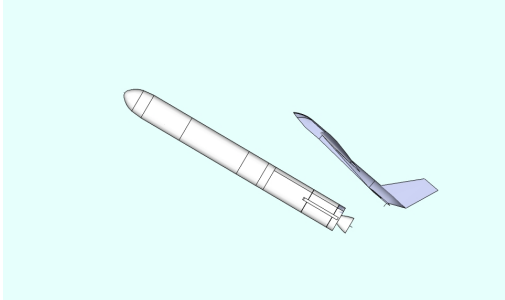
	
<p>3-When ready-to-launch and proper conditions are reached, the A/C performs the following operations:</p> <ul style="list-style-type: none"> <li>• Engines to idle,</li> <li>• Zero-lift angle-of-attack,</li> <li>• Aerobrakes open</li> </ul> <p>in order to make the separation ease and fast. The launcher is released.</p>	<p>4- The A/C falls at about 0-g; the lift of the launcher allows to keep increasing the altitude (1-g 1.5-g). The high A/C drag reduces a rearward relative motion of the launcher with respect to the A/C. The dynamic is such that the separation distance rapidly rises, clearing the A/C fin in less than 1.5 s .</p>
	
<p>5-The aerodynamic configuration of the launcher is such that its angle of attack tends to increase following separation (no movable surfaces). In this way a pull-up maneuver (up to more than 2.5g) is performed by the Aero-Module which converts part of the velocity into a vertical component exploited by the launch dynamics. In particular, loads before separation are reduced, aerodynamic effects are limited, induced drag on the launcher are contained (reduced loads before separation, lower interference effects, lower induced drag on launcher); still, a vertical velocity component, needed at the ignition, is assured.</p>	<p>6 - The A/C keeps falling at 0-g; throttle is pushed to 100% to increase separation from launcher. At a certain point, lift is re-established and a tight turn is performed to leave the launcher flight plane. In about 10-12 s from release, the separation distance is more than 1000m. The aerodynamic surfaces are separated from the launcher and 1st stage is ignited.</p>

Table 4.3: Separation manoeuvre sequencing

In the initial part of chapter 5 the analyses according to two possible separation maneuvers are shown:

1. horizontal release in which the separation occurs during horizontal flight;
2. inclined release, where the effect of a possible pull-up maneuver performed by the A/C carrier is assessed (separation with a positive Flight Path Angle, FPA).

It has to point out that the Aero-Module characteristics relevant to the requirements described in section 4.6 have been exploited in both cases.

Using high performance wing the required characteristics result, for aerodynamic surfaces and centres of pressure seen in section 3.1 :

1-g angle of attack [deg]	$cl_{\alpha}^{wing-tail}$ [1/deg]	$cd_0^{wing-tail} = 1/15cl_{1g}$	$cd^{wing} = cd^{wing} + C_d$
6.5	0.12	0.0765	0.11

Table 4.4: Aerodynamic characteristics for the Aero-Module

where for the wing it has considered an increase due to the launcher contribution of  $C_d$ , which has been set equal to 0.4 from [17] and has been spread on the wing thus obtaining an increase of about 0.04 with respect to that of the tail.

Aerodynamic coefficients are chosen and calculated conservatively according to other examples available for wings (refer to [12] and [18]).

As already mentioned, the A/C is assumed to be controllable in the vertical plane, assuring a fixed angle of attack during the current phase. Results reported in the next sections hypothesize a dive of the carrier and do not pay attention to the A/C manoeuvres end as soon as the Aero-Module is released.

The carrier is not full loaded during the manoeuvres and presents the characteristics reported in table 5.14:

Mass	$S_{wing}[m^2]$	$cl_{airbrake}$	$cd_{airbrake}$
200000	362	-0.53	0.34

Table 4.5: Aerodynamic characteristics for Airbus A330

It has to put out that in the configuration treated the maximum load is equal to 2, which is contained in the load envelope for this type of plane. This allows the plane to perform the described manoeuvre.

## Chapter 5

# Guidance and control simulation and results

This chapter is conceptually divided in two parts. In the first part the release manoeuvre and the ascent phase simulations for a typical mission are provided.

In the second part some sensitivity analyses on the launcher has been performed in order to evaluate how the delivered payload mass capabilities vary. This operation is necessary because it gives noticeable information about the predictable performances, which in general are expected to decrease during the development and effective realization of the work.

### 5.1 Release manoeuvre results

As described in section 4.7, two strategies has been studied and their simulations performed: the horizontal and the inclined separation.

While margins for optimization of the aerodynamic configuration and of the separation dynamics exists, in both cases the capability to reach a successful separation and good initial conditions for ignition will be demonstrated.

#### 5.1.1 Separation during horizontal flight

In this case the A/C releases the launcher with a horizontal velocity. By taking into account that the aerodynamic surfaces are fixed (no control surfaces), the launcher initial angle of attack is a driving parameter for dynamics; in the presented results the initial

AoA is 6.5degrees (with respect to zero-lift line).

Such a choice can be read as the request to have the launcher risen above the A/C by the erection mechanism before release to get the needed attitude with respect to the air velocity (see point 2 of table 4.3). In this way during the flight to the release area, it would be reduced the aerodynamic and load effects of the launcher on the carrier.

By the integration for 13 s of the equations 4.1, 4.2 and 4.3 it is possible to study the manoeuvre, considering the most important variables, that are the position of the Aero-Module and launcher with respect to the carrier, and the angle of attack that influences the normal loads.

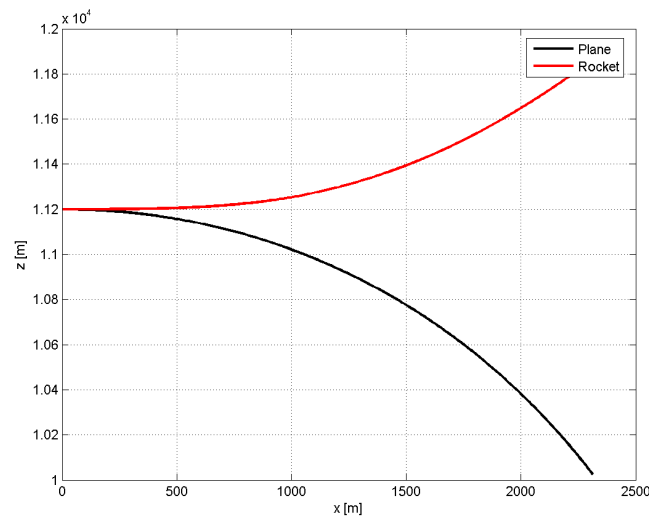


Figure 5.1: A/C and launcher position

Figure 5.1 shows the trajectories in the vertical plane of the A/C and of the launcher (as the model is bi-dimensional, it is assumed that the A/C is not leaving the vertical plane), referring to the initial separation manoeuvre position. Actually, the integration has been stopped because after 13s the vertical velocity reaches the maximum value and then begin to slow down. When considering the first phases after release, in close proximity to the A/C, the relative positions of the launcher with respect to the A/C are shown in figure:



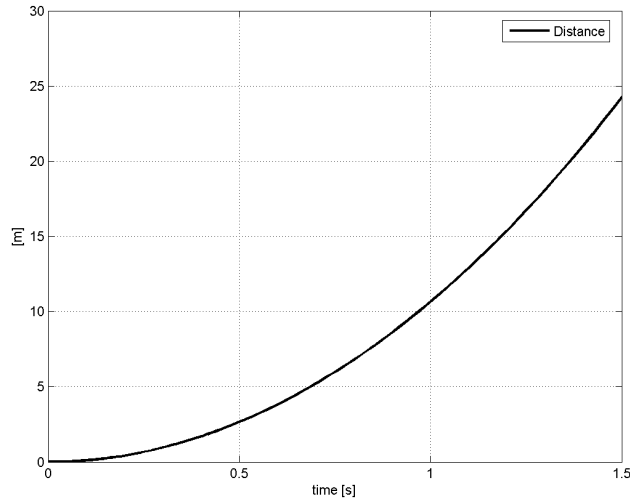


Figure 5.2: A/C and launcher relative module distance

After 1 s the launcher has cleared the A/C fin (about 10 m height); the launcher has moved only 2.5 m forward, as a result of the A/C actions related to air-brake deployment and engine-to-idle.

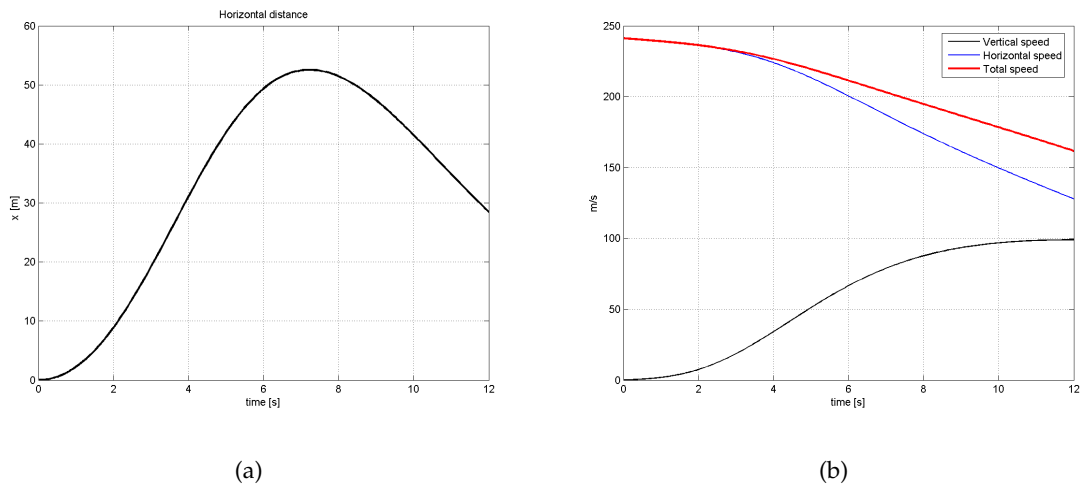


Figure 5.3: Horizontal separation and launcher speed components

After 13 seconds from release, the pull-up maneuver, induced by the launcher aerodynamic configurations, put the launcher in the proper state conditions for the ignition to start:

- the launcher has reached a vertical velocity of about 100 m/s; this is the minimum

## 5.1. RELEASE MANOEUVRE RESULTS

---

value assumed as a good compromise between the difficulty of the manoeuvre and the gain in terms of performances;

- horizontal velocity at ignition (about 130 m/s, see fig. 5.3-b) has not decreased too much, thus having a beneficial effect on performance, because it is possible to use this value to reduce the out of plane manoeuvres, which is basically a speed loss; in this case, in fact, the propellant consumption do not increase the speed tangentially;
- separation distance between A/C and launcher is more than 1800 m; actually, the separation between the two vehicles is expected to be even larger and rapidly increasing; in case of explosion at ignition, this distance is assumed to be a safe one for the A/C; in case of deviation from expected trajectory following ignition, the system dynamics (relatively small accelerations at beginning of first stage firing) allows to perform the safety range actions (see [19]) with no harm for the A/C.

Figures 5.4, 5.5 and 5.6 present the behavior of other significant parameters:

1. the normal load factor on the launcher for an effective pull-up is limited to less than 2.8 g, when the maximum value was set to 3g;

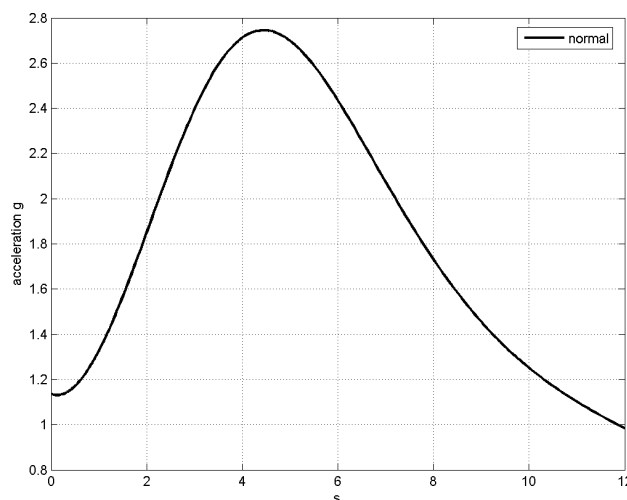


Figure 5.4: Normal loads on launcher

the maximum value is the combination of both velocity and angle of attack; it has to point out that the load factor is equal to 1 when the Aero-Module reaches the maximum vertical component; that naturally proceeds from the fact that the vertical speed reaches a maximum speed;

- the flight path angle increases continuously up to about 38degrees at the time of ignition;

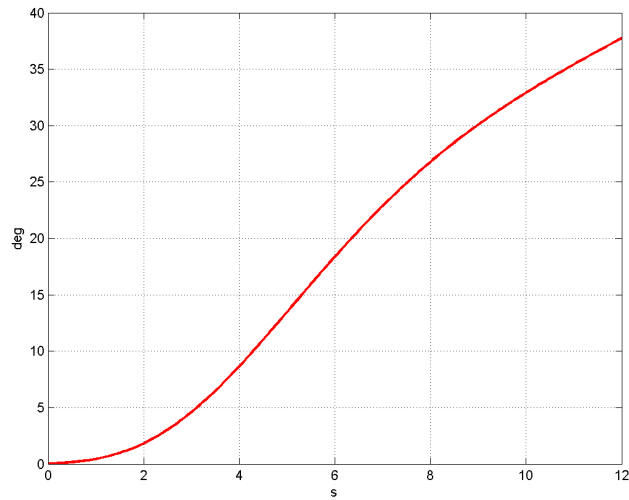


Figure 5.5: Flight path angle

- the AoA, remains within limited values of less than 19 degrees;

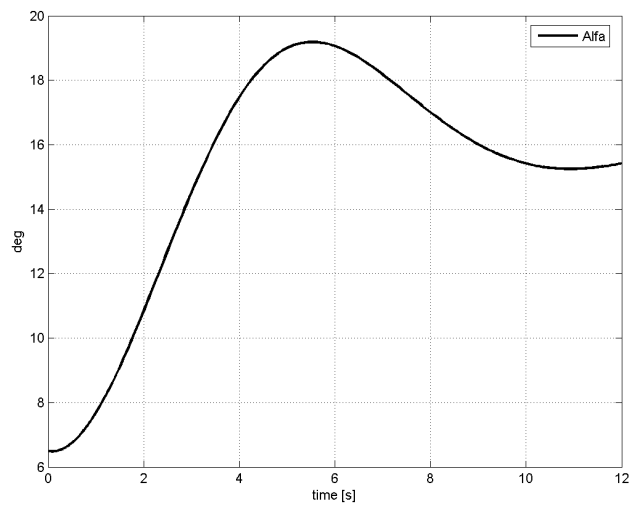


Figure 5.6: Angle of attack

the angle of attack grows up to the maximum value of 19 degrees and then decrease to a lower equilibrium angle of about 15 degrees, because in that situation the aerodynamic forces reaches their maximum value as confirmed also by figure 5.4. Actually, the value of 15degrees would be the equilibrium value if the Aero-Module

conserved its speed in that condition.

High angles of attack are critical for the wing behaviour. It would cause the wing to stall at lower angle than that reached. This means that the wing has to be design in order to increase the angle for which the stall occurs. For classical profiles this is possible adding flaps which increase the maximum lift and corresponding maximum angle of attack; otherwise delta wings offer similar performance (see [20]). In both the situation the maximum achievable angle of attack is more than 30 degrees with a maximum lift coefficient up to 4. For the designed wing the maximum lift coefficient is achieved at about 20 degrees, where it is about 2.4, less than other high performances wings.

### 5.1.2 Inclined separation manoeuvre

In this case, the A/C performs a moderate pull-up maneuver releasing the launcher with a vertical velocity component, to be further augmented by the launcher dedicated pull-up manoeuvre. The A/C maneuvering possibilities at this altitude are limited, the engines not being able to provide enough thrust for a steady climb; for the presented case, a flight path angle of about 11degrees at the moment of release resulted to provide some good results in terms of vertical velocity at release (about 45 m/s) and limited loss of overall velocity (energy). A/C velocity in horizontal flight at beginning of its pull-up maneuver is 240 m/s (as in the previous case); at launcher release, when the flight path angle calculated to be 11.7degrees, the velocity module is 235 m/s.

The launcher angle of attack at release is about 3.4degrees, which is less than in the previous case (6.5 degrees), therefore reducing the requirement for erection of the launcher above the A/C before release. Never the less the initial vertical speed is more than 40m/s and this has a positive effect on the manoeuvre

Figure 5.7 shows the trajectories in the vertical plane of the A/C and of the launcher starting from release (as the model is bi-dimensional, it is assumed that the A/C is not leaving the vertical plane). In this case, the carrier goes along parabolic trajectory.

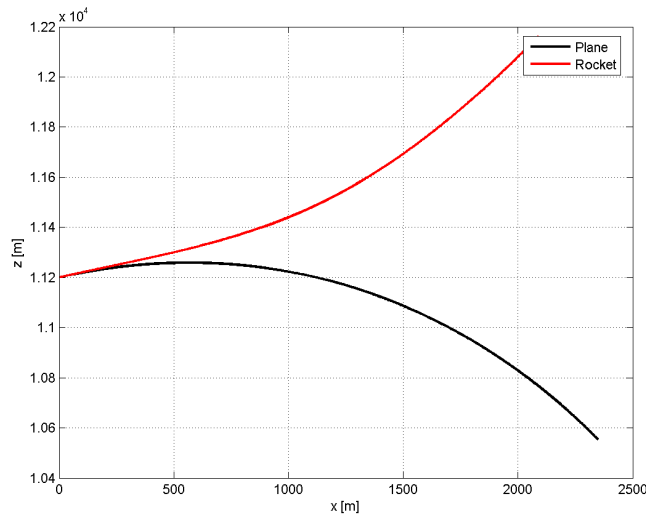


Figure 5.7: Inclined release: A/C and launcher position

When considering the first phases after release, in close proximity to the A/C, the relative positions of the launcher with respect to the A/C are shown in figure 5.8:

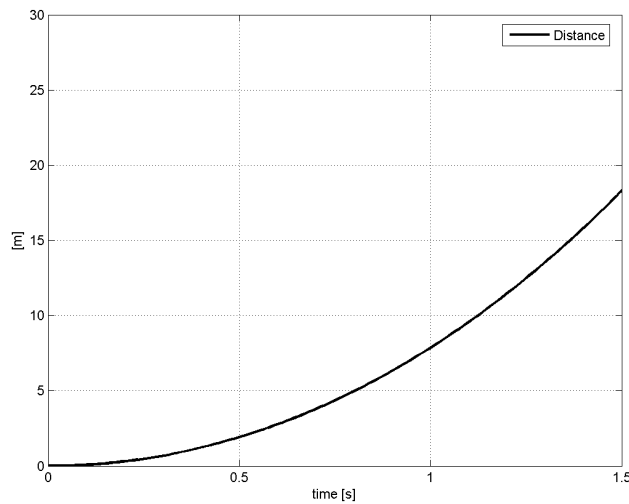


Figure 5.8: Inclined release: A/C and launcher relative module distance

After about 1.5 s, the launcher has cleared the A/C fin (about 8 m height on A330); the launcher has moved only 2m forward, as a result of the A/C actions related to air-brake deployment and engine-to-idle. In this situation the overall distance results 5m lower than that achieved in the horizontal manoeuvre, because at the beginning the carrier follows a trajectory nearly parallel to that of the Aero-Module, as also confirmed by figure

5.9-a.

Figure 5.9-b shows the the speed trend after the release from the carrier, in which it can be seen that the overall dynamics is about 4 seconds faster than in the horizontal separation, in reaching the vertical speed of 100m/s.

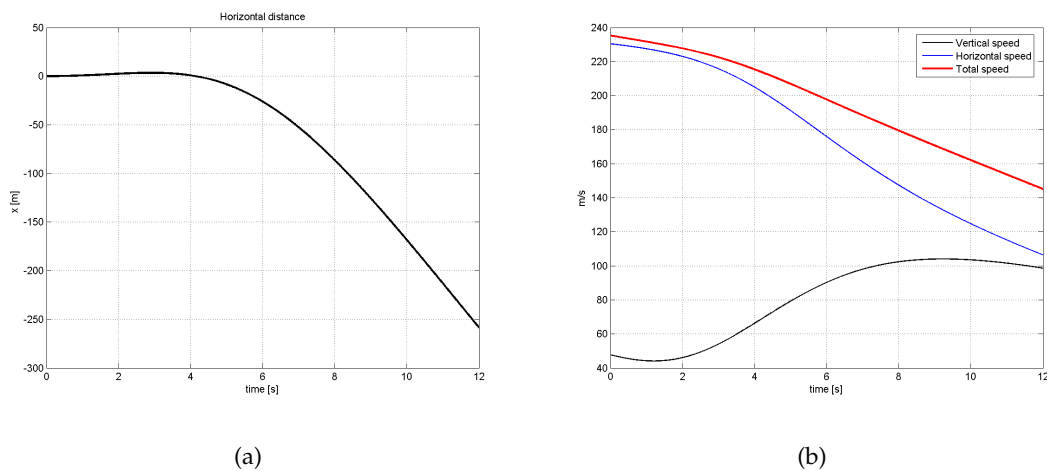


Figure 5.9: Inclined release: horizontal separation and launcher speed components

After about 10 seconds from release, the additional pull-up maneuver induced by the launcher aerodynamic configurations, put the launcher in the proper state conditions for the ignition to start:

- the launcher has a vertical velocity of 104 m/s, a little bit higher than the horizontal separation manoeuvre case;
- horizontal velocity at ignition (about 127 m/s, see figure 5.9) is lower than in the horizontal maneuver but has a minor effect on launch performance in SSO;
- Separation distance between A/C and launcher is more than 1000 m; according to this aspect, the same considerations done in the previous section can be applied.

Figures 5.10, 5.11 and 5.12 present the behavior of other significant parameters:

1. the normal load factor on the launcher is limited to 2.3 g less then previous case; also in this case it is a load case enveloped by the usual load conditions for a launcher; this occurs because the initial angle of attack implies an initial load factor of 0.5 g;

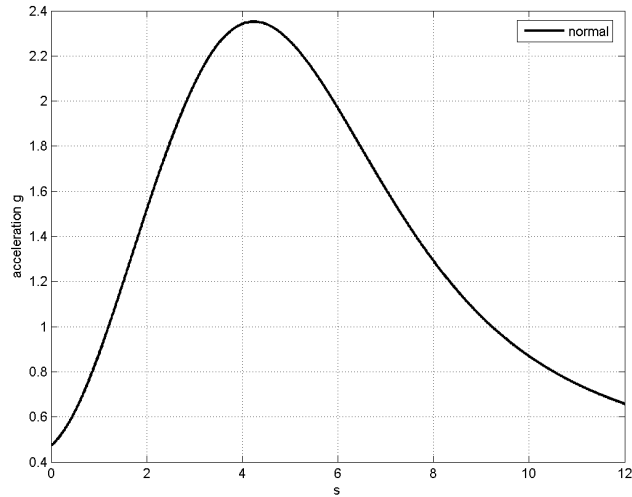


Figure 5.10: Inclined release: normal loads on launcher

also in this case, it has to point out that the load factor is equal to 1 when the Aero-Module reaches the maximum vertical component; that naturally proceeds from the fact that the vertical speed reaches a maximum speed;

2. the flight path angle increases continuously up to about 40 deg. at maximum vertical speed, higher than before thanks to the initial positive FPA and a bit lower horizontal speed components;

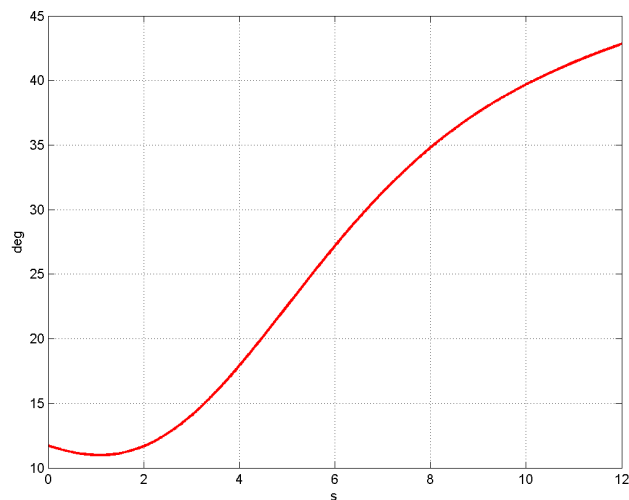


Figure 5.11: Inclined release: flight path angle

3. the angle of attack reaches a value of about 21deg;

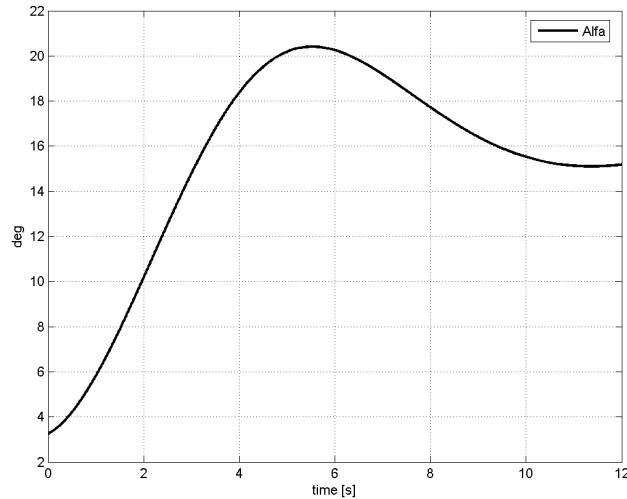


Figure 5.12: Inclined release: angle of attack

the angle of attack grows up to the maximum value of 21 degrees and then decrease to a lower equilibrium angle of about 15 degrees, because in that situation the aerodynamic forces reaches their maximum value as confirmed also by figure 5.4. Actually, the value of 15degrees would be the equilibrium value if the Aero-Module conserved its speed in that condition. It has to be pointed out that, since the aerodynamic configuration is the same, the equilibrium angle is the same of those obtained in the horizontal separation manoeuvre.

The same remarks on the wing characteristics, done at the end of section 5.1.1, can be applied to inclined separation manoeuvre, with the only difference that in this case the maximum  $C_l$  is 2.5, widely included in the high performances wings range for this coefficient.

## 5.2 Considerations

It is here underlined that the analyses presented so far include no control at all. If this is theoretically possible, in practice no control could be not realizable because the system would be too dependent from the initial conditions and the final performances could be excessively worsened. On the other hand the presence of an active control could allow to increase the initial vertical speed component. This effect has been comprised in the sensitivity analyses of performances in section 5.6. Nevertheless the selected approaches



confirms the feasibility of the captive on-top air-launched in both horizontal and inclined separation.

Furthermore, the carrier could be pointed to a direction so that the horizontal speed component can be used to reduce the out of plane component given by the Earth rotation, conserving a good vertical speed component. Those two effects are important and represent one of the aspects which make the air-launch different from the ground-launch.

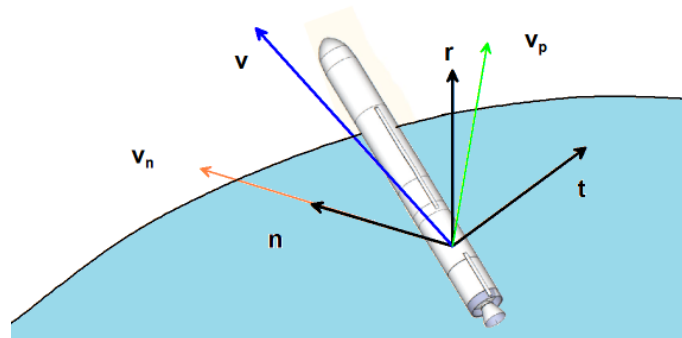


Figure 5.13: Attitude consideration

So if it is considered a horizontal speed component of  $130m/s$ , which is the highest value according to a vertical speed of  $100m/s$  resulting from analyses of sections 5.1.1 and 5.1.2, in the direction normal to the orbital plane  $n$ , as shown in figure 5.13, the overall speed offers two components in the orbital plane whose flight path angle is important in the analyses reported in section 5.3:

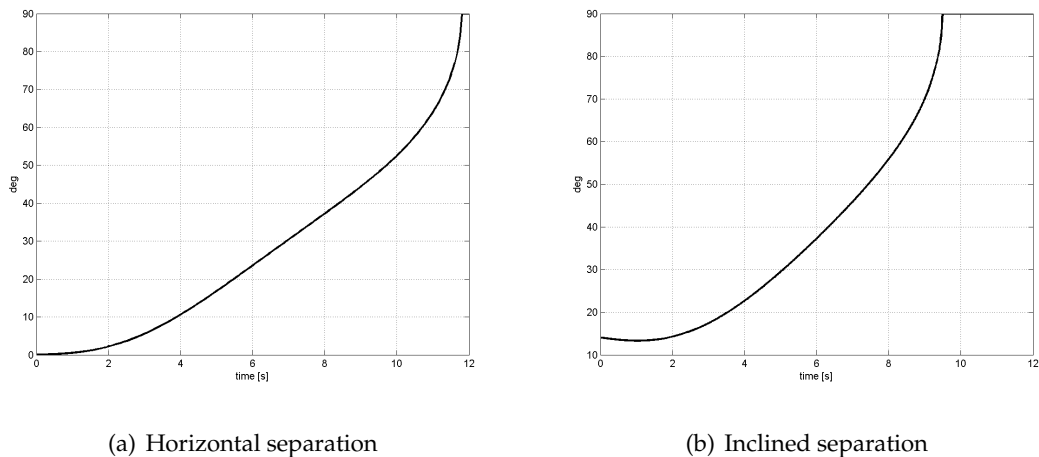


Figure 5.14: Flight path angle relative to the orbital plane

A high initial path angle in the orbital plane offers the possibility to reduce speed losses

avoiding to perform costly manoeuvre (in terms of propellant mass consumption) to point the absolute speed on the orbital plane.

From the figure 5.14 this angle can takes every value comprised between 0 and 90degrees, that is a positive aspect because it allows to have the degree of freedom necessary to make the launcher trajectory optimization during the ascent phase.

### 5.3 Power ascent simulation

This paragraph reports the simulation for inserting about 300kg payload on circular 600 km Sun-Synchronous orbit. The aim of this work is to develop the launcher able to carry this payload. So this main objective has been assessed.

Table 5.1 reports the initial state vector at first stage ignition. It has to be noted that the state vector is given in local coordinates centred at 60 deg of latitude and 0 deg of longitude ( that are included in the launch area described section 2.1.1) Initial condition, that are represented by vectorial position (given by altitude) and speed in local frame (remember that the local frame is on the the orbital plane with x-y axis and z-axis corresponding to the normal to orbital plane as defined in section 4.5.2 ). Third third stage mass is 570kg:

	$x_p$	$y_p$	$z_p$
Position [km]	$R_{earth} + 12$	0	0
Speed [m/s]	99.7	7.8	130

Table 5.1: Third stage 570kg: initial condition

By the values reported in table 5.1 it can be gathered that in the orbital plane the initial flight path angle is of 85.5 degrees, for  $FPA = \arctan v_{px}/v_{py}$ .

Table 5.2 reports the timeline only for the power ascent phase with the consequent altitude reached:

### 5.3. POWER ASCENT SIMULATION

Time [s]	$\Delta t$ [s]	Altitude[km]	Event	Control type
0	0	12	First stage ignition	Out of plane control
117	117	63	First stage burn-out and separation	
120	3	65	Second stage ignition	Out of plane control and in plane FPA control
180	60	93	Fairing separation	
500	320	123	Second stage burn-out and separation	
503	3	123	Third stage ignition to transfer orbit	Thrust tangential to absolute speed $v$
623	120	123	Cut-off	
3326	1703	608	Apogee firing and orbital insertion	None
3408	82	608	Cut-off	Thrust tangential to $v$

Table 5.2: Power ascent timeline

Figures 5.15 and 5.16 show in details the flight profile starting from the first stage ignition to the 600 km orbit insertion.

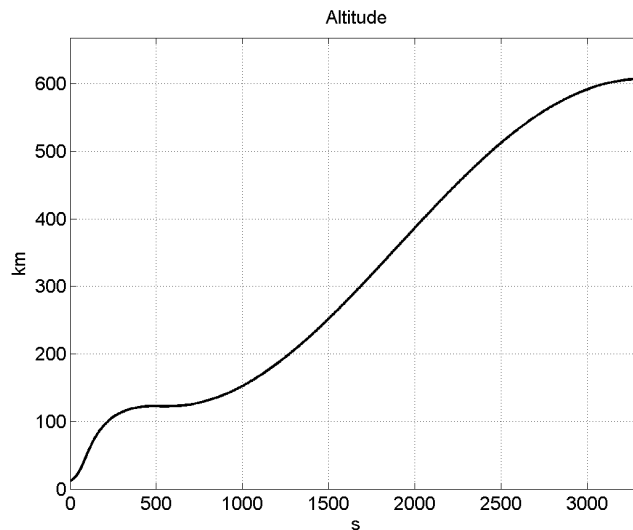


Figure 5.15: SSO at 600 km launch: altitude vs time

It can be noted in fig.5.16 that during the upper stage ignition the altitude does not change significantly, and altitude can be considered constant. The first approach described in section 4.5.3 has been used in this case. The only difference from the second approach is due to the fact that it is not an ideal Hohmann transfer because the burning time is not impulsive but lasts 120s.

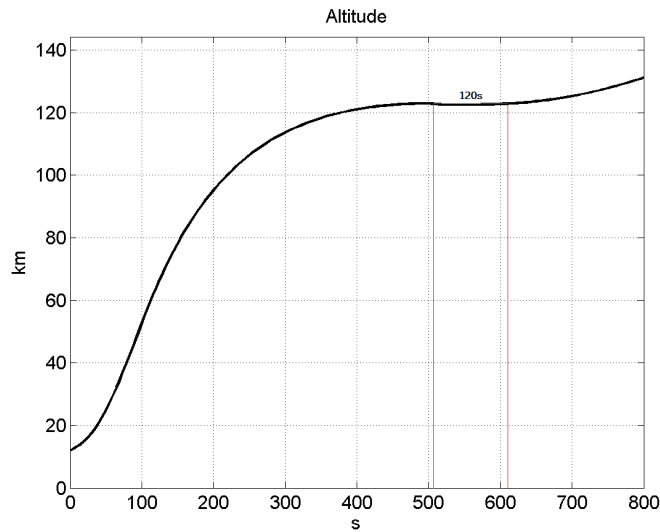


Figure 5.16: SSO at 600 km launch: altitude vs time - detail

This power ascent phase corresponds in the first stage to the trajectory reported in figure 5.17, where it can be seen that the launcher flies over the sea, reducing hazard for populated area:

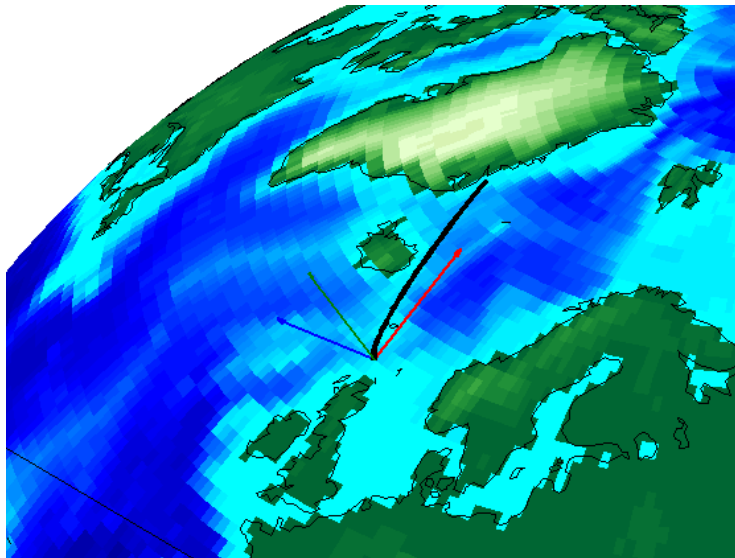


Figure 5.17: SSO at 600 km launch: trajectory - 3D detail

Figure 5.18 shows how the speed increases till it has reached the value corresponding to that necessary for orbiting on a 120km circular orbit (i.e.  $\approx 7.8 km/s$ ) after 500s, before the apogee motor ignites.

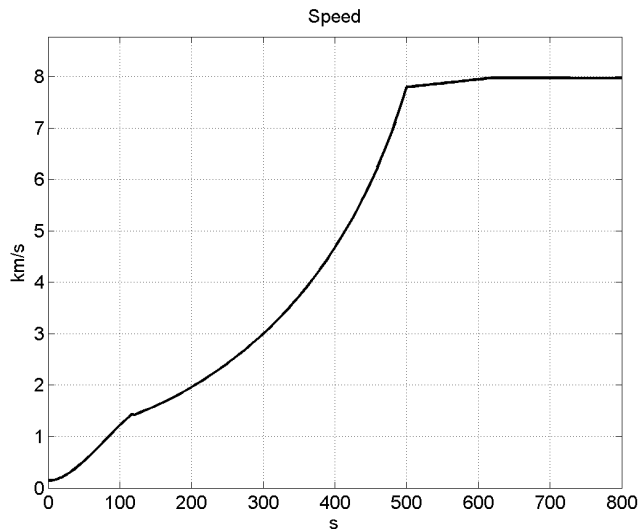


Figure 5.18: SO at 600 km launch: velocity vs time

Fig. 5.19 shows that the maximum acceleration is less than  $46m/s^2$ , i.e. 4.7 g. and is obtained at the end of second stage firing, which sensibly less than ground small launcher, for which this value rises up to 7-8 g (see [21]). The discontinuity at 117s and 500s are due to the engines burnout. Moreover, in the first 117s there is a peak because the thrust to mass ratio reaches the maximum value and the thrust decreases according to section 2.2.1. Maximum acceleration under first stage thrust is 2.2 g and acceleration at the beginning of second stage firing is less than 1g.

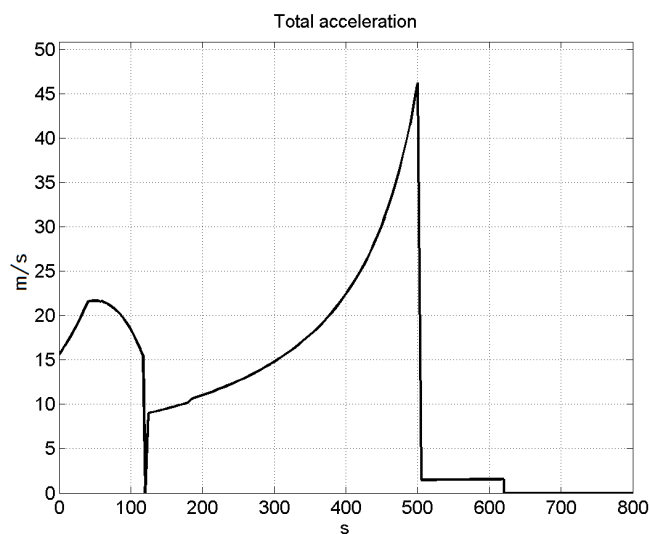


Figure 5.19: SSO at 600 km launch: acceleration vs time

Figure 5.20 relevant to thrust level vs time shows also the out-of-plane thrust component required by the out-of-plane control. According to the control law and control coefficients adopted, such thrust component is very high at the beginning (about 140000 N) then rapidly decreases to less than 1000N in about 65 s.

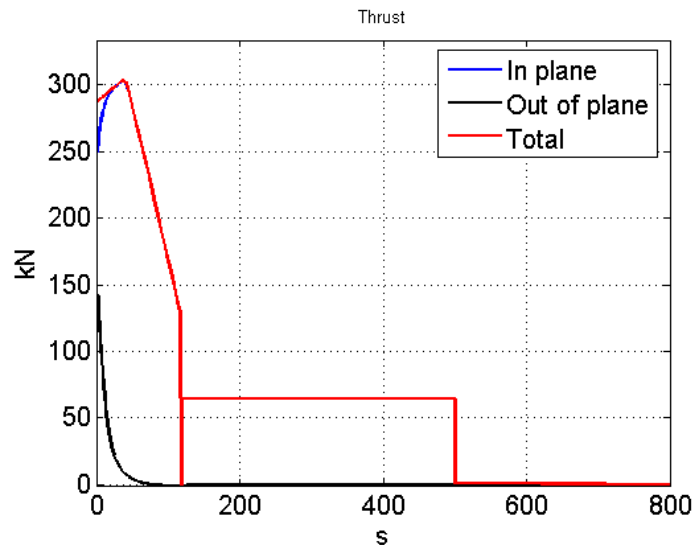


Figure 5.20: SSO at 600 km launch: thrust vs time

The peak at 40 s is due by the fact that the environmental pressure drops and the normal to plane thrust reduces sharply, because the launcher is completely on the plane. Moreover, after that time the available thrust begins to decrease, according to Z9 performances in section 2.2.1

Figure 5.21 shows the effect of this out-of-plane control on the out-of-plane absolute velocity. This velocity is about -92 m/s at the beginning, deriving from the combination of Earth rotation effect eastward and heading of the vehicle at separation from aircraft (see sect.5.1). In less than 25 s overpasses the zero value and then, with an overshoot cycle, tends to a stable zero value in about 3 minutes (also the second stage contributes to the out-of-plane control, with very small thrust components).

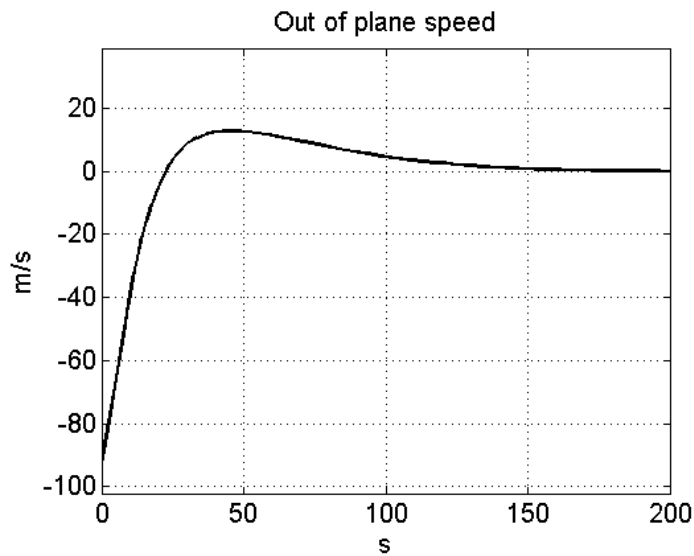


Figure 5.21: SSO at 600 km launch: out-of-plane velocity vs time

The angle of attack diagram in figure 5.22 shows that the orientation of the vehicle axis with respect to its velocity vector reaches significant values. During second stage burn, in order to follow the required path (commanded FPA vs time) the angle of attack reaches values up to 32degrees.

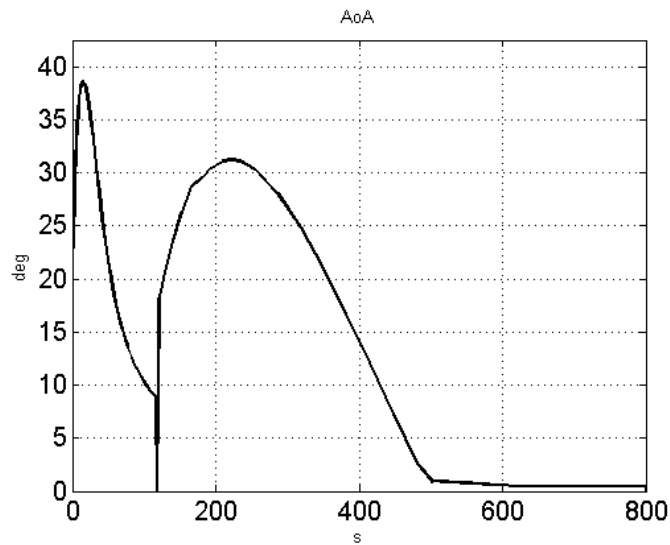


Figure 5.22: SSO at 600 km launch: angle of attack vs time

Also at the beginning of first stage ignition, the angle of attack has considerable values: 23 degrees at the beginning and up to 36degrees after 20 s. According to the

aircraft separation analysis , the angle of attack of the launcher at ignition is 15degrees, the launcher just after ignition should maneuver with thrust vectoring to reach the required thrust higher angle required by the flight trajectory strategy (this has not been implemented in the simulation model).

It seems, that in order to reduce such initial maneuvering and high angle of attack in atmosphere, further investigations and optimizations has to be sought working on the characteristics of the aircraft-launcher separation maneuver (ratio between vertical and horizontal initial velocities, aerodynamic characteristics of the Aero-module,etc.).

It has to be highlighted that the aerodynamic definition and separation analysis done in section 5.1 aimed only at demonstrating the conceptual feasibility of the separation maneuver; therefore definition and optimization margins are wide.

Moreover, the AoA reported has been calculated without considering a rotational dynamic but it is the angle between the thrust vector and the relative speed, as

$$\alpha = \arccos \frac{\mathbf{T}' \mathbf{v}_{wind}}{\|\mathbf{T}\| \|\mathbf{v}_{wind}\|} \quad (5.1)$$

This, of course, leads to different value.

Moreover the thrust vector control capability allows a nozzle rotation of about 10 degrees. In this way the effective angle of attack can be lower, and so no discontinuities is envisaged between the Aero-Module separation phase and the first stage ignition.

In the same way the second stage TVC can accomplish the necessary control in order to perform the 8 degrees AoA difference between first stage burnout and second stage ignition.

The flight path angle diagram of figure 5.23 shows the angle as projected in the nominal orbital plane (thus the out-of-plane velocity component is neglected) and it is computed using the speed with respect to the local orbit frame; as altitude increases and out-of-plane motion becomes negligible (after 200-250 s) this angle is very close to the *absolute* flight path angle.



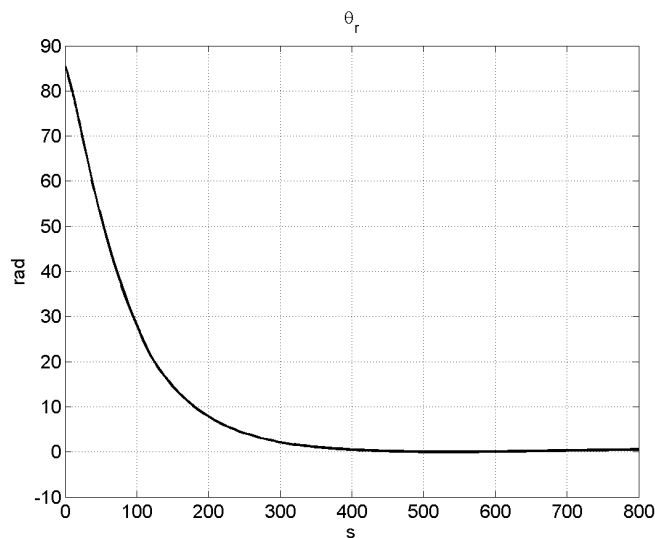


Figure 5.23: SSO at 600 km launch: plane flight path angle vs time

At the end of second stage firing, the vehicle is about at the apogee (flight path angle equal to 0 degree) of a trajectory profile which could bring the second stage to reenter; furthermore, the first firing of the third stage has to start at this point with the Hohmann transfer orbit.

Fig.5.24 presents the behavior of the dynamic pressure during the flight. Since the  $CdS$  parameter (drag coefficient  $\times$  cross section of the launcher) is 1.13, corresponding to a drag coefficient  $C_d$  equal to 0.4, the figure is also indicative, by a factor 1.13, of the drag force.

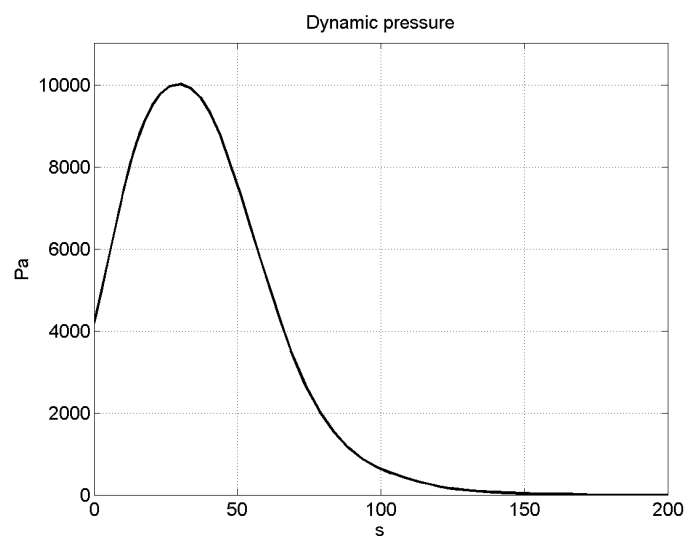


Figure 5.24: SO at 600 km launch: dynamic pressure vs time

The dynamic pressure has maximum value of about 10000 Pa. This is much lower than the usual values for a vehicle launched from ground (e.g., for VEGA the figure is greater than 50000 Pa) and it means that lower acoustic loads are affecting the payload.

## 5.4 Heat fluxes on fairing

Fairing separates from launcher when heat fluxes reaches a minimum value. Literature [15] offers a wide range of formulas to calculate heat fluxes, but it is preferable to use simple expressions with few parameters.

Neglecting radiative contribution and thermal transient, the model results are valid when heat fluxes are less than  $5000W/m^2$ . Fairing temperature is given by:

$$T_{fairing} = T_e + \frac{Pr}{2c_p} v^2 \quad (5.2)$$

where

- $T_{fairing}(K)$  is the fairing temperature,
- $T_e(K)$  is environment temperature as calculated in section 4.2,
- $Pr(-)$  is Prandtl number for air,
- $c_p(J/(KgK))$  is specific heat coefficient at constant pressure.

$Pr$  and  $c_p$  have been assumed constants in all the altitude range as reported in table 5.3:

Pr	$c_p \left[ \frac{J}{KgK} \right]$
0.7	1004.5

Table 5.3: Prandtl number and specific heat coefficient

In this way the heat flux  $q(W/m^2)$  results:

$$q = \frac{1}{2} \rho v \frac{C_d}{4} c_p (T_{fairing} - T_e) \quad (5.3)$$

A typical limit value for heat fluxes used to establish when fairing separation should occur is about  $1000W/m^2$  (the Vega and the Falcon launchers use this quantity [3]-[22]).

figure 5.25 shows heat flux acting on the fairing in the last separation might occur at about 150 seconds after first ignition.

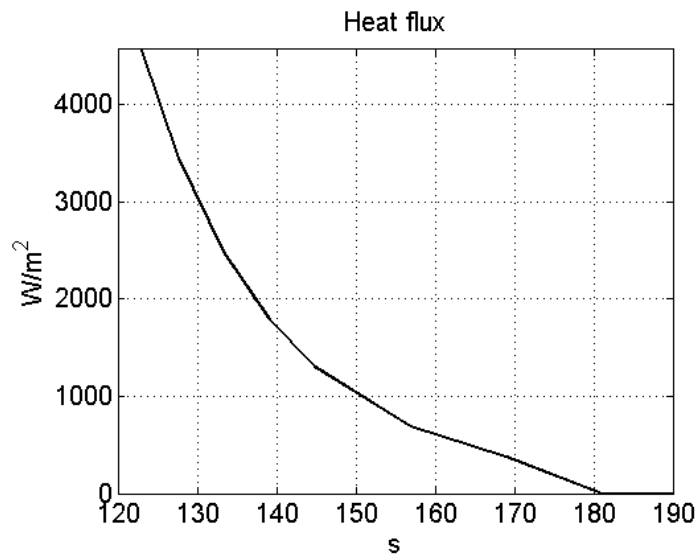


Figure 5.25: Heat fluxes on fairing

This instant can not be stated *a priori* and during the analyses the value of 180 seconds it has been assumed fixed for all configuration<sup>1</sup>.

## 5.5 Flight trajectory optimization

During the second stage firing the trajectory is controlled as seen in the section 4.5.2, and follows a flight path angle defined by a function of time.

In order to achieve the maximum performance in terms of mass on circular orbit, three functions have investigated:

$$\theta_{parabolic} = \theta_0(1 - t/t_f)^2 \quad (5.4)$$

$$\theta_{tangential} = \arctan((1 - t/t_f) \tan \theta_0) \quad (5.5)$$

$$\theta_{exponential} = a \exp(-b \cdot t) - c \quad (5.6)$$

where

- $t_f(s)$  is a typical time, coincident with the firing time of the second stage,
- $\theta_0(rad)$  is the initial FPA in the orbital plane
- $a(rad), b(1/s), c(rad)$  are suitable coefficients for the exponential law.

<sup>1</sup>in the sensibility performances it will be varied

The coefficients  $a, b, c$  allow to change the shape of the curve. They are calculated on the base of:

- initial flight path angle  $\gamma_0$ , as resulting from previous flight phase ;
- final flight path angle, at an hypothetical case of  $t = \infty$ , in this case equal to  $-0.2\text{deg.}$ ;
- time at which the flight path angle reaches the zero value, which coincides with the burning time in this comparison; this parameter basically defines how steep is the slope of the profile.

These laws are reported in figure 5.26 with respect to the initial flight path angle at the second stage ignition:

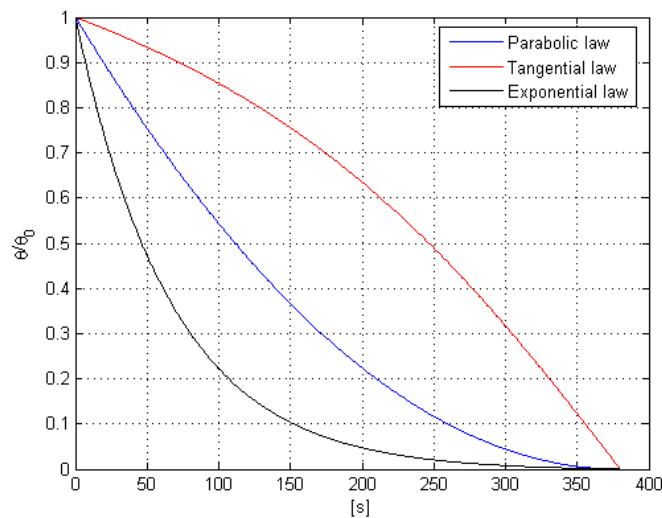


Figure 5.26: Control laws

Because the tangential and parabolic laws are less modellable than the exponential law, it is considered a *Hohmann* transfer, so that the final altitude is the same. Table 5.4 reports the simulation results comparison:

	Parabolic law	Tangential law	Exponential law
Mass on orbit [kg]	534	480	514
Circular orbit altitude[km]	170	235	608
Mass on 600 km orbit	494	448	514

Table 5.4: Control laws: performances comparison

The exponential law proves to allow the more suitable performances if compared to the other examined laws. This is due essentially to the fact that the thrust can accelerate nearly tangentially the launcher, minimizing the gravity losses.

Moreover the presence of three different parameters gives the possibility to manipulate them and to define for different settings of mass on third stage the best controlled profile and performances.

## 5.6 Performances

Optimizing the shape of the controlled phase it is possible to calculate the best performance in the nominal case, which is a speed component in the orbital plane of 100m/s and 130 m/s in the normal to plane direction.

The project of the rocket is susceptible to many variables which could affect the effective performance in terms of payload on circular orbit. So it is important to show the impact of some element on this result.

The figure 5.27 presents the sensitivity of the launcher performance to mass changes of different items of the launcher: first stage, second stage. allocated to uncertainties on the interstage and interfaces to the aircraft.

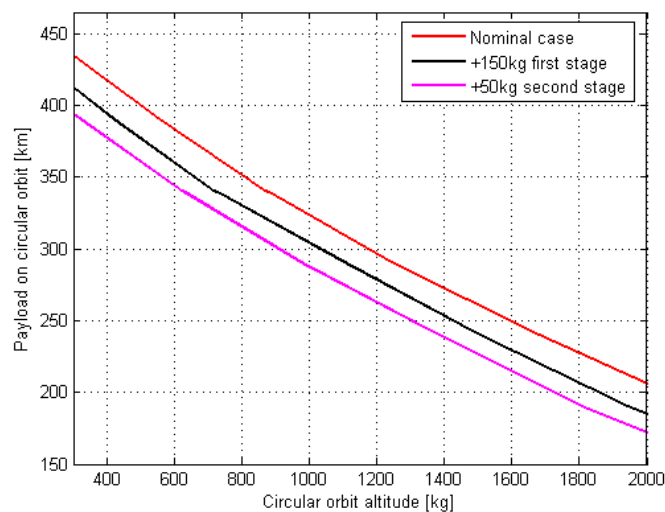


Figure 5.27: Sensitivity on mass

Obviously the most significant impact is on the second stage mass, where most of the assumed 50 kg increase becomes a correspondent reduction of payload.

Sensitivity to first stage and fairing mass changes is much softer. Considering that the Z9

mass uncertainty is very limited, the considered 150 kg mass change on first stage can be. Table shows the payload capability decrease for this the case.

Payload capability on circular orbit [kg]			
Altitude orbit[km]	Nominal	Stage1+150kg	Stage2+50kg
300	432.5	410.4	392.0
600	384.6	360.7	344.1
900	334.9	315.6	300.
1200	297.2	279.7	264.1
1500	260.4	239.2	225.4
1800	225.4	207.0	191.4
2000	206.1	185.8	173.0

Table 5.5: Sensitivity analysis on stage mass

The payload loss capability is about 20 kg in the first case and of about 40kg in the second. An initial vertical velocity 50% larger (150 m/s) has been combined with a reduced horizontal velocity component (30 m/s); in fact, during the pull-up maneuver following the separation from the aircraft, the horizontal component decreases as the vertical one increases.

The feasibility of reaching a 150 m/s vertical velocity by a proper aerodynamic maneuver and with a suitable aerodynamic configuration seems uncertain considering that to reach the 100 m/s vertical velocity, the overall velocity drops during the maneuver from 230 m/s at separation from aircraft to about 170 m/s at ignition; reaching a 150 m/s vertical component would require more time (unless higher loads are accepted), thus further velocity losses, which would make difficult to reach the result.

The presented sensitivity analysis shows in any case that, if feasible, the performance gain is marginal with respect to an increase of the complexity of the system: it appears that the 100 m/s initial vertical velocity combined with a horizontal component of about 130 m/s, is a good compromise between performance and pull-up maneuver possibilities.

The lower curve in the figure 5.28 is relevant to an initial vertical velocity of 50 m/s. The initial horizontal component is 130 m/s; a larger horizontal component would be available which should aid in performance; the analysis has shown a marginal sensitivity of performance to horizontal velocity (3-6 kg of payload depending on the orbital altitude).

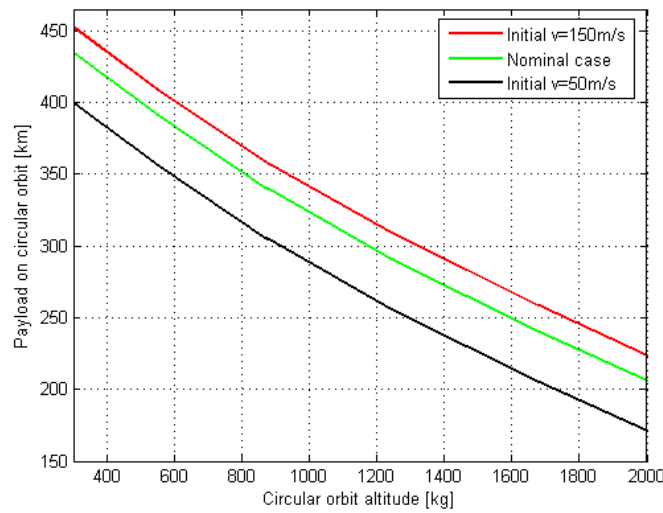


Figure 5.28: Sensitivity on initial in plane speed

It has been also assessed the sensitivity of performance on the occurrence of the fairing separation time, assumed to occur nominally at 180 second from first stage ignition, between 70-90 km altitude.

Figure 5.29 compares this nominal case with the performance resulting with a fairing separation occurring 30 s before, between 60-75 km<sup>2</sup>. A 5-6kg payload increase results, depending on the orbital altitude.

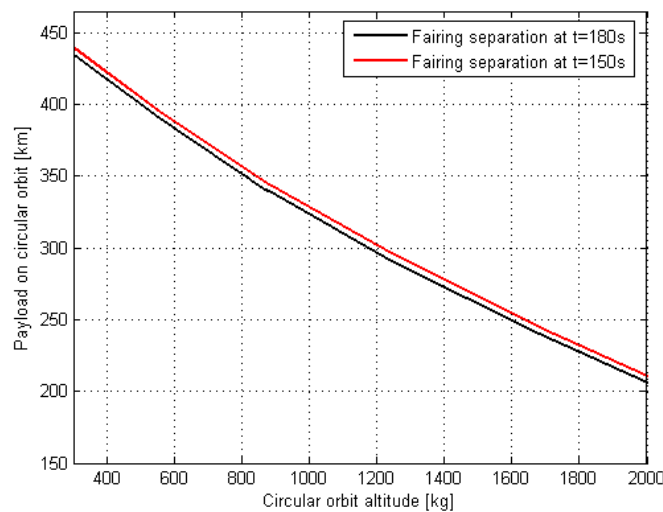


Figure 5.29: Sensitivity on fairing separation time

<sup>2</sup>this has been done because of the thermal fluxes reported in section 5.4

Table 5.6 shows the payload capability variation for the jettison time and initial speed:

Payload capability on circular orbit [kg]				
Altitude orbit[km]	Nominal	Fairing 150s	initial vert speed 150m/s	initial vert speed 50m/s
300	432.5	437.1	445.4	392.92
600	384.6	388.3	397.4	346.69
900	334.9	340.4	350.3	298.65
1200	297.2	302.7	313.1	261.49
1500	260.4	265.9	275.9	225.23
1800	225.4	230.0	239.7	186.25
2000	206.1	210.7	224.	172.66

Table 5.6: Sensitivity analysis on initial vertical speed and fairing separation



## Chapter 6

# Design of Kerosene-LOx launcher

Whenever considering the design and performances of the launcher, a limitation is applied because the overall configuration depends on the components of the corresponding elements of European launcher, especially for the first stage which remains unchangeable. By keeping that constraints an optimal mass distribution among the stages cannot be achieved.

Furthermore the selection of three different kinds of motors for propulsion goes in the opposite direction of having a simple and reliable system.

The cryogenic propulsion engine represents the major problem, because of the safety problems which can occur, considering that the burst during the release can cause, besides the failure of the mission, the lost of the carrier and its crew.

For this reason this chapter has the goal of studying the performances of a launcher, which propulsion system is driven by a liquid, non cryogenic system, whose propellants are liquid kerosene *RP-1* and oxygen.

### 6.1 Falcon I architecture

It can be noted that liquid *RP-1* and oxygen architecture is the same as that used on *Falcon 1*, which is a medium launcher developed by Space-X with private funding and has successfully delivered its first satellite 14 July 2009. The main characteristics of this launcher are listed in table 6.1:

## 6.1. FALCON I ARCHITECTURE

	Stage I	Stage II
Length	21.35m (both stages with fairing and interstage)	
Diameter	1.7m	1.7m;Fairing 1.52m
Dry Mass	1360	550
Usable Propellant Mass	21500kg	4050
Fairing	Aluminum skin and stringer,biconic:	
Structure Type	Monocoque	Monocoque
Material	Aluminum	Aluminum
Engine	Liquid pressure fed on gas generator cycle	Liquid Pressure fed
Engine designation	Merlin 1C	Kestrel 2
Number of engines propellant	LOX/Kerosene	LOX/Kerosene
Thrust	347kN	31kN
Isp	300s	317s
Propellant Feed system	Turbo-pump	Pressure fed
Tank pressurization	Heated Helium	Heated helium
Attitude Control: pitch, yaw	Hydraulic TVC	Electro-mechanical actuator TVC
Attitude control: roll	Turbo-pump exhaust	cold gas thrusters
Nominal burn time	169	418
Shutdown process	Burn to depletion	Predetermined velocity
Stage separation	Explosive bolts with pneumatic pushers	Marmon clamp with pneumatic pushers

Table 6.1: Falcon 1: features



Figure 6.1: Falcon 1

It is noticeable that at the end of the optimization, the launcher system has similar characteristics of *Falcon 1*.

## 6.2 Parametric design for liquid engine rocket

In order to optimize the mass distribution and evaluate performances, it is necessary to design in a parametric way the overall launcher. First of all the configuration used is the same as that studied hitherto, i.e. stages are two with the upper stage and fairing unchangeable with reference to the paragraph 2.3.3.

The propulsion system, meant as sum of nozzle, engine, feed system and tanks, is overriding in the mass budget if compared to the structural items.

The goal of sizing the mass distribution can be fulfilled with the use of nozzle gas-dynamics starting from the knowledge of the thrust furnished by the nozzle, and some physical data about propellants and state of art similar engines<sup>1</sup>.

The main assumptions done, about the engine, are:

1. the specific impulse is 300s at the adaptation altitude: this value is a little less than that of the Merlin 1C in vacuum; the overall effect of the adaptation altitude is to increase the specific impulse of the engine in vacuum, but the difference is amply included in advanced work by Space X which is developing a new kerosene-Lox

---

<sup>1</sup>the reference is the Falcon class of Space X which is improving the overall performances of kerosene-LOx engines

engine with specific impulse equal to 340s; the adaptation pressure has been varied linearly with the thrust in order to reduce the overall dimension but transversal and longitudinal, especially for diameter which is limited to less than 1.5m (for Falcon's engines is less than 1.25m);

2. the combustion chamber pressure is 67atm like Merlin 1C: this value is used for both first and second stage engines; using this values could seem excessive for the second stage, but it implies a heavier propulsion system<sup>2</sup>;
3. the combustion chamber temperature is 3700K, the same of Delta II;
4. the mass ratio of oxidizer/propellant, the heat specific ratio descend from Merlin 1C, meanwhile the values of Mach number and characteristics length of combustion chamber are drawn from literature [23] and listed in table 6.2:

mass ratio $\lambda$	heat specific ratio $k$	Molar mass $m_{mol}[kg/kmol]$	Mach number $M_c$	$l^*[m]$
2.56	1.24	23.1	0.1	1

Table 6.2: Useful data for engine sizing

Furthermore, turbo-pumps with heated helium feed the propulsion system and the nozzle is protected by ablative-radiative layer as it is done for the Falcon 1<sup>3</sup>.

Once imposed the thrust  $T$ , the steps are the following:

1. mass flow

$$\dot{m}_f = \frac{T}{I_{sp}g_0} \quad (6.1)$$

where

- $\dot{m}_f(kg/s)$  is the propellant mass flow,
- $I_{sp}(s)$  is the specific impulse;

2. nozzle throat cross section

$$A_t = \frac{\dot{m}_f \sqrt{\frac{R_{gas} T_c}{m_{mol}}}}{P_c \sqrt{k \left( \frac{2}{k+1} \right)^{\frac{k+1}{k-1}}}} \quad (6.2)$$

---

<sup>2</sup>it has to be taken into account that this assumption, as the following ones, has the only consequence on mass and dimensions, because the performances are imposed by thrust, specific impulse and adaptation altitude

<sup>3</sup>the payload-orbit targets as seen in the previous sections are inferior to these of the Falcon, and so the functioning and heating of the nozzle result limited

- $A_t(m^2)$  is the nozzle throat cross section,
- $R_{gas}(J/(mol \cdot K))$  is the universal gas constant,
- $m_{mol}(kg/mol)$  is the molecular mass of combusted gases,
- $T_c(K)$  is the combustion chamber temperature,
- $P_c(Pa)$  is the combustion chamber pressure;

3. combustion chamber cross section

$$\frac{A_c}{A_t} = \frac{1}{M_c} \sqrt{\left[ \frac{2}{k+1} \left( 1 + \frac{k-1}{2} M_c^2 \right) \right]^{\frac{k+1}{k-1}}} \quad (6.3)$$

- $A_c(m^2)$  is the combustion chamber cross section
- $M_c(-)$  is the Mach number of gases in the combustion chamber;

4. combustion chamber length

$$l_c = l^* \frac{A_t}{A_c} \quad (6.4)$$

- $l_c(m)$  is the combustion chamber length,
- $l^*(m)$  is a characteristic length of the engine;

5. nozzle exit cross section

$$\frac{A_t}{A_e} = \left( \frac{P_e}{P_c} \right)^{\frac{1}{k}} \left( \frac{k+1}{2} \right)^{\frac{1}{k-1}} \sqrt{\frac{k+1}{k-1}} \left[ 1 - \left( \frac{P_e}{P_c} \right)^{\frac{k-1}{k}} \right] \quad (6.5)$$

where

- $A_e(m^2)$  is the nozzle cross section,
- $P_e(Pa)$  is the external pressure acting on the exit section;

6. divergent conic nozzle length with a semi-aperture angle of 30deg

$$l_n = \frac{\sqrt{A_e/\pi} - \sqrt{A_t/\pi}}{\tan \alpha_{semi-aperture}} \quad (6.6)$$

where

- $l_n(m)$  is the nozzle divergent length
- $\alpha_{semi-aperture}$  is the semi-aperture angle of the

The overall propulsion system mass has been calculated on the base of a statistical approach, derived from [23]. This method uses the mass of the an element for establishing the mass of the system; it could be used the engine mass but its small dimension, due to the mass flow rate, leads to lighter engines. On the contrary the nozzle mass allows to obtain mass system comparable to Merlin and to HM7B engines<sup>4</sup>.

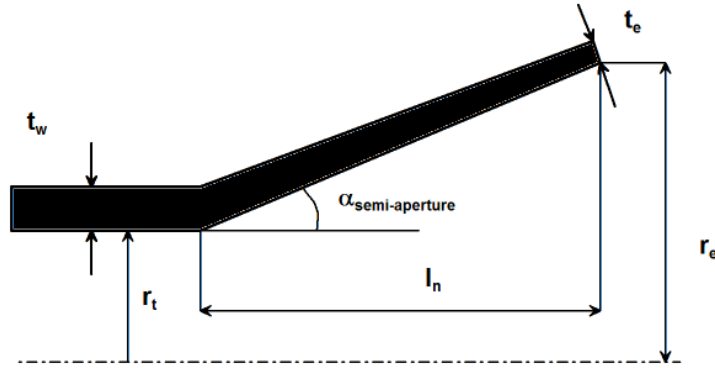


Figure 6.2: Nozzle definitions

Considering the figure 6.2, the mass of the nozzle, in tapered wall configuration, results:

$$m_n = 2\pi\rho l_n \left[ \frac{1}{3}f_1f_2l_n^2 + \frac{1}{2}(f_1r_t + f_2t_t)l_n + r_t t_t \right] \quad (6.7)$$

where

- $\rho_{Ni}(kg/m^3)$  is material density, that for the chosen nickel alloy is equal to  $8500kg/m^3$
- $t_t(m)$  is the throat thickness, assumed equal to that of the combustion chamber;
- $t_e(m)$  is the exit thickness, assumed as a fraction  $3/4$  of the throat thickness;
- $f_1(-)$  and  $f_2(-)$  are dimensionless parameters based on the nozzle geometry:

$$f_1 = \frac{t_e - t_t}{l_n} \quad (6.8)$$

$$f_2 = \frac{r_e - r_t}{l_n}. \quad (6.9)$$

The wall thickness of the combustion chamber,  $t_w(m)$  comes from

$$t_w = \frac{P_b r_c}{F_{tu}} \quad (6.10)$$

where

<sup>4</sup>adaptation pressure plays a considerable role in defining masses and sizes

- $P_b(Pa)$  is the burst pressure, equal to that of combustion chamber multiplied for a safety margin of 2;
- $r_c(m)$  is the combustion chamber internal radius,
- $F_{tu}(Pa)$  is the ultimate stress, that for the chosen nickel alloy is 310MPa.

Following the statistic approach the overall mass of the propulsion system  $M_{prop-system}$  results (see [23]):

$$M_{prop-system} = \frac{m_n}{0.168}$$

### 6.3 Parametric design for the structures

Once established the burning time for each stage it is possible to size all structural elements in terms of mass and dimensions. The transversal dimension of the launcher is the same as that used for the previous launcher, i.e. 1.9 m.

The procedure follows the same step using characteristics margin of safety as those seen in section 2.3, with the only difference is the presence of kerosene, whose density is  $\rho = 810 kg/m^3$  :

1. tank pressure for both oxygen and kerosene is 3 atm
2. tank mass derives from eq.2.1 to eq.2.3
3. helium mass is calculated from eq.2.7
4. helium tank derives from eq.2.4
5. insulation layer is a fraction of the tank mass
6. structural mass is obtained assuming aluminum alloy panels of 1mm thick

Using two stages, besides the structures seen, it has to be considered an interstage whose mass is summed to that of the first stage. Because the dimensioning of the interstage can not prescind from the knowledge of the power spectrum, it has been used a 2.5mm thick aluminum annular ring as for the previous launcher, with a margin of 50% on mass.

Other elements included in the sizing are the separation system of 35kg, the CPU and other devices with overall mass of 40kg.

The third stage is unchangeable with respect to the previous launcher.

## 6.4 Optimization procedure

The search for a solution that has to fit a certain number of constraints has been done exploiting a minima search algorithm<sup>5</sup>. Besides the standpoint of the sizing about the third stage, it has assumed that the fairing separation occurs after about 160s, a value inferior to that used for the previous analyses.

The function that has been minimized is represented by the amount of the propellant burnt to circularize the orbit at the second stage burnout taking into account some constraints.

In general the number of constraints can be different from the number of the independent variables involved in the minimization problem. In this case it has been chosen to use the same number with some constraints that can be considered redundant. Nevertheless the problem is highly non linear; this causes the presence of multiple minima, and the solution can converge to a non optimal minimum, because optimization is strongly dependant from the initial conditions.

The constraints imposed are:

1. the amount of propellant used to be less than 40kg<sup>6</sup>;
2. the circular orbit altitude, after second burnout, limited between 100 and 150 km, similar to the case treated in chapter 5;
3. maximum acceleration less than 5.8g;
4. overall launcher mass less than 25000kg;
5. path angle at second stage ignition less than  $\pi/8$ <sup>7</sup>;

The variables, which allows to define the launcher in its size and dimensions, are the thrust and the burning time. Another variable is represented by the initial path angle, because of the gravity turn phase which has a considerable effects on the final altitude. Thus the vector on which the optimization has been performed is:

$$[ T_1 \quad T_2 \quad t_{burning1} \quad t_{burning2} \quad \theta_0 ] \quad (6.11)$$

where

---

<sup>5</sup>the *fmincon* function of *Matlab* [24]

<sup>6</sup>this is redundant but necessary for avoiding non optimal minimum

<sup>7</sup>this helps accelerating the launcher tangentially



- $T_1(N)$  is the first stage vacuum thrust,
- $T_2(N)$  is the second stage vacuum thrust,
- $t_{burning1}(s)$  is the first stage burning time,
- $t_{burning2}(s)$  is the second stage burning time,
- $theta_0(rad)$  is the initial FPA.

### 6.4.1 Discussion

Table 6.3 report optimization results in terms of thrusts and burning time compared to the assembled case:

	$T_1[kN]$	$T_2[kN]$	$t_{burning1}[s]$	$t_{burning2}[s]$	$\theta_0[deg]$
Kerosene/LOx launcher	361.46	48.76	94	364.8	78.9
Assembled launcher	310	64.8	117	380	85.5

Table 6.3: Optimization kerosene/LOx launcher

As it can be seen those parameters differ considerably, except for the second stage burning time which is almost equal. It has to be highlighted that the ratio between thrusts in the optimized launcher is about 9, which is close to the value of Falcons' reported in table 6.1.

Performances are similar to the assembled launcher for what concerns the mass on orbit and altitude at second stage burnout and circularization:

	Circular orbit altitude 2 <sup>nd</sup> stage	Mass on orbit
Kerosene/LOx launcher	120	558
Assembled launcher	123	566

Table 6.4: Optimization kerosene/LOx launcher

The mass distribution results different from the assembled case, but the effect on performances is not so predominant:

	Mass at first ignition [kg]	Mass at second ignition [kg]
Kerosene/LOx launcher	18837	5878
Assembled launcher	18385	7265

Table 6.5: Kerosene/LOx launcher: mass subdivision

#### 6.4. OPTIMIZATION PROCEDURE

---

As it can be inferred from table 6.4 and 6.5, the optimization leads to a system whose characteristics are different from the assembled launcher and whose performances are very almost equivalent.

Table 6.6 shows the two engines mass and size characteristics:

	First stage engine	Second stage engine
Mass [kg]	790	136
Overall length [m]	1.71	1.50
Nozzle diameter [m]	1.06	0.64

Table 6.6: LOX-Kerosene launcher: engines characteristics

Those results are noticeable especially for what concerns the second stage whose characteristics are coherent with those of HM7B (see section 2.2.2), considering the thrust difference.

The position of the center of gravity moves forward (table 6.7) :

	Mass [kg]	Position [mm]
Engine 1	790	1400
TVC device 1	55.3	1500
Insulation+structure 1	150.5	4152
Tank+Propellant 1	11929.6	3662
Tank helium+ devices 1	33.7	6397
Interstage	189.3	7495.5
Engine 2	136	8096
TVC device 2	16.4	8296
Tank+Propellant 2	4655.8	9158
Insulation + structure 2	61.6	9304
Tank Helium+guide	48.8	10063
Third stage	270	11213
Fairings	200	11213
Payload	300	12713
Rocket	18837	5370.

Table 6.7: LOx-Kerosene:Elements mass and CoG with complete mass budget

Furthermore, third stage mass and assembly have great influence on the center of gravity

#### 6.4. OPTIMIZATION PROCEDURE

with severe consequences on the separation manoeuvre. As far as a variable payload from 150 to 400 kg, center of gravity varies considerably:

$$5300 - 5450mm$$

Thanks to the use of kerosene in place of the hydrogen in second stage, the launcher results to be more compact with an overall length of about 15 m.

Although the fairing envelope is assumed equal to the assembled launcher, considering also the second stage mass and thrust reduction, it is also reasonable to reduce its dimensions, which could lead to a decrease of the mass with beneficial effects on the payload on orbit.

The mass breakdown for the two stages is reported in figure 6.3 and table 6.8; it has not been included the mass of the fairing for the second stage :

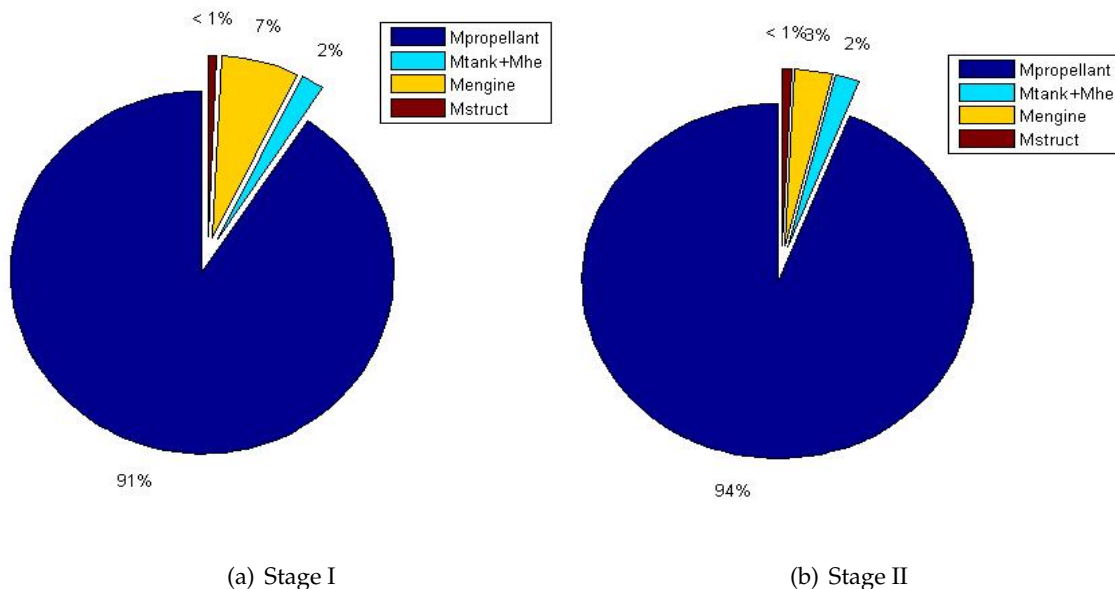


Figure 6.3: Mass breakdown

First stage mass [kg]	Second stage mass [kg]
12959	5308

Table 6.8: Stage masses

Considering the overall mass of the launcher the structural ratio is about the 10%, which is higher than other system such as the Falcon 1, and it is due to the high margin used. This gives robustness to the results obtained, but this paper represents a *phase A* study for estimating the feasibility of the air-launcher and its performances.

### 6.4.2 Performance

Table 6.4 reports the comparison between the performances<sup>8</sup> of the RP1-oxygen launcher and the assembled one, in terms of payload mass on circular orbit:

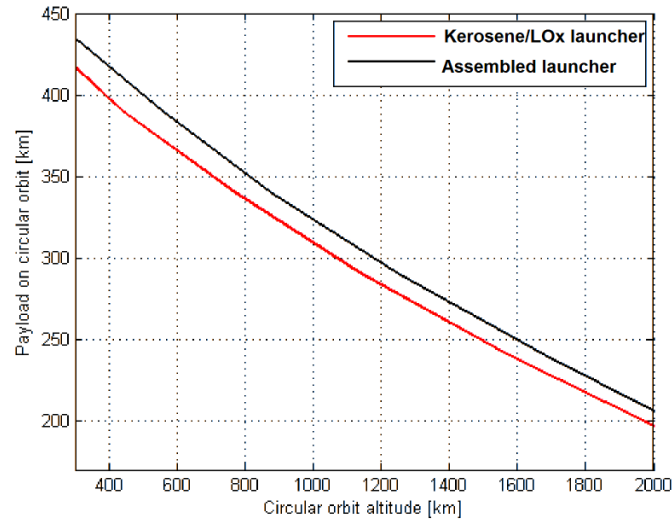


Figure 6.4: Performance comparison in nominal condition

Despite the differences in propulsion and in mass, the kerosene launcher conserves good performances as reported in table 6.9. The difference is in mean terms of about 20kg.

Payload capability on circular orbit [kg]		
Altitude orbit[km]	Assembled launcher	Kerosene launcher
300	432.5	415.1
600	384.6	363.4
900	334.9	319.4
1200	297.2	280.2
1500	260.4	241.0
1800	225.4	209.5
2000	206.1	195.2

Table 6.9: Comparison between assembled and kerosene launcher

It has to be noted that the difference in mass and configuration between the launchers allows the use of the same system designed for the release manoeuvre of the assembled

<sup>8</sup>the difference may be more than that seen in table 6.4 because of the optimization done for the controlling phase

launcher modifying only the relative position of the wing with respect to the center of gravity (see table 6.10).

Arm of the horizontal surface lift wrt CoG	4.3 m (geometrically defined)
Arm of the body-wing lift wrt CoG	0.74 m in front of CoG

Table 6.10: The Aero-Module for LOx-kerosene launcher: trimming and centers of pressure

The first stage has a greater structure to overall mass ratio if compared to other launcher such as the Falcon, which has 6.5% ratio, and strengthening are required for the release manoeuvre; all that in mind, a sensitivity analysis has been performed, reducing the inert mass to 7%.

Furthermore the fairing mass can be reduced on the basis of a smaller envelope , with an height of 3.5 m, which implies a fairing mass of 135kg. The effect of the two is then considered in a third sensitivity analysis reported in figure 6.5:

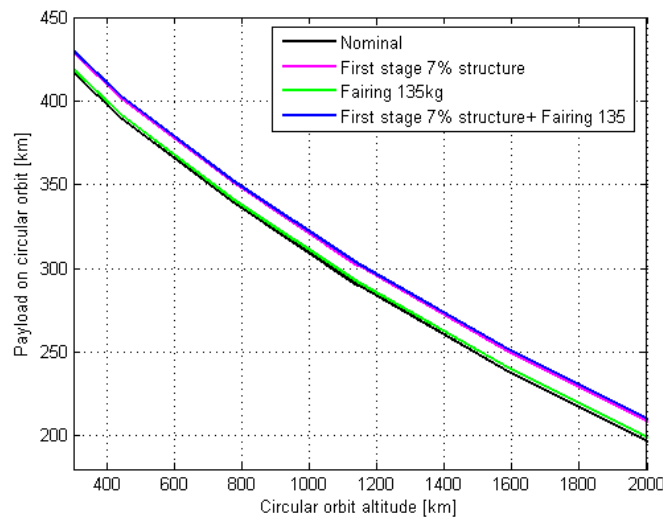


Figure 6.5: LOx-Kerosene: sensitivity analysis

The effect of structure mass reduction on the first stage is predominant, with an increase of about 12 kg with respect to the nominal case. Table 6.11 reports the payload capabilities variation for the different configuration.

Payload capability on circular orbit [kg]				
Altitude orbit[km]	Nominal	Fairing mass 135kg	Stage1 structure	Stage1+Fairing
300	415.1	416.1	424.7	427.9
600	363.4	367.8	378.27	378.9
900	319.4	322.1	331.5	333.2
1200	280.2	282.5	295.2	297.6
1500	241.0	245.4	258.9	260.5
1800	209.5	211.2	230.5	231.3
2000	195.2	197.7	209.2	210.9

Table 6.11: Sensitivity analysis on kerosene launcher mass

The fairing mass has a low impact on the performance, because the increase is only of about 2 kg. This effect is shown also in the third sensitivity analysis. In this way the performances of the LOx-Kerosene launcher result to be almost similar to that of the assembled one, thanks to the optimization conducted for establish the mass ratios.

### 6.4.3 Direct insertion

For the kerosene-LOx launcher the direct insertion problem has been considered too. A Genetic Algorithm has been exploited to avoid being trapped in local minima. The aim was to assess a different launch strategy which allows to reduce the overall time passing from the release to the payload insertion on the orbit.

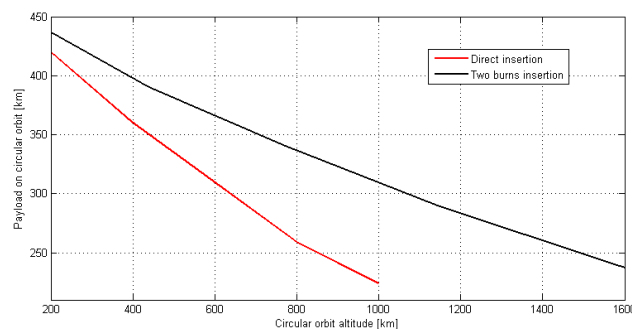


Figure 6.6: Two burns insertion and direct insertion for kerosene-LOx launcher

This difference is due to the fact that direct insertion increases gravity losses, with the result of a reduced delivered payload mass capability. Table 6.12 shows that this

difference is in the order of more than 60kg.

Payload capability on circular orbit [kg]		
Altitude orbit[km]	Two burns	Direct insertion
200	437.7	419.7
400	399.1	362.5
600	363.4	314.8
800	338.7	267.0
1000	312.2	234.1

Table 6.12: Comparison between direct and two burn insertion

As it can be seen in the figure 6.6, the trend of the curves are very similar to that are shown in the Falcon User’s Manual and reported in figure 6.7.

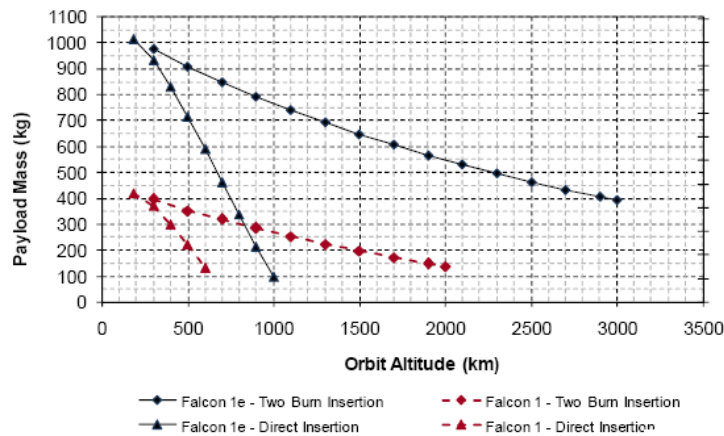


Figure 6.7: Two burns insertion and direct insertion for different Falcon launcher

The different slope of the curves can be attributed to the different launch strategy.

## Chapter 7

# Refined model for performances evaluation

The rocket is released from the carrier in a manner that its attitude is not that which is exactly needed to the initial phase of the power ascent. The estimation of the control needed to rotate the launcher and put it on the orbital plane allows to obtain some further information about the effective payload put on orbit.

This chapter briefly analyzes some aspects that should be developed in future works.

### 7.1 Rocket Attitude

With the set of equations used in chapter 5 is not possible to consider how rocket has to correct its attitude in order to direct thrust and obtain the desired position on the orbital plane.

Rocket has its own attitude with respect to the inertial frame, which can be expressed by a matrix  $A$ . It is useful to write this matrix in terms of quaternions, then (see [25]):

$$A = (q_4^2 - \mathbf{q}^T \mathbf{q}) I + 2\mathbf{q} \cdot \mathbf{q} - 2q_4 [\mathbf{q} \times] \quad (7.1)$$

where  $\mathbf{q} = [q_1, q_2, q_3]^T$ ,

$$q_1 = e_1 \sin \frac{\chi}{2} \quad (7.2)$$

$$q_2 = e_2 \sin \frac{\chi}{2} \quad (7.3)$$

$$q_3 = e_3 \sin \frac{\chi}{2} \quad (7.4)$$

$$q_4 = \cos \frac{\chi}{2} \quad (7.5)$$



where

$$\chi = \arccos \left( \frac{1}{2} (tr(A) - 1) \right) \quad (7.6)$$

$$e_1 = \frac{A_{23} - A_{32}}{2 \sin \chi} \quad (7.7)$$

$$e_2 = \frac{A_{31} - A_{13}}{2 \sin \chi} \quad (7.8)$$

$$e_3 = \frac{A_{12} - A_{21}}{2 \sin \chi} \quad (7.9)$$

Momentum equations are necessary to define how thrust has to be controlled in order to achieve and remain on orbital plane with respect to the local tangent. In this case it is convenient to write those equations in principal axis :

$$I_{inertia} \frac{d\omega}{dt} + \omega \times I_{inertia} \omega = \mathbf{M}_c \quad (7.10)$$

where

- $\omega(rad/s)$  is the angular velocity vector of  $\omega_x, \omega_y$  and  $\omega_z$  components,
- $M_c(Nm)$  is the control momentum vector proportional to attitude error of  $M_{c,x_r}, M_{c,y_r}$  and  $M_{c,z_r}$ ,
- $I_{inertia}(kgm^2)$  contains *inertiae* momentum about principal axis.

Adding this equation to those seen the launcher behavior is described as a six degrees of freedom body.

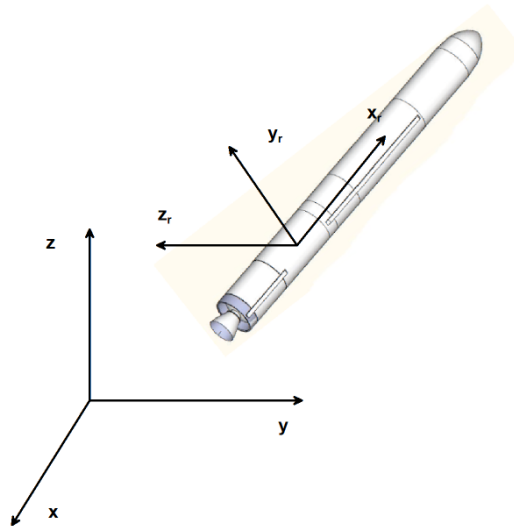


Figure 7.1: Rocket principal axis

Referring to figure 7.1 and considering axial symmetry , *inertiae* result in table 7.1:

$I_{x_r} \text{ Kgm}^2$	$I_{y_r} \text{ Kgm}^2$	$I_{z_r} \text{ Kgm}^2$
10785.31	501908.21	501908.21

Table 7.1: First stage *inertiae*

Finally attitude must be updated:

$$\frac{d\mathbf{q}}{dt} = \begin{bmatrix} 0 & \omega_{z_r} & -\omega_{y_r} & \omega_{x_r} \\ -\omega_{z_r} & 0 & \omega_{x_r} & \omega_{y_r} \\ \omega_{y_r} & -\omega_{x_r} & 0 & \omega_{z_r} \\ \omega_{x_r} & \omega_{y_r} & -\omega_{z_r} & 0 \end{bmatrix} \mathbf{q} \quad (7.11)$$

The attitude determination is with respect to the local on-orbit plane frame (see figure 7.2):

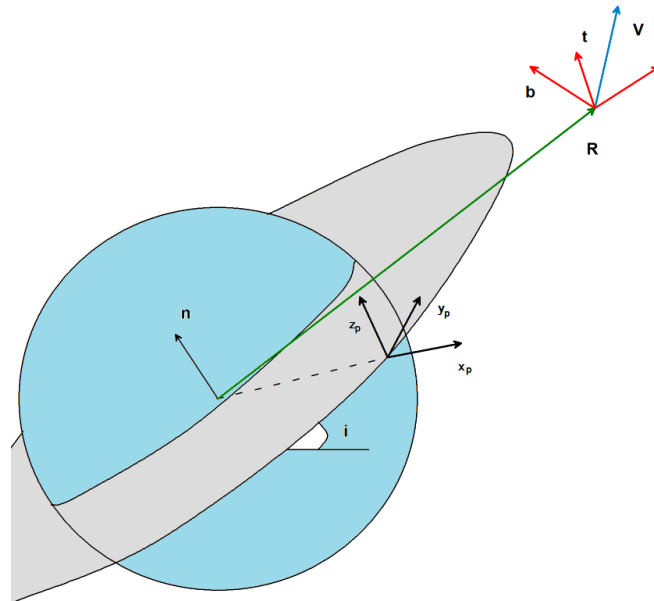


Figure 7.2: Attitude reference frames

As seen in section 4.5 local on-orbit plane frame is defined by the normal to plane  $z_p$ , the projection of  $\mathbf{R}$  on the local plane  $x_p$ , and  $y_p$  completes the frame.

The other frames, whose center is on the rocket, is defined by the versor  $\mathbf{r}$ , in  $\mathbf{R}$  direction, the projection of  $\mathbf{v}$  normal to  $\mathbf{r}$ , and  $\mathbf{b}$  completes the frames.

## 7.2 Rocket controller

The aim of controller is to put rocket on the plane and to assure that it will follow a determinate path angle, so that the global speed lies in the orbital plane. Once reached the plane, the problem can be solved by the same method exposed in section 4.5.2. In this way the target matrix is represented by:

$$A_{target} = [\mathbf{x}_p, \mathbf{y}_p, \mathbf{z}_p] \quad (7.12)$$

Defining the second frame with respect to the local on orbit plane by a generic matrix  $A_{rtn}$ , the matrix error results:

$$A_e = A_{target} \cdot A_{rtn}^T$$

Remembering that thrust vector control is limited on the plane normal to  $\mathbf{x}_r$ , control is done only about  $\mathbf{y}_r$  and  $\mathbf{z}_r$ . In this way the error due to misalignment and in the plane results:

$$err_y = \frac{1}{2} (A_{e21} - A_{e12}) \quad (7.13)$$

$$err_z = \frac{1}{2} (A_{e32} - A_{e23}) \quad (7.14)$$

$$(7.15)$$

Therefore also the error about  $\mathbf{x}_r$  is considered because it couples the dynamic about the other two axis:

$$err_x = \frac{1}{2} (A_{e12} - A_{e21}) \quad (7.16)$$

Control *momenta* in eq. 7.10 behave as a spring-damper system and result:

$$M_{c,x_r} = 0; \quad (7.17)$$

$$M_{c,y_r} = -k_{yz} \cdot err_z - k_{yx} \cdot err_x - c_y \cdot \omega_{y_r}; \quad (7.18)$$

$$M_{c,z_r} = -k_{zy} \cdot err_y - k_{zx} \cdot err_x - c_z \cdot \omega_{z_r}. \quad (7.19)$$

The first is set to zero because of the previous hypothesis. Coefficients are different at each latitude and each inclination. Control momentum is limited by the maximum value achievable by the thrust vector control:  $M_c$  is limited to:

$$M_{cMAX} = \pm T_{x_r-y_r} \cdot l_{cg}.$$

where

- $M_{cMAX}(N)$  is the maximum control momentum norm on  $x_r$  and  $y_r$  axis,

- $T_{x_r-y_r}(N)$  is the thrust norm on  $x_r$  and  $y_r$  axis,
- $l_{cg}(m)$  is the exit section, on which the thrust is localized, distance from the centre of mass.

Finally components of thrust on  $y_r$  and  $z_r$  are calculated by inverting the previous expression, meanwhile along  $x_r$  is given by:

$$T_{z_r} = \sqrt{T^2 - T_{y_r}^2 - T_{x_r}^2}$$

then they are rotated in the local frame, because attitude is expressed in global frame:

$$\mathbf{T}_1 = A\mathbf{T}_r \quad (7.20)$$

### 7.3 Results

It has been tested the case reported in the section 5.3, with the following assumption, i.e. the rotational phase, also called Eulerian phase, controls the first stage till the attitude reaches a certain angle, after which the control can be accomplished by the thrust vector control of the nozzle. Then the second stage behaves as exposed in chapter 5.

The difference between this method and the previous is that also first stage is controlled in order to achieve at the burnout the orbital plane and the desired orientation of  $\mathbf{V}_{in}$ <sup>1</sup>. As initial condition, it has assumed that the launcher axis forms an angle of about 80 deg with the plane:

---

<sup>1</sup>control is limited and the definition of optimal control is not the purpose of this work

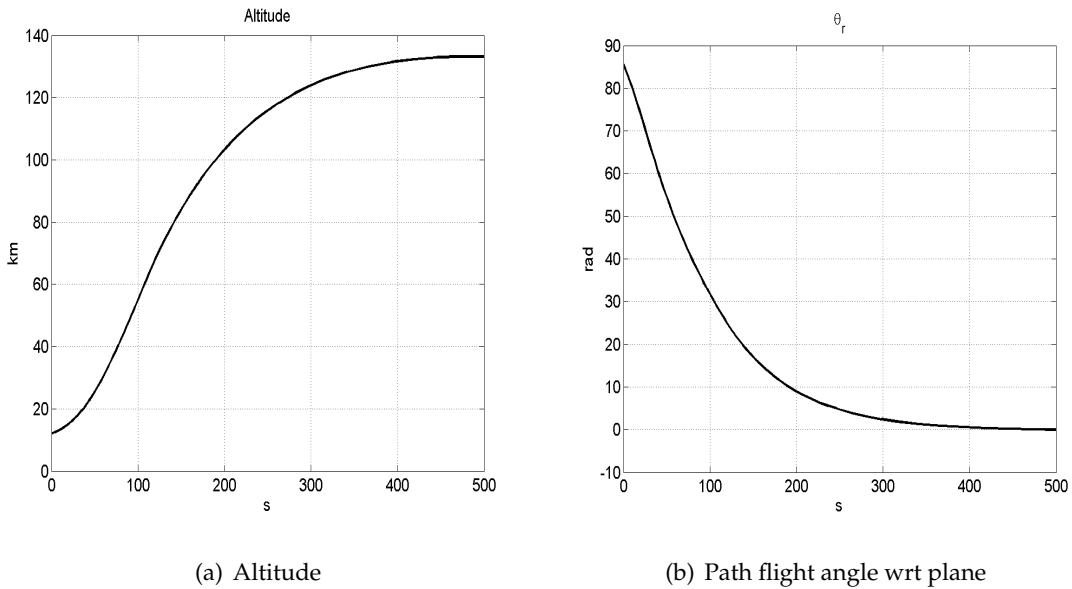


Figure 7.3: 6 DoF Assembled launcher: Altitude and  $\theta_r$ .

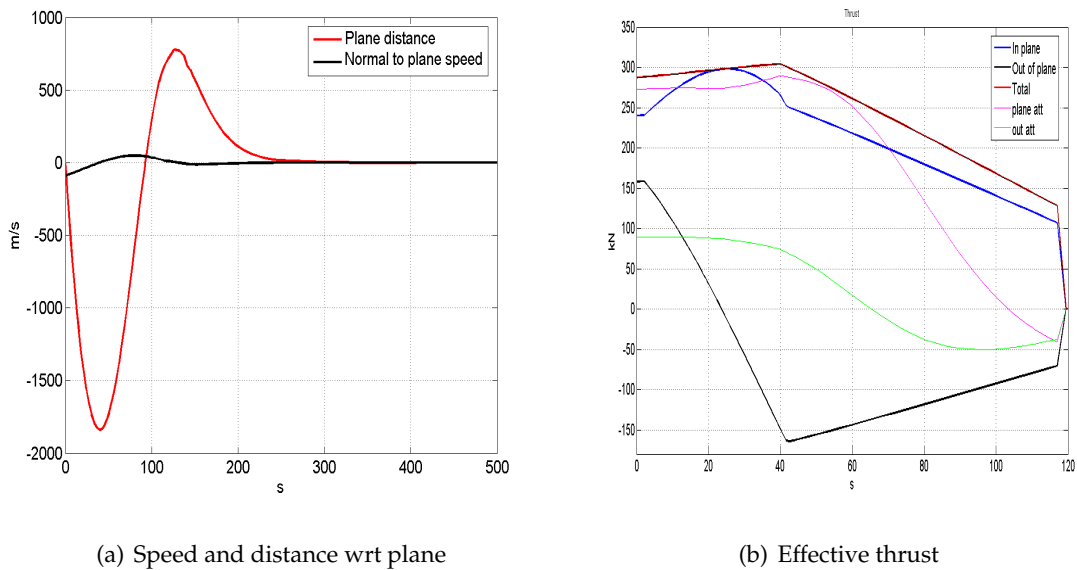


Figure 7.4: 6 DoF Assembled launcher: parameters and thrust wrt plane

As can be seen by figures 7.3 and 7.4, the effect of this kind of control is a kind of *strengthening*, because the launcher maintains a vertical attitude so that it achieve higher altitude of about 130 km (instead of 123), paying a major propellant consumption of about 4kg.

The passage from one phase to the other has been done in the second stage burn:

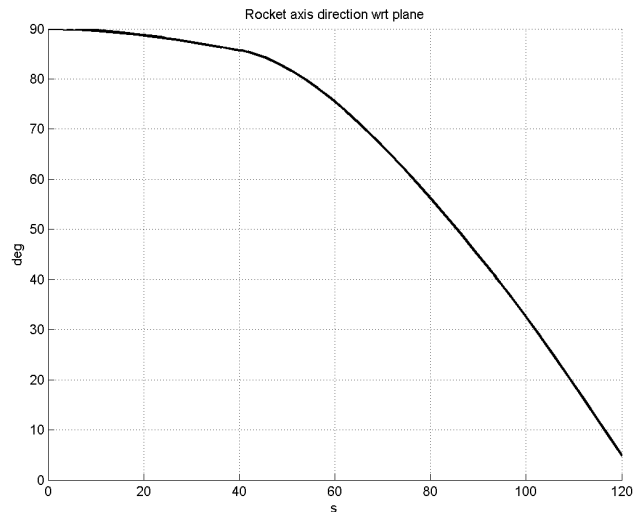


Figure 7.5: Angle between  $x_r$  projection on  $z_p - y_p$  plane and orbital plane

Figure 7.5 reports the trend of Angle between  $x_r$  projection on  $z_p - y_p$  plane and orbital plane: the launcher axis, at the first stage burn-out, is nearly on the plane so the control can be accomplished by the thrust vector control.

## 7.4 Consideration

The attitude assumption on the initial condition is very demanding and it represents a hint for further study, because this means that the Aero-Module has to detach from the launcher, giving a rotation so that the final angle reduce the control loss.

In fact for lower angle the payload capabilities tend to decrease considerably, for example for an angle of 70deg the loss is of about 20kg.

This tendency has been highlighted also by Darpa's studies on the Falcon Small Launch Vehicle program (see par.1.3.6 and [26]).

## Chapter 8

# Conclusions

The results obtained along this study has fulfilled the objective of obtaining a robust and sufficiently detailed preliminary models for Boreas air-launch vehicle, which in the industrial field, is defined as phase A. It has been demonstrated the feasibility of the overall configuration, with the availability of sensitiveness and performances analyses. Thanks to the use of a conservative approach, those results have been enforced with the comparisons to equivalent systems.

### 8.1 Innovative aspects

From the conceptual point of view the main innovative aspect is related to the launch method which occurs on the top of the aircraft. The second thing concerns the fact that the so called Aero-Module, the winged part of the launcher, is separated soon before the ignition of the first stage engine. This strategy allows to reduce the inert weight of the system, and differs from all existing or proposed systems, where the wings are separated with the first stage, beyond the fact that their dimension is reduced with respect to the Boreas' ones.

For what concerns the project and the design of the system, it has be pointed out that during the work the methodology has progressively got inside a Multidisciplinary Design, exploiting the synergies of mutually interacting phenomena. Optimization tools, both local and global, have been used to identify a pool of preferred solution.

During the study for the assembled launcher the possibility to exploit sinergies has been limited to the control system and structure due to the fact of using components off the shelf. The design of the kerosene-LOx launcher, instead, led the exploitation of the

interactions of the subsystems, mainly propulsion, structure and control which concur to the mass definition.

The assembled launcher presents different types of propulsion systems ( solid, cryogenic and storable propellant are used) which imply strong hazards during the transportation on the top of the A/C from take-off up to the release of the launcher, because of the thermal loads due to the aerodynamic drag and the time taken to reach the launch area from the ground base.

The hydrogen could be internally carried in the A/C and provided few minutes before the release, but this would make the system more complicated. Moreover this strategy would reduce only the hazard related to the transportation during flight but would introduce other concerns on the supplying interface between A/C and the launcher.

On the contrary the kerosene-Lox launcher results safer under this point of view thanks to the use of more stable propellants.

For what concerns the release manoeuvres, both horizontal and inclined strategies have proved to be able to give suitable initial conditions for the ascent phase. The second strategy seems to be less reliable because of the complexity with which it has to be performed. In order to reduce possible hazards during the release the first one has to take into account for future developments.

Nevertheless the release manoeuvre without active control represents an open issue, because the external environmental conditions, such as gust and lateral wind, together with the aerodynamic influence between A/C and Aero-Module could affect the overall manoeuvre, in terms of hazards, performances reduction or mission abort.

## 8.2 Future developments

For what concerns the use of the launchers studied in this thesis some hints for future developments can be proposed, in order to produce a more faithful model:

1. to develop the software including extensively the six-degrees of freedom of the rocket as treated in chapter 7.4
2. to study the critical aerodynamic aspects of separation at the initial phase of flight
3. to study the Aero-Module interference with rocket at separation and impacts on performances (as it has been highlighted in the section 7.4)



4. to analyze in detail and size the structural impacts of the attachment points on the launcher and the A/C, including the study of erection system on the top of the A/C,
5. to analyze in detail the thermal loads impact on the configuration,
6. to assess the feasibility of the identified control laws by the control actuation system.

These developments should take into account a more structured Multi Disciplinary Optimization approach to get the benefits of the method.

Moreover from the practical point of view, it can be proposed to valuate the costs of the system, considering also the possibility to recover and reuse the Aero-Module and the first stage, which are the most expensive element of the launcher, though this possibility could imply the presence of a parachute and other components with the task of protecting critical elements. The reuse of a recoverable system offers two primary promising advantages. First the obvious saving in costs reusing launch system components, rather than building new components for each flight. Secondly, by spending less money on manufacturing new flight vehicle each time they are flown, more money may be spent on developing a launch operations infrastructure that permits a higher flight frequency, reducing recurring costs per flight (which are also limited by the use of air-launch).

An interesting hint for the use of the system it is represented by the commercial application of this system for sub-orbital space tourism flights. This choice would require a complete re-design, for example including the Aero-Module in the manned module with active surface control for the re-entry and return to a ground base.

# References

- [1] C. Bonnal C. Talbot. Surrey university guest lecture: Air launch solutions for microsattellites. CNES, September 2008.
- [2] Kosmotras. *Dnper User's Manual*, 2001.
- [3] Arianespace. *Vega User's Manual*. Arianespace, March 2006.
- [4] Eurockot. *Rockot User's Manual*, 2004.
- [5] Russian Space Agency. <http://www.russianspaceweb.com/cosmos3.html>, June 2009.
- [6] Indian Space Research Organisation. <http://www.isro.org/>, June 2009.
- [7] Eugene F. Megyesy. *Pressure vessel handbook, 14th edition*. PV PUBLISHING, INC., 2008.
- [8] Z.T.C. Zandbergen. <http://www.lr.tudelft.nl/live/pagina.jsp?id=416497e6-bd6b-44f0-8889-14231a648af4&lang=en>, July 2009.
- [9] Charles D. Brown. *Elements of Spacecraft Design*. American Institute of Aeronautics and Astronautics, 2002.
- [10] Luigi De Luca. Appunti del corso di sistemi di propulsione e potenza per lo spazio, March 2008.
- [11] Giampiero Bindolino. Dispense dell' insegnamento costruzioni aeronautiche, 2004.
- [12] Airbus. *A330, Airplane Characteristics*, February 2009.
- [13] Airbus. *A300, Airplane Characteristics*, February 1983.
- [14] A.C. Kermode. *Mechanics of flight*. Pearson, Prentice Hall, 1996.
- [15] Anandkrishnan Frank J. Regan. *Dynamics of atmospheric re-entry*. American Institute of Aeronautics and Astronautics, 1993.

- [16] Martin JL Turner. *Rocket and Spacecraft Propulsion*. Elsevier Publishing Co., 2005.
- [17] Zucrow Bonney and Besserer. *Principles of guided missile design*. Grayson Merrill, 1952.
- [18] John Anderson. *Fundamentals of Aerodynamics*. 2005.
- [19] Range Safety Office. Eastern and western range, 1997.
- [20] Maurizio Boffadossi. Appunti del corso di complementi di aerodinamica, 2007.
- [21] Orbital Company. *Pegasus User's Manual*, 6.0 edition, 2006.
- [22] SpaceX Company. *Falcon 1 User's Manual*, 2008.
- [23] Larson Humble, Henry. *Space Propulsion Analysis And Design*. McGraw-Hill Companies, 1995.
- [24] Mathworks. <http://www.mathworks.com/access/helpdesk/help/toolbox/optim/ug/fmincon.html>, November 2009.
- [25] Franco Bernelli Zazzera. Appunti del corso di dinamica e controllo di assetto, 2008.
- [26] Gary C. Hudson Marti Sarigul-Klijn, Nesrin Sarigul-Klijn and and Chris Webber Livingston Holder. Gravity air launching of earth-to-orbit space vehicles. *AIAA Space*, 7256, 2006.
- [27] Carlo Grillo Pasquarelli. *Dinamica del missile, 1ed*. Torino: Lito-Copisteria Valetto-Marcorello, 1972.
- [28] Hammond. *Design Metodologies for space transportation systems*. American Institute of Aeronautics and Astronautics, 2001.
- [29] Hammond. *Space Transportation: a systems approach to analysis and design*. American Institute of Aeronautics and Astronautics, 1999.
- [30] Thompson. *Space Vehicle Dynamics and Controll*. American Institute of Aeronautics and Astronautics, 1998.
- [31] Frederick Boltz. *Optimal Ascent Trajectory for Efficient Air Launched into Orbit*. American Institute of Aeronautics, 2004.
- [32] [http://en.wikipedia.org/wiki/pressure\\_vessel](http://en.wikipedia.org/wiki/pressure_vessel), June 2009.
- [33] Seiji Matsuda. Affordable micro satellites launch concepts in japan. 2008.

- [34] [http://en.wikipedia.org/wiki/space\\_shuttle\\_program](http://en.wikipedia.org/wiki/space_shuttle_program), July 2009.
- [35] Silvio Cammarata. *Sistemi Fuzzi: un'applicazione di successo all'intelligenza artificiale*. ETASLIBRI, 1994.
- [36] Randy L.Haupt and Sue Ellen Haupt. *Practical Genetic Algorithms*. John Wiley & Sons, Inc., 1997.
- [37] Gary C. Hudson Bevvin McKinney et al. Marti Sarigul-Klijn, Nesrin Sarigul-Klijn. Selection of a carrier aircraft and a launch method for air launching space vehicles. *AIAA Space*, 7835, 2008.
- [38] Marti Sarigul-Klijn and Nesrin Sarigul-Klijn. A study of air launch methods for RLVs. *AIAA Space*, 4619, 2001.
- [39] Michael D. Griffin and James R. French. *Space Vehicle Design*. American Institute of Aeronautics and Astronautics, 1991.
- [40] James Barrowman. Calculating the center of pressure of a model rocket. Technical report, Centuri Engineering Company, 1988.
- [41] Gregg Liesman Marti Sarigul-Klijn, Dan Fritz and Maurice P. Gionfriddo. Flight testing of a gravity air launch method to enable responsive space access. *AIAA*, 6146, 2007.

# Appendix A

## Software Validation

The software developed for the rocket dynamic described in chapter 5 has been validated both using a Fortran routine available in Carlo Gavazzi Space and testing it taking the Pegasus launcher as reference.

The first comparison is necessary to avoid numerical problem giving robustness to the software written, meanwhile the second is useful to state if the software is reliable.

### A.1 Comparison with Fortran

The Fortran software, to which the software developed in this thesis has been compared, was tested for many conditions and has proven to give results coherent with the *Matlab* one.

The results reported hereafter in figures A.1, A.2, A.3 and A.4 descend from the simulation with the same initial flight conditions in the section 5.3:

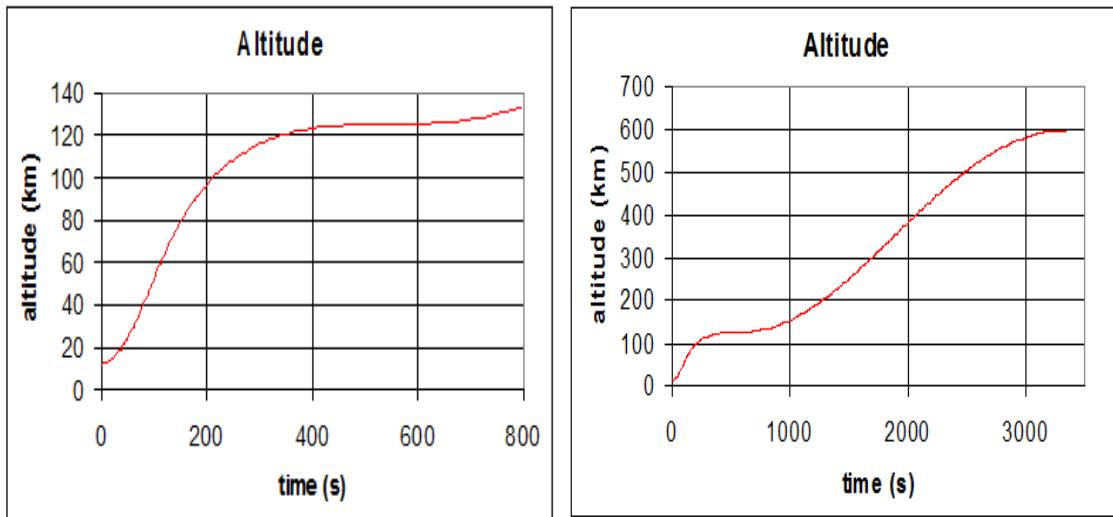


Figure A.1: Fortran simulation results: Altitude

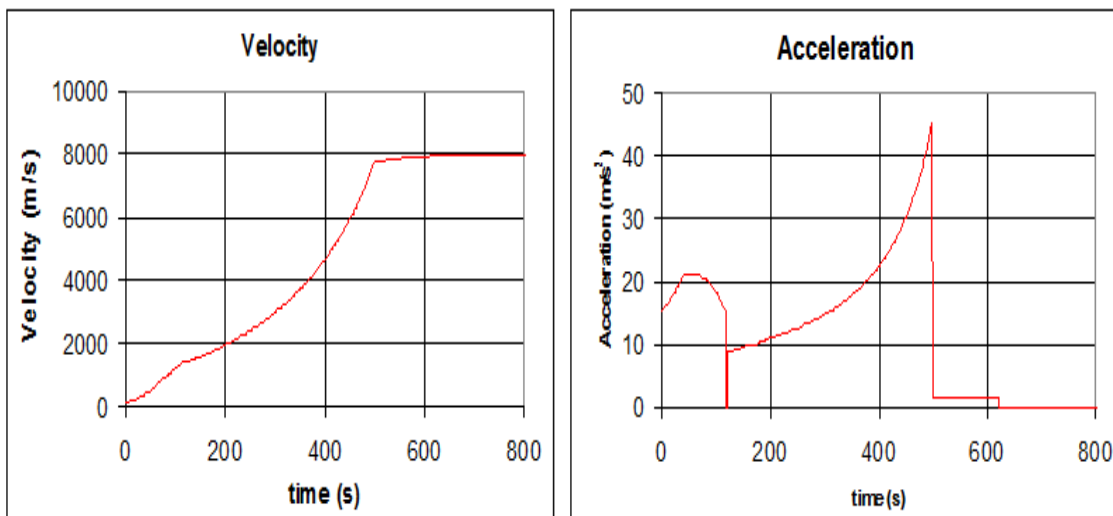


Figure A.2: Fortran simulation results: speed and acceleration

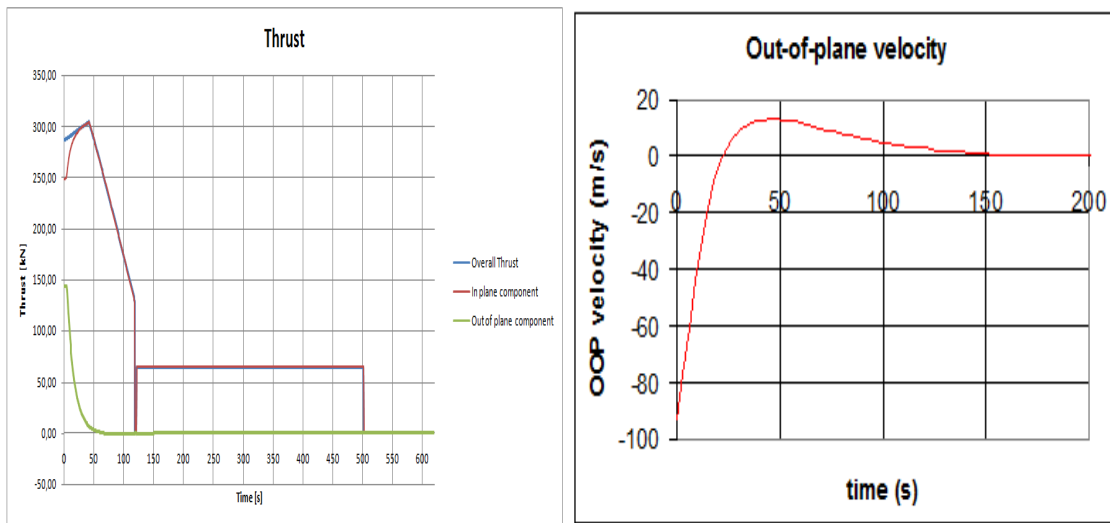


Figure A.3: Fortran simulation results: thrust and out of plane velocity

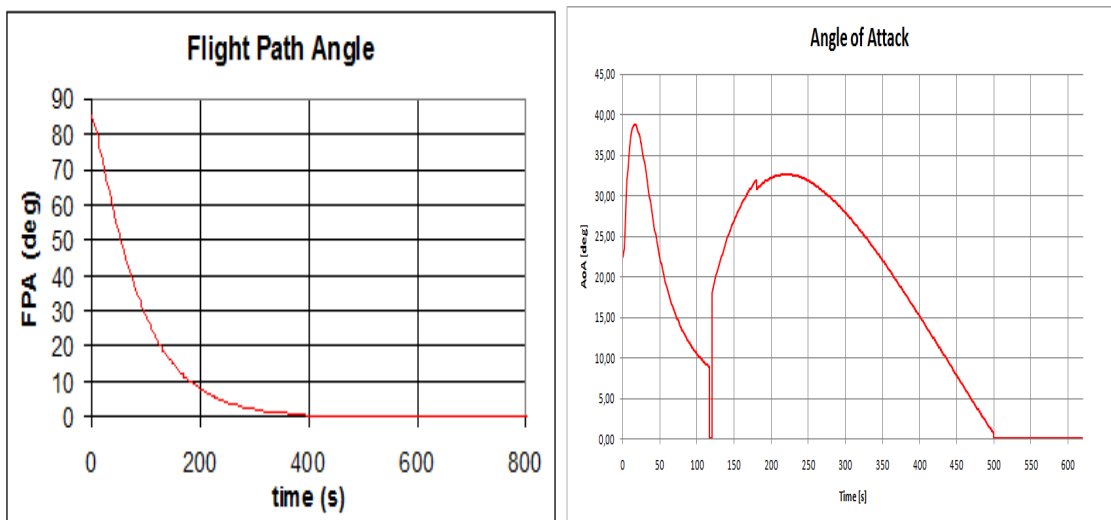


Figure A.4: Fortran simulation results: flight path angle and angle of attack

Comparing the figures above with those reported in the section 5.3, the Fortran ones show to be practically indistinguishable from those obtained by the *Matlab* software.

## A.2 Pegasus characteristics

Pegasus XL is a winged, three-stage, solid rocket booster that weights approximately 23130 kg, and measures 16.9 m (55.4 ft) in length and 1.27 m in diameter, and has a wing

## A.2. PEGASUS CHARACTERISTICS

span of 6.7 m. The main characteristics about stages and motors are reported in the table A.1:

	Stage 1 Motor Orion 50S XL	Stage 2 Motor Orion 50 XL	Stage 3 Motor Orion 38
Overall length [cm]	1027	311	134
Diameter [cm]	128	128	97
Inert Weight [kg]	1386	416	108
Propellant Weight [kg]	15032	3923	770
Total Vacuum Impulse [kN-s]	43325	11176	2182
Burn Time [s]	68.3	69.8	67.8
Mean Thrust [kN]	634.3	160.1	10.4

Table A.1: Pegasus's main characteristics

Thrust levels have been used in terms of mean value because there are not information available about the exact profile.

Furthermore, in order to have a correct overall mass of 21130 kg it has been assumed a fairing mass of 120 kg ( the length is about 3.5 m with a diameter of about 1 m), and it has been added about 800 kg for the wing mass, because the maximum payload is about 460 kg, as it can be deduced by figure A.5 in which are shown the performances for different location of launch and orbit inclination:

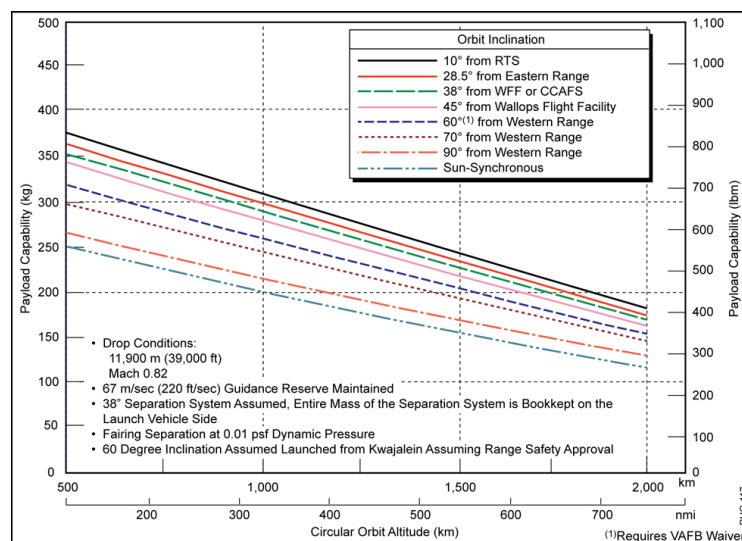


Figure A.5: Pegasus XL Performance Capability

Pegasus is lifted by the orbital carrier aircraft to a level flight condition of about 11900 m



and Mach 0.82. Five seconds after release from the orbit carrier aircraft (OCA) when the launcher has reached a speed of approximately 450 m/s, Stage 1 motor ignition occurs. The vehicle's autonomous guidance and flight control system provide the guidance necessary to insert payloads into a wide range of orbits.

### A.3 Test case

During this operation, some hypotheses has been done because data available also in the Pegasus User's Guide are conflicting, probably because they represent an industrial secret. Furthermore it has to take into account that the flight trajectory could be different especially for what concern the first phases of flight after the release from the carrier. Table A.2 reports the typical attitude and guidance modes sequence (see [21]):

Approximate time [s]	Event	Guidance mode	Attitude Mode
0	Drop	Open-loop	Inertial euler angles
5	Stage 1 ignition	Open-loop	Inertial euler angles
16	Maximum pitch-up	Open-loop	AoA limit
30	Pitch down	Open-loop	Inertial euler angles
65	Minimize AoA	Open-loop	Gravity turn
87	Stage 2 Explicit guidance		Gravity turn
90	Fins zeroed		Gravity turn
91	Stage 2 ignition	Closed-loop	Command Attitude
190	Explicit guidance calculations		Attitude hold
500	Stage 3 ignition	Open-loop	Command Attitude
575	Payload events as required		Command Attitude

Table A.2: Pegasus's typical attitude and guidance modes sequence

The time values are also contrasting with those corresponding to the stages burning time. A mission profile was tested with the simple software (i.e. that which consider an initial gravity turn, followed by the controlled phase). The mission, tested with burning times reported in table A.5, is that able to carry a payload of about 230 kg to a 741 km circular polar orbit.

For the validation it was assumed an initial path angle and then was established the control law which allows the third stage to reach the designed altitude consuming all the

### A.3. TEST CASE

---

propellant of the third stage.

Those assumption are necessary because the Pegasus launcher performs rotational manoeuvres in order to direct the thrust in a proper way. This is not possible with the model, and for this reason the initial path angle, together with the control law, are these which ,in mean terms, allows to describe the launcher mission profile. The effect of lift was not considered for lack of information about wind characteristics.

After some iteration those values have been determinate (see table A.3):

$\theta_0$ [deg]	Characteristic control time [s]	Final control path angle [deg]
62.7	1980	0.25

Table A.3: Pegasus's simulation parameters for 230 kg on 741 km circular orbit

A free flight phase between the two stages takes about 12s and fairings separations occur after about 116 s. The speed component normal to the plane has been set to 200 m/s. Those data and assumptions lead to the results reported in figures A.6 and A.7:

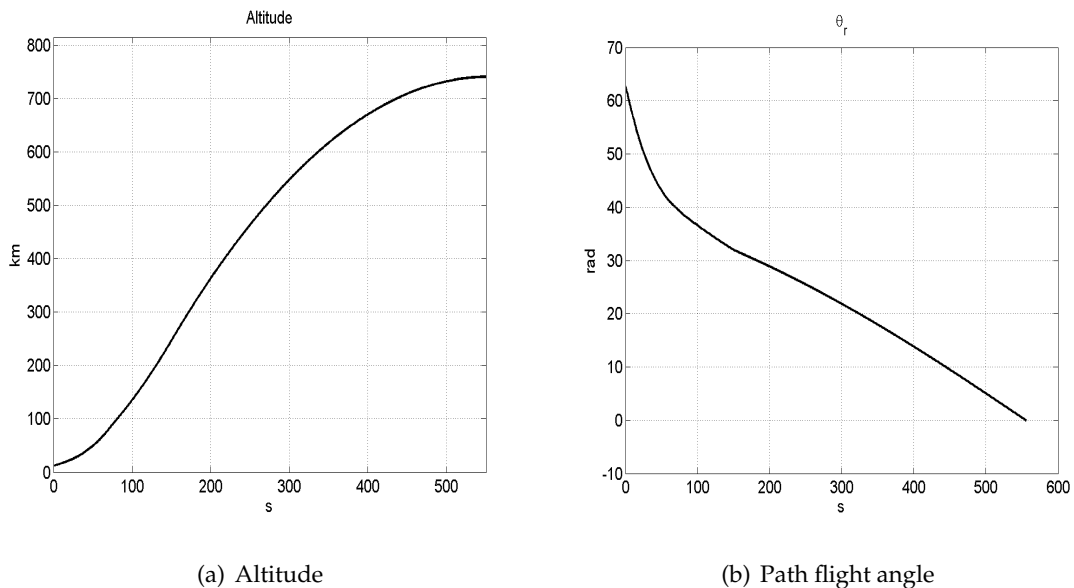


Figure A.6: Pegasus's simulation results for 230 kg on 741 km circular orbit: altitude and  $\theta_r$ .

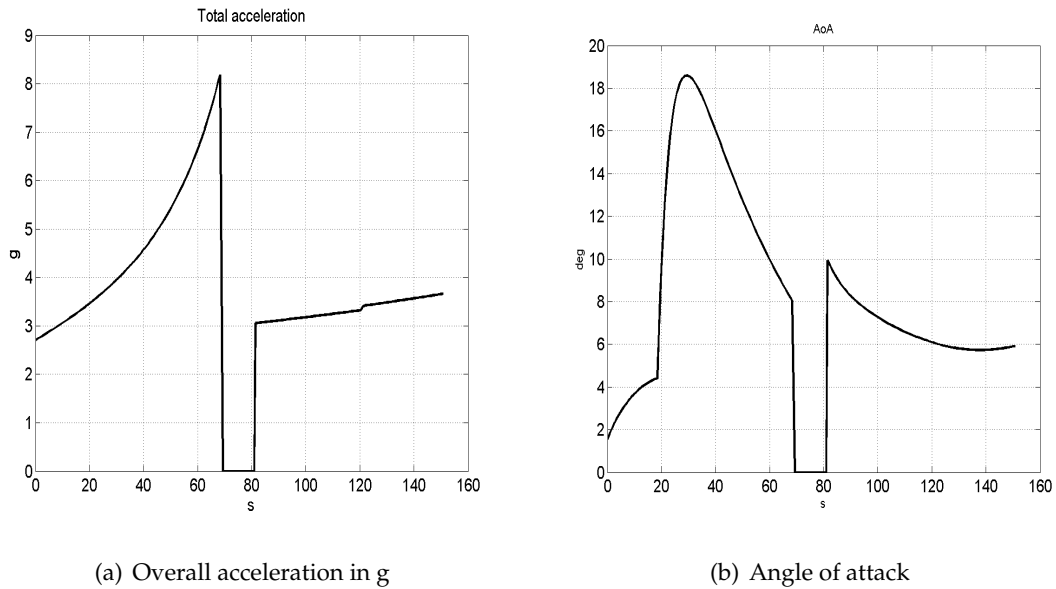


Figure A.7: Pegasus's simulation results for 230 kg on 741 km circular orbit: acceleration and AoA

All the propellant of the third stage is consumed in the injection at 741 km, where the path angle is clearly 0 deg. Thanks to the high thrust level the angle of attack remains limited to a max value of 18 deg, which can be considered coherent with the presence of the wing during the fire of the first stage.

The acceleration of Pegasus is considerably higher than that obtained with these of the launchers studied in this work.

## A.4 Consideration

The software used for estimating the performance has proven to be robust, thanks to the confront with the Fortran software, and reliable, able of describing and being applied to other launcher if the necessary assumption are taken.

## Appendix B

# Genetic Algorithms

Optimization search is a problem regarding the finding of zeros of the function derivatives, that correspond to the minimum or to the maximum of it. The main difficulty with optimization is determining if a given minimum is the best, global, minimum or a suboptimal, local, minimum.

During this work two are essentially the problems dealt and solved thanks to optimization procedure:

- the definition of the best conditions and control law for performance evaluation has been done by an optimization procedure;
- the design of the kerosene-LOX launcher.

This operation has been difficult because both the objective function are highly nonlinear ones. In the search for the condition which enables the launcher to reach a certain altitude with the minimum amount of propellant for circularization at the the second stage burnout; in the second case this object function has been correlated to a set of constraints (see par. 6.4).

Typical approaches to highly nonlinear problems involve either linearizing the problem in a very confined region or restricting the optimization to a small region.

In all the analyzed cases the parameters have limits and constraints, which are expressed incorporating equalities and inequalities into the cost function.

The minimum search algorithms try to minimize the cost function by starting from an initial set of parameter value. These minimum seekers easily get struck in local minima but are relatively fast. They are the traditional optimization algorithms and are generally based on calculus methods, with some determinant sequences of step.

On the other hand, random methods use probabilistic calculations to find parameters sets. They tend to be slower but have greater success at finding the global minimum.

## **B.1 Optimization based on genetic algorithms**

The largest category of optimization methods fall under the general title of successive line minimization methods ([35] and [36]). An algorithm begins at some random point in the cost function, chooses a direction to move, then moves in that direction until the cost functions begins to increase. Next the procedure is repeated in another direction.

There is a broad variety of methods developed but unfortunately those do not prove to be reliable, failing to find the global minimum. The genetic algorithms can solve this problem because they model natural selection and evolution, generating new points in the multidimensional space by applying operators to current points in the search space and statistically moving toward more optimal places in the search space. Genetic algorithms rely upon an intelligent search of large but finite solution space using statistical methods. Those algorithms do not require taking cost function derivatives.

The genetic algorithm is a subset of evolutionary algorithms that model biological processes to optimize highly and complex cost functions. It allows a population composed of many individuals to evolve under specified selection rules to a state that maximize the fitness. Some advantages of this calculation include that it :

- does not require derivative information,
- simultaneously searches from a wide sampling of the cost surface,
- deals with a large number of parameters,
- optimizes parameters with extremely complex cost surfaces as in the cases treated; they can jump out of a local minimum.

The genetic algorithm have origin from the observation of the natural world, where there is a tremendous diversity among the organisms of the same specie. This diversity is the product of the effect of the natural selection of best elements which fit the natural environment.

A group of individuals with their particularities is called population. Each individual is characterized by genes that are the basic unity of heredity; the genes form the chromosome of the individual, that is an array of parameter values. Under static

condition, the characteristics of the population conserve the same statistical distribution, though each individuals show great variety. When the population is no longer static, the statistical distribution changes between generations and evolution occurs thanks to an external forcing. The forcing may be grouped into four specific types:

1. mutations; it is a random change in the characteristics of a gene/element
2. gene flow; it results from the introduction of new organisms into the population
3. genetic drift; certain gene may sometimes be eliminated
4. natural selection; it operates to choose the most fit individuals for further reproduction/combination

In genetic algorithms the genetic drift is not considered because each gene of the chromosome corresponds to a parameter involved in the cost function.

### B.1.1 Components of the genetic algorithm

The problem of optimization via genetic algorithm starts with the definition of the cost function and the parameter that have to be optimized. In the case of the direct insertion handled in par.6.4.3, the cost function was defined in order to find the maximum payload mass carried by they launcher to a defined altitude  $h_{target}$ , with a certain thrust profile along all the power ascent:

$$f = (h - h_{target}) + mult(M_{circularization} - M_{available}) \quad (B.1)$$

where

- $h(m)$  is the reached altitude obtained in
- $mult(-)$  is a proper multiplier defined to take into account the order difference;
- $M_{circularization}(kg)$  represents the propellant mass necessary to circularize at the altitude  $h$ ;
- $M_{available}$  is the available propellant mass for circularization, which depends also from the altitude itself.

The available mass is less than third stage propellant , as seen in chapter 2:

$$M_{available} = M_{prop} - 0.011r_{target} \quad (B.2)$$

where

- $M_{prop}(kg)$  is the third stage embarked propellant;
- $r_{target}(km) = R_{Earth} + h_{target}$  is the target circular orbit radius.

It can be easily seen that in this way the cost function is highly nonlinear. The logic of the genetic algorithm is the following:

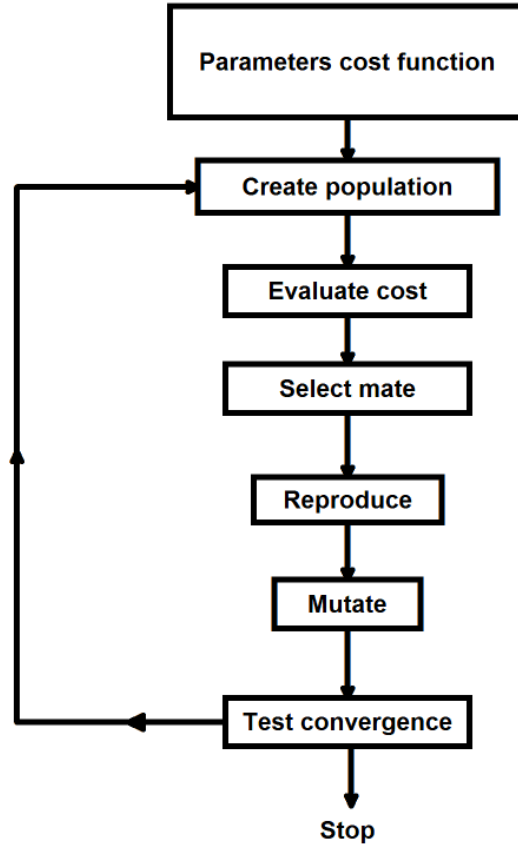


Figure B.1: Flow chart of a genetic algorithm

- Initial population

The search for the individual that best fits the cost function starts by the definition of the population of  $N_{ipop}$  individuals of chromosome, whose elements are defined by an array of  $N_{par}$  parameters containing a gene corresponding to the payload and the others to a thrust angle for the control law:

$$chromosome = [M_{payload}, \theta_1, \theta_2, \theta_3, \dots, \theta_n]$$

where

- $M_{payload}(kg)$  is the payload mass, and

–  $\theta_i(rad)$  is the control FPA at the time  $t_i(s)$

Each chromosome is randomly generated considering the constraint represented by the parameter range. All the individuals are grouped in a matrix of the initial population:

$$IPOP = (hi - ho) \cdot random\{N_{ipop}, N_{par}\} + lo \quad (B.3)$$

where hi and ho are the highest and lowest number in the parameter range.

- Natural selection

To each individual is associated a cost found by evaluating the cost function,  $f$ :

$$f = f(chromosome) = f(payload, \theta_1, \theta_2, \theta_3, \dots, \theta_n)$$

All the costs and associated chromosome are ranked from the lowest cost to the highest cost. The best  $N_{pop}$  members of the initial population are retained for the next iteration. The rest die off. This process of natural selection occurs at each iteration of the algorithm to allow the population to evolve over the generation to the most fit members as defined by the cost function. From this point on, the size of the population at each generation is  $N_{pop}$ .

Not all the survivors are deemed fit enough to mate. Of the  $N_{pop}$  chromosome in a given generation, only the top  $N_{good}$  are kept for mating and the bottom  $N_{bad}$  are discarded to make room for the new offspring (where  $N_{good} + N_{bad} = N_{pop}$ ).

- Pairing

The  $N_{good}$  most fit chromosomes form the mating pool. Mothers and fathers pair in some random fashion. Each pair produces two offspring that contain traits from each parent. In addition, the two parents survive to be part of the next generation. The most effective pair choice is based on the weighted cost selection. Parents are randomly chosen and rarely selected from the bottom half of the population, because their costs are so much bigger than those, at the top of the list.

- Mating

Two parents are chosen and the offspring are some combinations of these parents. The genetic algorithms used often the so called heuristic crossover, which allows the offspring to have to have the generic parameter  $p$  that goes outside the values of the two parent parameter:

$$p_{new} = \beta(p_{mn} - p_{dn}) + p_{mn}$$

where



- $\beta$  is a random number chosen on the interval  $[0,1]$  and
- $p_{mn}, p_{dn}$  are the  $n$  gene in the mother and father chromosome respectively.

If the value generated is outside of the allowed range, then the offspring is discarded and algorithm tries another  $\beta$ .

- Mutations

If care is not taken, the genetic algorithm converges too quickly into one region of the cost surface. If this area is in the global minimum, that is good. However the cost function have many local minima. To avoid the problem of overly fast convergence, the routine is forced to explore other areas of the cost surface by randomly introducing changes, or mutations, in some of the parameters. A mutation rate 1% and 20% often works well. If the mutation rate is above 20%, too many good parameters are mutated, and the algorithm stalls